Volume III | Number 2 | December 2015 | ARO ISSN: 2410-9355 | DOI: 10.14500/2307-549X

ARO

The Scientific Journal of Koya University

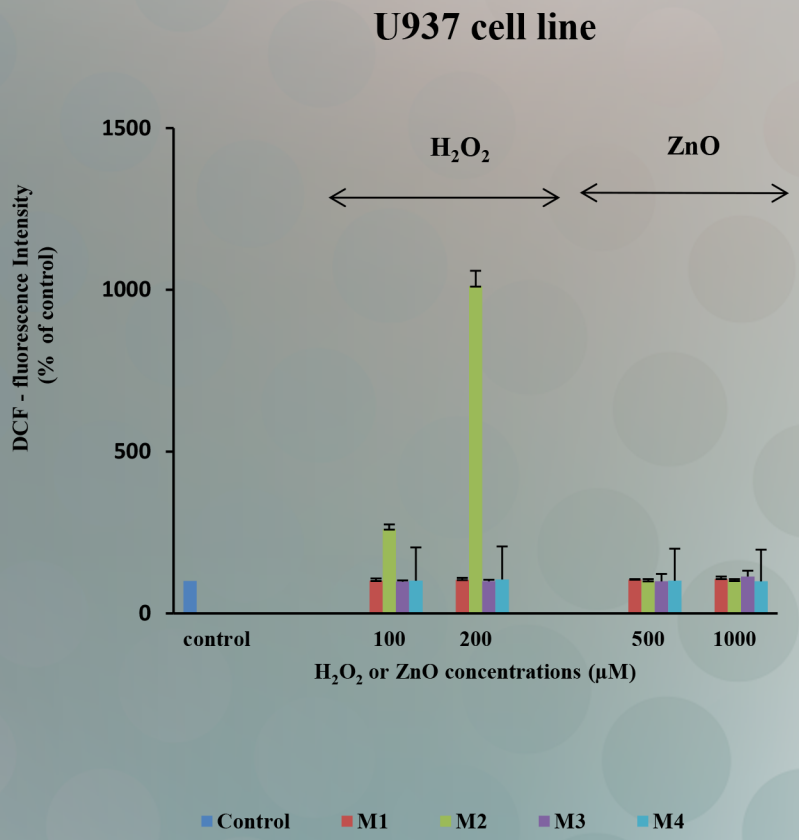

Issue Highlights

KOYA UNIVERSITY
aro.koyauniversity.org

ARO; The Scientific Journal of Koya University

The Aro (“Today” in Hewramí Kurdish), is an international scientific journal published by the Koya University with p-ISSN: 2410-9355, e-ISSN: 2307-549X and DOI: 10.14500/2307-549X. Aro is a journal of original scientific research, global news, and commentary. The Aro Scientific Journal is a peer-reviewed, open access journal that publishes original research articles as well as review articles in all areas of Science.

ARO the Scientific Journal Office
Koya University
University Park
Danielle Mitterrand Boulevard, Koya KOY45
Kurdistan Region - F.R. Iraq

Tel.: +964(0)748 0127423
Mobile: +964(0)7502257080
E-mail: aro.journal@koyauniversity.org
url: aro.koyauniversity.org

ARO

The Scientific Journal of Koya University

Vol III, No 2(2015)

Contents

♦♦♦

DOI: 10.14500/2307-549X ARO p-ISSN: 2410-9355, e-ISSN: 2307-549X

ARO p-ISSN: 2410-9355, e-ISSN: 2307-549X DOI: 10.14500/2307-549X

Aro Editorial Words

Dear readers, you are holding the fifth issue (Vol III, No 2) of Aro, the Scientific Journal of Koya University in your hand. With this issue Aro has concluded its third year journey in leading the quality of regional scientific publication with global impact. The editorial team is determined to keep the path of such a mission and sustain Aro's future publications with quality and reliability in mind.

Despite the economic downturn which have had a great impact on scientific research and universities our region in particular, Aro has received good numbers of well-motivated quality papers which shows its steadily growing trust among researchers in the region. With increasing demands by volume of submission, Aro's Associate Editorial has grown larger and our meetings are richer. Our colleagues with great passion are contributing to Aro's long-term visions.

Aro was created with long-term visions of becoming accessible to all researchers in Kurdistan and beyond, and covering a wide range of scholarly disciplines in sciences. The focus of the journal is to reflect that of the Koya University, namely promoting scientific knowledge and research in Kurdistan and secure a brighter future in education. Aro aspires to become a channel for exchange of scholarly research by establishing academic connections between scholars and listed by reliable institutes.

Aro is a journal of original scientific research, global news, review paper, letters and commentary. The Aro Scientific Journal is a peer-reviewed, open access journal that publishes original research articles as well as review articles in areas of natural sciences and technology. In this issue you will have access to genuine research paper in variety of areas, such as petroleum, physics, chemical engineering, biochemistry, engineering and material.

Aro is a member of CrossRef, which is a not-for-profit membership association whose mission is to enable easy identification via dedicated DOI and use of trustworthy electronic content by promoting the cooperative development and application of a sustainable infrastructure. Aro is also has become member and indexed of many organizations, e.g., ICI, ROAD, Google Scholar, ResearchGate, WorldCat, etc. Beside its online publications, Aro has a semi-annual hard copy publication which is available free-of-charge.

The warm response from researchers, academics and professionals in the last two years has made us to create a wider Editorial Board which serves the wider submitted scientific manuscripts. However, it is clear that having a dedicated and well organized editorial board for the journal is only one side of the coin. The other is the ability to attract submissions of quality research and scholarly work. We are thankful to all of those who put their trust in Aro and presented their original research work for publication in Vol III, No 2 of the journal, as well as, our thanks are extended to the 13 peer-reviewers from the Universities worldwide for their efforts in reviewing this issue of Aro publications.

Your support and feedback are invited and appreciated.

Sincerely

Wali M. Hamad
Executive Publisher

Dilan M. Rostam, Shwan K. Rachid, Salah I. Yahya and Sarkawt S. Abdulrahman
Executive Editorial Board

DOI: 10.14500/2307-549X ARO p-ISSN: 2410-9355, e-ISSN: 2307-549X

ARO p-ISSN: 2410-9355, e-ISSN: 2307-549X DOI: 10.14500/2307-549X

Optimizing the Flexural Strength of Beams Reinforced with Fiber Reinforced Polymer Bars Using Back-Propagation Neural Networks

Bahman O. Taha[1], Peshawa J. Muhammad Ali[2] and Haval A. Ahmed[2]

[1]Department of Civil Engineering, Erbil Technical Engineering College
Erbil, Kurdistan Region of F.R. Iraq

[2]Department of Software Engineering, Koya University
Daniel Mitterrand Boulevard, Koya KOY45, Kurdistan Region of F.R. Iraq

***Abstract*—The reinforced concrete with fiber reinforced polymer (FRP) bars (carbon, aramid, basalt and glass) is used in places where a high ratio of strength to weight is required and corrosion is not acceptable. Behavior of structural members using (FRP) bars is hard to be modeled using traditional methods because of the high non-linearity relationship among factors influencing the strength of structural members. Back-propagation neural network is a very effective method for modeling such complicated relationships. In this paper, back-propagation neural network is used for modeling the flexural behavior of beams reinforced with (FRP) bars. 101 samples of beams reinforced with fiber bars were collected from literatures. Five important factors are taken in consideration for predicting the strength of beams. Two models of Multilayer Perceptron (MLP) are created, first with single-hidden layer and the second with two-hidden layers. The two-hidden layer model showed better accuracy ratio than the single-hidden layer model. Parametric study has been done for two-hidden layer model only. Equations are derived to be used instead of the model and the importance of input factors is determined. Results showed that the neural network is successful in modeling the behavior of concrete beams reinforced with different types of (FRP) bars.**

***Index Terms*—Concrete, fiber reinforced bars, fiber reinforced polymer (FRP), neural networks.**

I. Introduction

Fiber-reinforced polymers (FRP) are composite materials which made of fibers embedded in a polymeric resin. FRP has become an alternative to steel reinforcement for concrete structures. Since FRP materials are nonmagnetic and noncorrosive, the problems of electromagnetic interference and steel corrosion can be avoided using FRP reinforcement. FRP materials have a high tensile strength which makes them suitable for use as a structural reinforcement. The anti-corrosion characteristic of FRP concretes is useful for structures in marine environments, in chemical and other industrial plants, in places where good quality concrete cannot be achieved and in thin structural elements.

The mechanical behavior of FRP reinforcement differs from the behavior of steel reinforcement. FRP materials are anisotropic and are characterized by high tensile strength only in the direction of the reinforcing fibers. FRP materials do not exhibit yielding; rather, they are elastic until failure. Design procedures should account for a lack of ductility in a concrete reinforced with FRP bar.

The neural network is a technique that can be used in modeling complicated and interrelated data. It simulates the way that human's brain works. Multilayer Perceptron (MLP) is a feed forward neural network, which can be used successfully in prediction and modeling. The neural network can learn from collected data only, without any prior knowledge about the nature of the relationships among factors. A supervised learning can be conducted by comparing the output with the target, the difference is propagated back to update all connecting links between nodes, this algorithm is called back-propagation. Neurons are arranged in layers, input, hidden layer(s) and output layer.

Experimental studies have been done in evaluating the flexure strength and behavior of concrete beams reinforced with different types of FPR bars having different concrete compressive strengths (Taha, 2013; Al-Shamaa, 2010; Chitsazan, et al., 2010; Barris, et al., 2009; Al-Sunna, 2006). Also, neural networks technique is used to predict the behavior of existing beams strengthened with FRP sheets (Leung, et al., 2006; Yousif and Al-Jurmaa, 2010; Mashrei, et al., 2013). Many other studies have been done in predicting the behavior of concrete members in shear reinforced with or strengthened with FRP (Perera, et al., 2014; Metwally, 2013;

ARO, The Scientific Journal of Koya University
Volume III, No 2(2015), Article ID: ARO.10066, 10 pages
DOI: 10.14500/aro.10066
Received 21 December 2014; Accepted 23 April 2015
Regular research paper: Published 25 June 2015
Corresponding author's e-mail: peshawa.jammal@koyauniversity.org

http://dx.doi.org/10.14500/aro.10066

Lee and Lee, 2014). The aim of this work is to modeling concrete beams in flexure reinforced with fiber polymer bars using back-propagation neural networks.

The objectives of this research work are;

1) Constructing and training the model on the collected data.
2) Using the model for predicting the flexural strength of concrete beams reinforced with FRP bars.
3) Writing mathematical equations to represent the model.
4) Determining the relative importance of input factors.
5) Doing a parametric study for major parameters that affect the flexural strength of high strength concrete beams.

For this purpose a number of high strength concrete beams reinforced with carbon and glass fibers were predicted taking different parameters into account. The parameters include; the effect of the effective depth (d), concrete compressive strength ($f'c$), and the flexural reinforcement ratio (ρ). The rest of the paper is organized as follows: Section II presents the neural network model, Section III presents the weights equations, Section IV shows the importance of input factors and parametric study is presented in Section V. Finally, Section VI concludes the paper.

II. The Neural Network Model and the Experimental Results

The system includes five phases: data collection, preprocessing, creation of the model, learning, and evaluation of the model. The system can be illustrated in the process diagram shown in the Fig. 1.

Fig. 1. Process diagram of the system.

A. Data Collection

Data are collected from different published papers, where different types of fiber reinforced polymer bars are used (carbon, aramid, basalt and glass). Most of researches done previously have been working on one specific type of fiber polymer bars, whereas, in this paper different types of fiber polymers are collected, therefore, the model can be used to predict the flexural strength of beams reinforced with all types of fiber polymer bars. Five important factors which influencing the strength of a beam in flexure are taken in consideration. Factors are, the width of the beam (b), the effective depth of the beam (d), cylindrical concrete compression strength ($f'c$), the ultimate tensile strength of fiber reinforced polymer bars (fu), and reinforcement ratio (ρ), the empirical moments capacity are used as target data. 101 samples were collected from nine sources (Taha, 2013; Al-Shamaa, 2010; Chitsazan, et al., 2010; Barris, et al., 2009; Al-Sunna, 2006; Toutanji and Saafi, 2000; Masmoudi, et al., 1998; Duranovic, et al., 1997; Benmoktane, et al., 1995), the collected data are arranged in Appendix A. The ranges of the collected data and measurement units are given in Table I.

TABLE I
Influenced Factors, Ranges of Data and Measurement Units

Factors and empirical strength	Unit	Minimum	Maximum
Width of the beam (b)	mm	80	500
Effective depth of the beam (d)	mm	70.48	509.00
Concrete compression strength ($f'c$)	MPa	31.20	100.82
Bars ultimate tensile strength (fu)	MPa	600	2300
Reinforcement ratio % (ρ)	----	0.15	4.05
Empirical moment caused the failure (Mu)	KN.m	5.43	181.70

B. Data Preprocessing

In this paper, Weka package (Hall, et al., 2009) is used for creating and learning the model. Weka is a software that can be used for all purposes of data mining and knowledge extraction. It provides a very easy to use and friendly environment. The package is imported to a self-created Java program and used for creating and learning the model. Using this package enables the user to specify the structure of the model like number of hidden layers and the number of nodes inside each layer and type of the transfer functions for each layer. Weka uses a random initialization for weights and bias values.

To minimize the bias of one feature over another, data normalization is necessary. This step has been done automatically by the Weka package which makes the input features within the same range of values. In this paper min-max [-1, +1] normalization is used which casts all features to the range [-1, +1].

C. Creating Models

In this paper, two models of MLP Neural Network are created. The first model was created with three layers: an input, a hidden layer and an output layer. The structure can be summarized as BPNN1(5-3-1), shown in the Fig. 2. The second model consists of input, two hidden layers and an output layer BPNN2(5-5-3-1), the structure of the second model is shown in Fig. 3. All activation functions of hidden layers for both models are sigmoid functions while the activation function of the output layer is a linear function. Notice that the word “layer” hasn’t been appended to the word “input”. This is because the input is not a real layer where there is no summation, no bias, and no transfer function (Muhammad Ali, et al., 2013; Muhammad Ali, 2014).

Choosing number of hidden layers and number of nodes in each layer depends on different factors. It depends on the complexity of the problem, the size of the training data set dealing with and the quality of the data. Usually, the number of nodes in the hidden layer is ranging between the number of nodes in the input and the number of the nodes in the output layer. To find a suitable structure of the neural model, different structures should be tested then the best can be selected.

D. Learning Process

The back-propagation is used for supervised learning. In this method, an artificial network learns from computing the error between the output values with target values, then

propagating back this error by justifying the weights of the connections between nodes. This backward-propagation of errors needs the transfer functions used in the nodes to be differentiable to ensure a smooth back-distribution of errors on the weights. Gradient descent with moment (GDM) algorithm is used for back-propagation. The detail of the learning process for both models is shown in Table II.

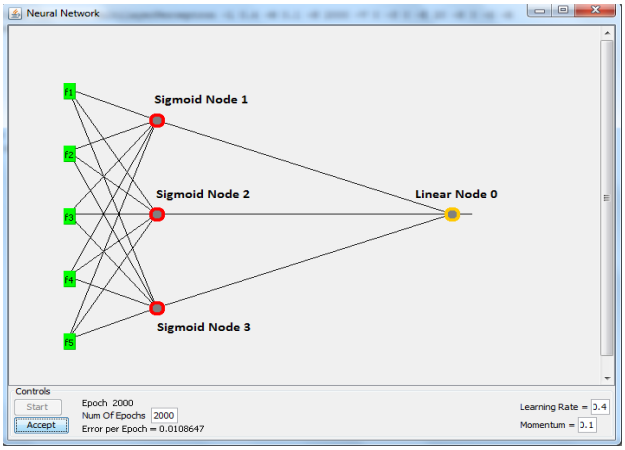

Fig. 2. The neural network model BPNN1(5-3-1).

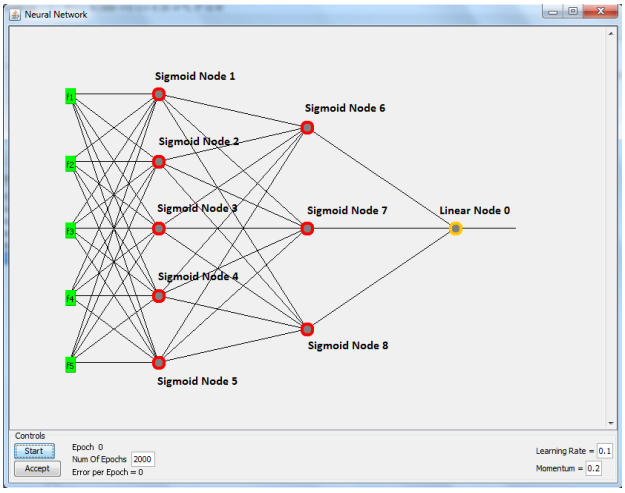

Fig. 3. The neural network model BPNN2(5-5-3-1).

TABLE II
LEARNING PROCESS DETAILS

Parameters	BPNN1(5-3-1)	BPNN2(5-5-3-1)
Learning rate	0.4	0.1
Momentum	0.1	0.2
Epoch	2000	2000

E. Evaluation

The 101 collected samples were divided into two parts, 91 of them (90%) were used for training the neural network models, and the other 10 items (10%) were used for testing. These 10 unseen data are used for finding the correlation of the model with the actual observed results. The results showed that the BPNN2(5-5-3-1) model (R=0.9832) is better correlated than the first structure. Therefore, the second model is used. Fig. 4 shows the correlation between predicted data and actual data for BPNN1(5-3-1), and Fig. 5 shows the same correlation for BPNN2(5-5-3-1) model.

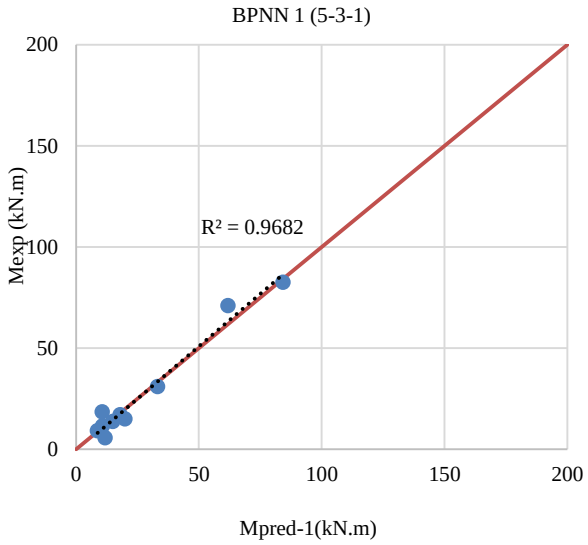

Fig. 4. The correlation between actual and predicted data for BPNN1 (test set only).

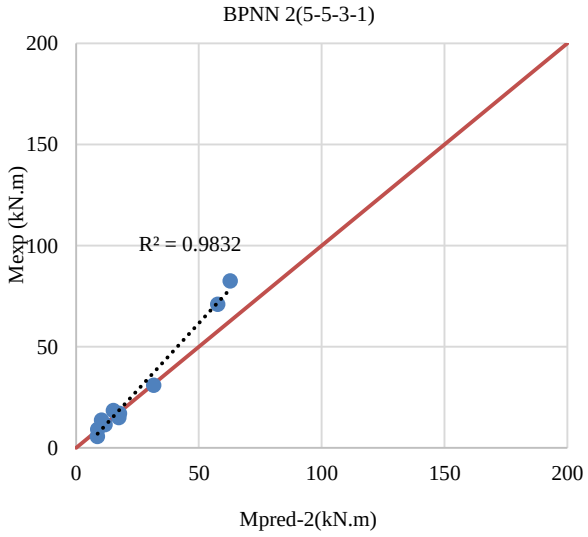

Fig. 5. The correlation between actual and predicted data for BPNN2 (test set only).

III. WEIGHTS AND EQUATIONS

The neural network model can be mathematically represented by one mathematical equation, but for the sake of simplicity, it's better to present the model in several simpler equations, especially for models have more than one hidden layer. In this section, the BPNN2 model is presented in (1) to (8). The min-max normalization is necessary to bring all features to the range [-1, +1] to eliminate the influence of one feature over another feature.

 http://dx.doi.org/10.14500/aro.10066

$$x' = 2*\left[\frac{x-min}{\max-min}\right]-1 \quad (1)$$

Where x' is the normalized values, x is the value before normalizing, *min* and *max* are minimum and maximum values of any feature shown in Table I.

$$A = \frac{1}{1+e^{\left[-1.9+0.1(b)+1.2(d)-2.4(fc)-0.02(fu)+3.1(r)\right]}} \quad (2)$$

$$B = \frac{1}{1+e^{\left[1.2-0.9(b)-4.5(d)+0.5(fc)-0.02(fu)-0.1(r)\right]}} \quad (3)$$

$$C = \frac{1}{1+e^{\left[0.6-0.2(b)-1.5(d)+0.4(fc)-0.7(fu)-0.5(r)\right]}} \quad (4)$$

$$D = \frac{1}{1+e^{\left[-1.9-0.1(b)-2.5(d)-0.7(fc)+0.5(fu)-3.96(r)\right]}} \quad (5)$$

$$E = \frac{1}{1+e^{\left[0.7-0.3(b)-1.6(d)+0.1(fc)-0.6(fu)-0.4(r)\right]}} \quad (6)$$

Where b is the width of the beam in mm, d is the effective depth in mm, fc is the concrete compression strength in MPa, fu is bars' ultimate tensile strength in MPa, and r is reinforcement ratio in %. e is the exponential function and other constant numbers are the weights of the trained model. A, B, C, D, and E are calculated and inserted to (7):

$$y' = 1.129 - \frac{1.755}{1+e^{\left[-0.36+1.39A+1.70B+0.51C+D+0.30E\right]}} - \frac{2.099}{1+e^{\left[-1.68+1.32A+2.09B+0.50C+1.68D+0.30E\right]}} - \frac{1.765}{1+e^{\left[-0.43+1.35A+1.66B+0.45C+1.09D+0.28E\right]}} \quad (7)$$

$$M = \left[\left(\frac{y'+1}{2}\right)(max-min)\right]+min \quad (8)$$

Where y' is the output of the model before denormalizing, M is the moment capacity in KN.m, *min* and *max* are the minimum and maximum values of target feature before normalization.

IV. Importance Factor

The relative importance study for input factors has been done based on the importance of weights using the method proposed by (Garson, 1991), see (9).

$$I_j = \frac{\sum_{m=1}^{m=Nh}\left(\left(\frac{\left|W_{jm}^{ih}\right|}{\sum_{k=1}^{Ni}\left|W_{km}^{ih}\right|}\right)\times\left|W_{mn}^{ho}\right|\right)}{\sum_{k=1}^{k=Ni}\left\{\sum_{m=1}^{m=Nh}\left(\left(\frac{\left|W_{jm}^{ih}\right|}{\sum_{k=1}^{Ni}\left|W_{km}^{ih}\right|}\right)\times\left|W_{mn}^{ho}\right|\right)\right\}} \quad (9)$$

Where, I_j is the relative importance of the jth input variable on the output variable, *Ni* and *Nh* are the numbers of input and hidden neurons, respectively, W is connection weights, the superscripts *"i"*, *"h"* and *"o"* refer to input, hidden and output layers, respectively, and subscripts *"k"*, *"m"* and *"n"* refer to input, hidden and output neurons, respectively. Table III shows the relative importance ratio for both models calculated according to Garson's method.

It's clear that in both models the effective depth (d) has the greatest influence on the moment capacity of the beams.

TABLE III
Relative Importance Ratio According to Garson Formula

Features	BPNN1 (5-3-1) %	BPNN2 (5-5-3-1) %
Width of the beam (b)	05	06
Effective depth (d)	44	42
Compression strength of concrete (f'c)	24	23
Ultimate tensile strength of re-bars (fu)	8	9
Reinforcement ratio (ρ)	19	20

V. Parametric Study

The most important benefit of creating models by the neural network is that it makes parametric study an easy job. Researchers can predict the influence of one factor by fixing all other factors. The parametric study focused on the carbon fiber polymer bars and glass fiber polymer bars which they are the common types mostly used. Parametric study has been done for BPNN2(5-5-3-1) model only which gains the higher correlation rate. The reason behind the difference in the accuracy of the two models is that BPNN2(5-5-3-1) model can save or remember higher numbers of relationships between nodes. It's an evident on the non-linearity relationships among influenced factors affecting the flexural strength of beams reinforced with FRP bars. 150 test samples are prepared (75 samples reinforced with carbon fiber polymer bars with fixed ultimate tensile strength (2300 MPa) and 75 samples reinforced with glass fiber polymer bars with fixed ultimate tensile strength (1000 MPa), all samples are high strength concrete (60 MPa, 80 MPa, 100 MPa)). Samples are fed to the BPNN2(5-5-3-1) model and moment capacity is predicted.

A. Parametric Study for Beams Reinforced with Carbon Fiber Polymer Bars

By using BPNN2(5-5-3-1) model, the flexural strength capacity of 75 concrete beams reinforced with carbon fiber polymer bars were predicted to evaluate the effect of parameters (effective depth, cylindrical concrete compressive strength and reinforcement ratio) on the flexural capacity of concrete beams reinforced with carbon fiber polymer bars.

Influence of Effective Depth

Effective depth is the most important parameter influencing the moment capability of a beam. Fig. 6 shows the BPNN2(5-5-3-1) neural network relationship between the effective depth

and moment capacity of the beam for different reinforcement ratios (0.15%, 0.30%, 0.45%, 0.60% and 0.75%).

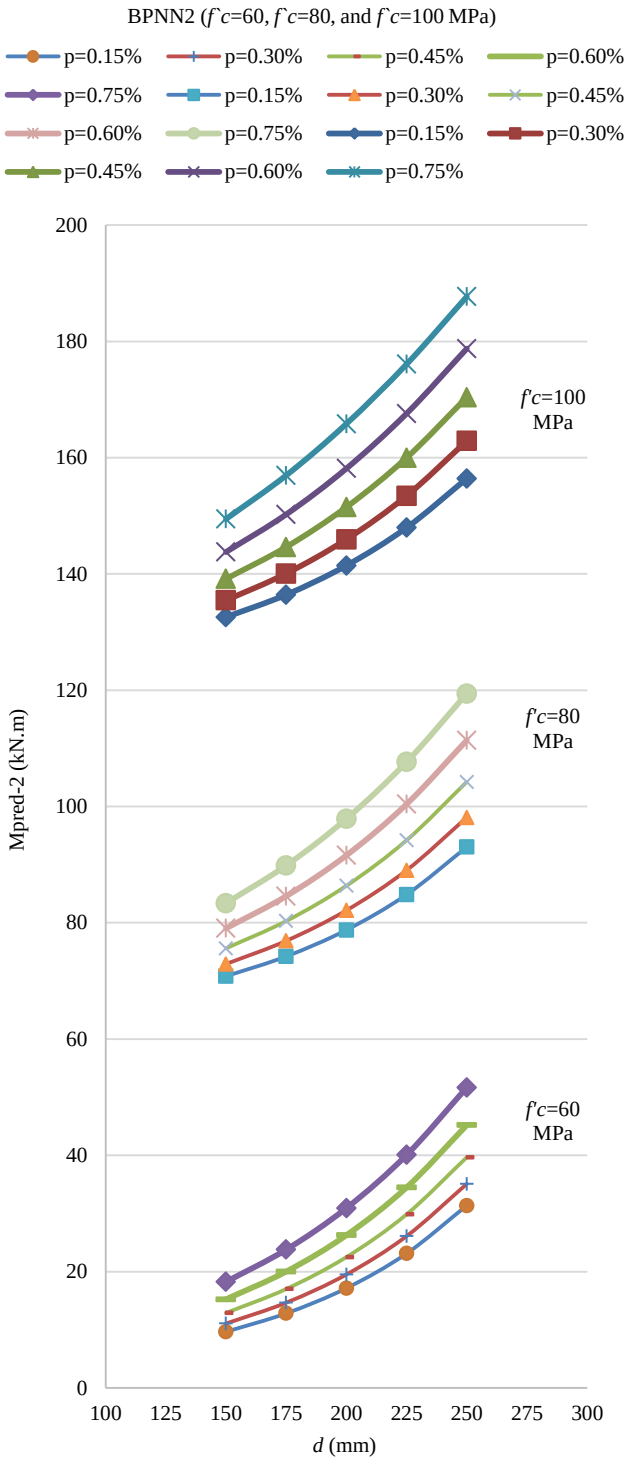

Fig. 6. Variation of the ultimate moment capacity with the effective depth and the reinforcement ratios.

In these relationships the ultimate tensile strength of the bars is already fixed to 2300 MPa, while the concrete strength is fixed to 60 MPa, 80 MPa and 100 MPa, different reinforcement ratio are used. Increasing the effective depth caused an increase in the moment capacity of beams with respect to the different reinforcement ratios. All curves look very normal and represent the realistic relationships of the effective depth and moment capacity.

A careful look to the three relationships in Fig. 6 shows that the slope of all curves being steeper when the effective depth of a beams increased. This means that the rate of increasing moment capacity is higher for beams having greater effective depth.

Influence of Compression Strength of Concrete

Fig. 7 is declaring the relationship between the cylindrical compressive strength of concrete and the predicted moment capacity of the beams. The relationships are created by fixing tensile strength of rebars to 2300 MPa as mentioned before and effective depth to (150 mm 175 mm, 200 mm, 225 mm, and 250 mm). Five curves are drawn for different reinforcement ratios (0.15%, 0.30%, 0.45%, 0.60% and 0.75%). By increasing the cylindrical compression strength, the sectional moment capacity will increase.

The slope of all curves in Fig. 7 increases with increase in the cylindrical compression strength of concrete (i.e. the rate of increase of the moment capacity when the concrete cylindrical compressive strength increased from 80 MPa to 100 MPa is greater than the rate of increase in the moment while the concrete compression strength increased from 60 MPa to 80 MPa). The increase in the moment capacity caused by increasing in reinforcement ratio is higher at 100 MPa concretes if compared with 60 MPa compression strengths.

Influence of Reinforcement Ratio

Fig. 8 shows the relationship between reinforcement ratio and predicted moment capacity of the beams. The Ultimate tensile strength of the bars is already fixed to 2300 MPa; different colored curves represent different concrete compressive strengths. The effective depths are (150 mm, 175 mm, 200 mm, 225 mm, and 250 mm) accordingly.

All curves in Fig. 8 look to be linear which means that the rate of increasing in moment capacity is constant, a small difference is sensible for green colored curves (100 MPa). The low compression strength concretes have flat slopes while higher compression strength concretes gives steeper gradient lines (i.e. increasing in the reinforcement ratio gives higher rates of increase in moment capacity for beams having higher concrete compressive strengths).

B. Parametric Study for Beams Reinforced with Glass Fiber Polymer Bars

Another set of 75 generated beams were used to represent the relationships among influenced factors for beams supposed to be reinforced with glass fiber polymer bars, BPNN2(5-5-3-1) is used to evaluate the effect of parameters (effective depth, cylindrical concrete compressive strength and reinforcement ratio) on the flexural capacity of concrete beams.

http://dx.doi.org/10.14500/aro.10066

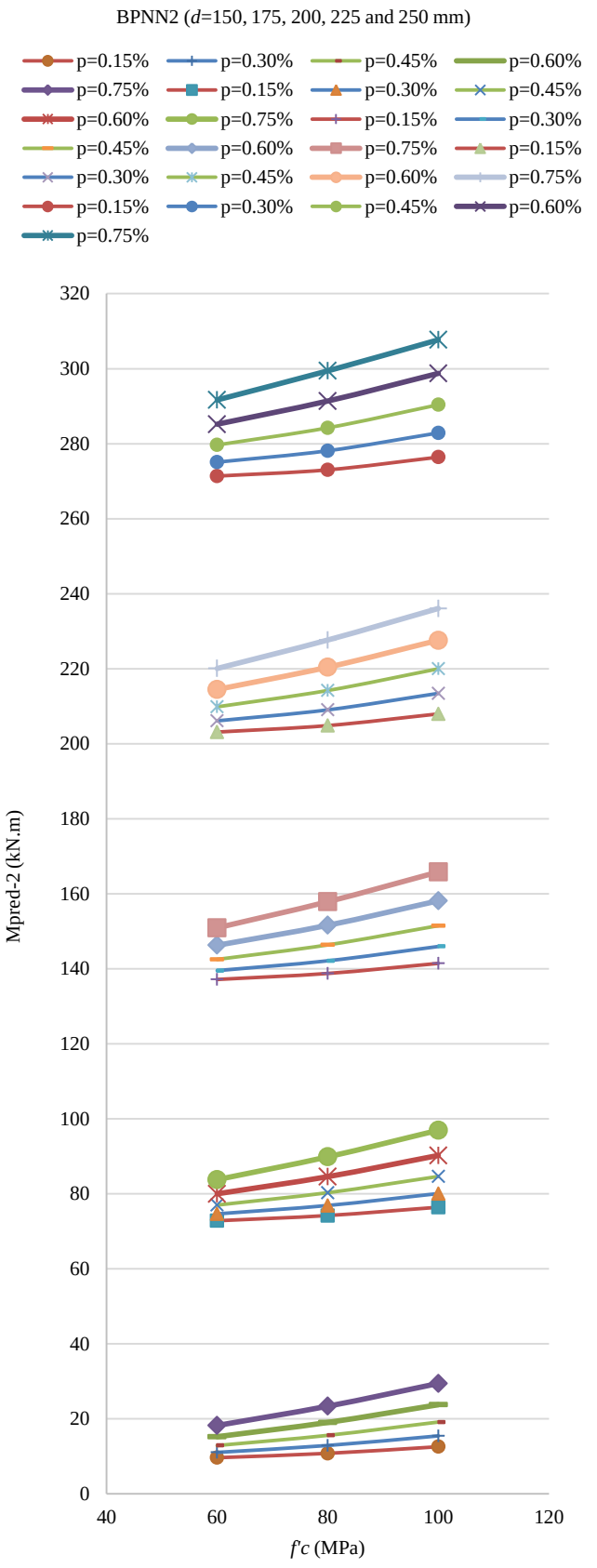

Fig. 7. Variation of the ultimate moment capacity with the cylindrical concrete compressive strength and the reinforcement ratios.

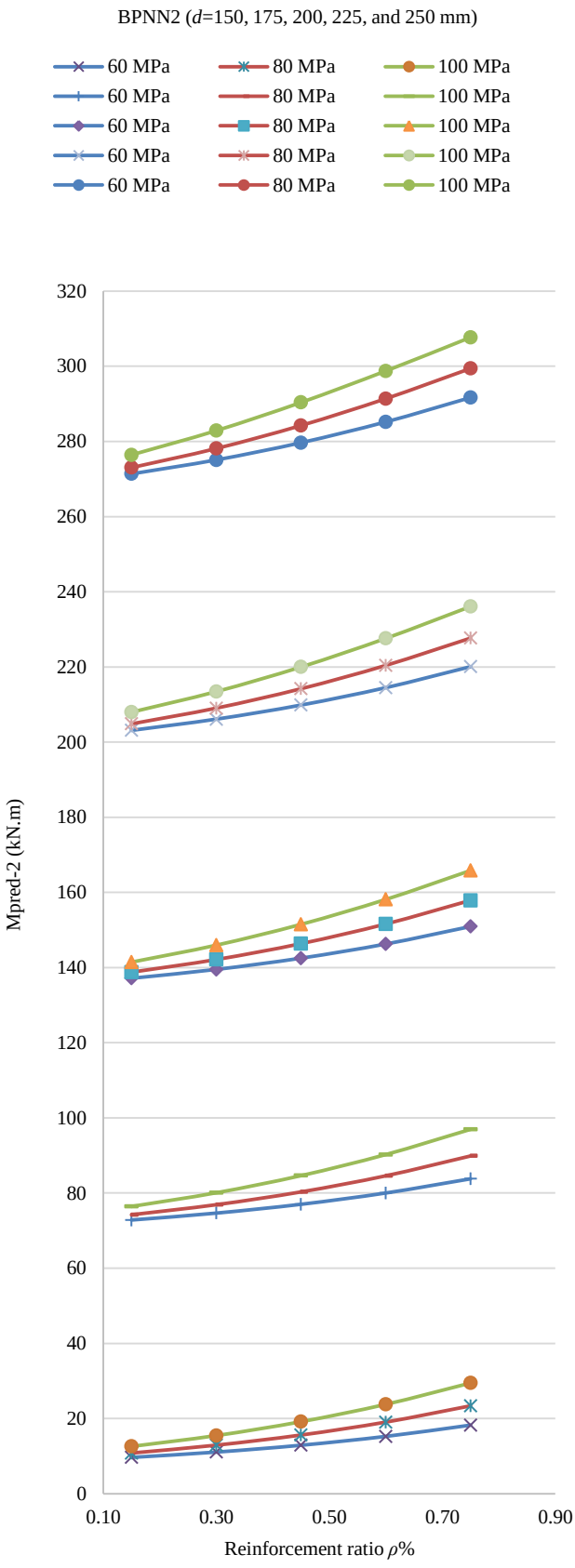

Fig. 8. Variation of the ultimate moment capacity with the reinforcement ratio and the cylindrical concrete compressive strengths.

Influence of Effective Depth

Fig. 9 shows the BPNN2(5-5-3-1) neural network relationship between the effective depth and the predicted moment capacity for beams having cylindrical concrete strengths 60 MPa, 80 MPa and 100 MPa respectively. Five curves are drawn representing the different reinforcement ratios (0.25%, 0.50%, 0.75%, 1.00% and 1.25%). The moment capacity of beams is increased by increasing the effective depth with respect to the different reinforcement ratios.

As shown in Fig. 9, the rate of increasing in moment capacity is higher in beams with greater effective depth (i.e. the slope of all curves being steeper when the effective depth of beams increased).

Influence of Compression Strength of Concrete

Fig. 10 shows the relationship between the cylindrical compressive strength of concrete and the predicted moment capacity of the beams. The relationships are created by fixing effective depth to 150 mm, 175 mm, 200 mm, 225 mm and 250 mm. Five curves are drawn for different reinforcement ratios (0.25%, 0.50%, 0.75%, 1.00% and 1.25%). By increasing the cylindrical compression strength, the sectional moment capacity will increase.

The rate of increase of the moment capacity when the concrete cylindrical compressive strength increased from 80 MPa to 100 MPa is greater than the rate of increase in the moment while the concrete compression strength increased from 60 MPa to 80 MPa (i.e., the slope of the curves increases with an increase in the cylindrical compression strength of concrete. The increase in the moment capacity caused by increasing in reinforcement ratio is higher at 100 MPa concretes if compared with 60 MPa concrete compressive strengths.

Influence of Reinforcement Ratio

Reinforcement ratio is one of the parameters that affecting the moment capability of a beams. Fig. 11 shows the BPNN2(5-5-3-1) neural network relationship between the reinforcement ratios and moment capacity of the beam for different concrete compressive strengths (60 MPa, 80 MPa and 100 MPa). In these relationships the ultimate tensile strength of the bars is already fixed to 1000 MPa (glass bar tensile strength), while the effective depth are 150 mm, 175 mm, 200 mm, 225 mm and 250 mm. Increasing the reinforcement ratio caused an increase in the moment capacity of beams with respect to the different concrete compression strengths.

After looking to the relationships in Fig. 11, it shows that the slope of all curves being steeper when the reinforcement ratios of a beams increased. This means that the rate of increasing moment capacity is higher for beams having greater reinforcement ratios. The amount of increasing in moment capacity obtained by increasing the concrete compressive strength at the reinforcement ratio 1.25% is greater than that obtained while the reinforcement ratio is 0.25% (i.e. Higher amount of moment capacity obtained by increasing the concrete compressive strengths at high level of reinforcement ratios while smaller amount obtained by increasing the concrete strengths at small level of reinforcement ratios).

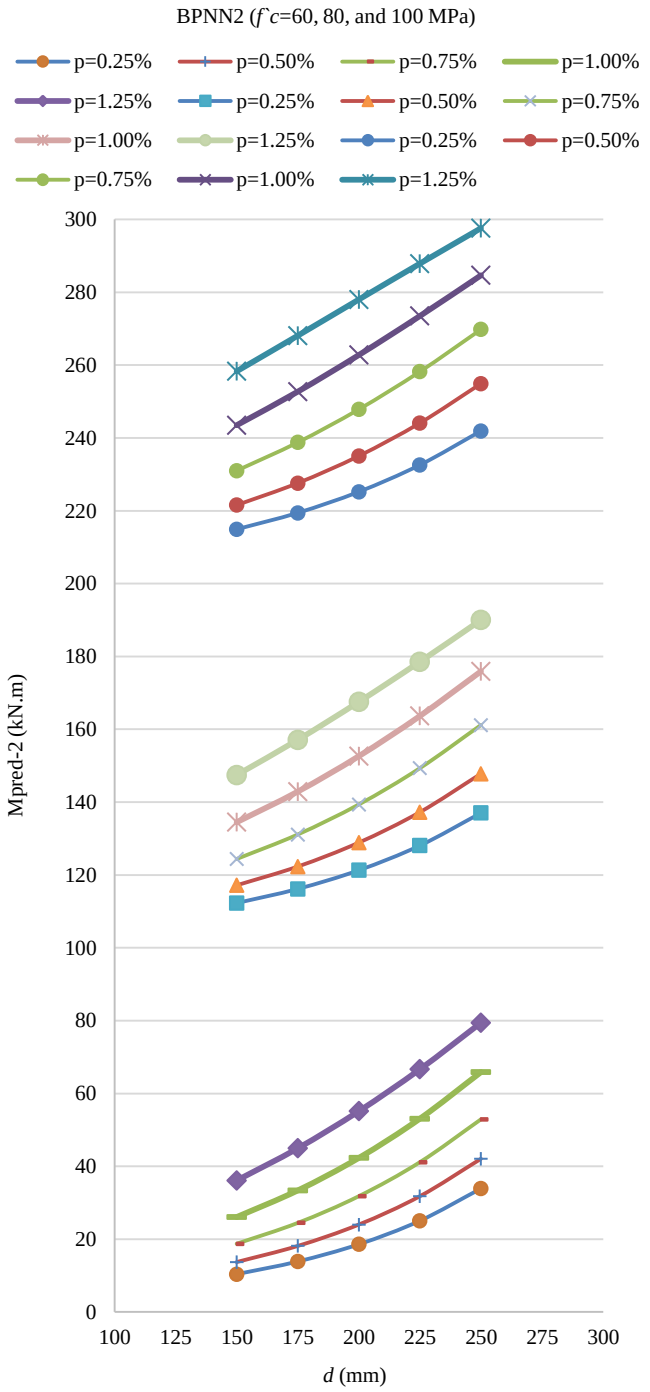

Fig. 9. Variation of the ultimate moment capacity with effective depth and reinforcement ratios.

VI. Conclusion

It is concluded that using a neural network model is successful in modeling the flexural behavior of beams reinforced with fiber reinforced polymer (FRP) bars.

http://dx.doi.org/10.14500/aro.10066

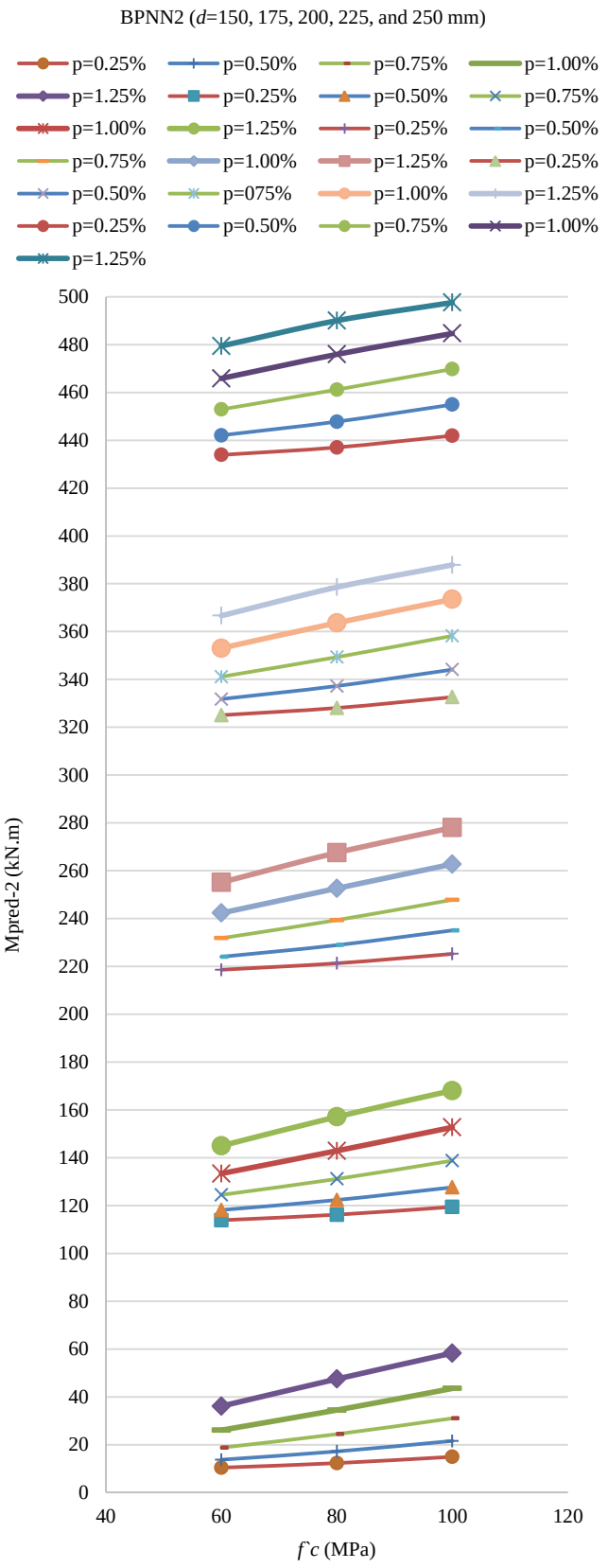

Fig. 10. Variation of the ultimate moment capacity with the cylindrical concrete compressive strength and the reinforcement ratios.

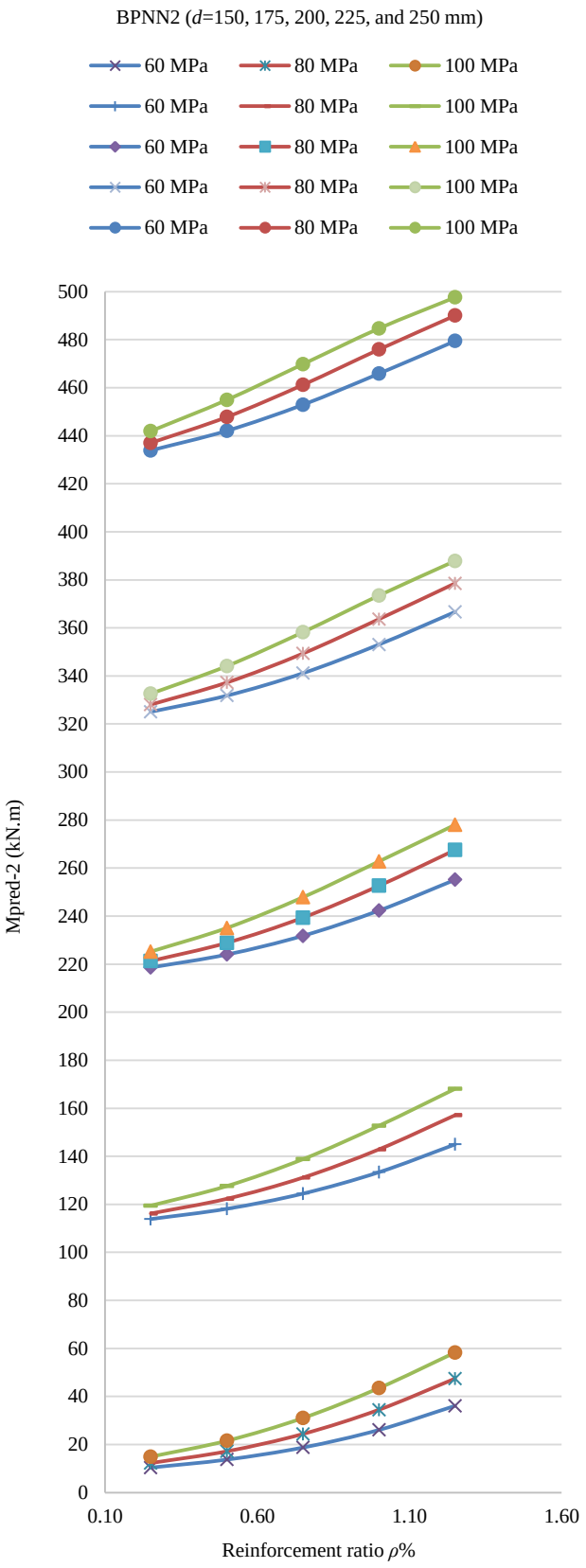

Fig. 11. Variation of the ultimate moment capacity with the reinforcement ratio and the cylindrical concrete compressive strengths.

The neural network with two hidden layers was more successful than the neural network with a single hidden layer in modeling the flexural behavior of beams reinforced with FRP bars which is evidence on the complex and high non-linearity of the relationships among influenced factors. The sigmoid transfer functions used in the hidden layers are acted successfully in the modeling process. Effective depth (*d*) has the largest effect among all other factors on the moment capacity of the beam, while width (*b*) has the least effect on the moment capacity of the beams. For data with high non-linearity such as reinforced concrete data "gradient descent with momentum" is a suitable back-propagation algorithm. The parametric study showed that the rate of increase in moment capacity of beams for higher levels of high strength concrete is much higher than the rate of increase in moment capacity of lower levels of high strength concrete beams.

APPENDIX A

SAMPLES COLLECTED FROM DIFFERENT SOURCES

No.	Beam notation	Source	b (mm)	d (mm)	f'c (MPa)	fu (MPa)	ρ%	Mexp (KN.m)
1	ISO2	(Benmokta ne, et al., 1995)	200	259.00	43.00	690	1.10	80.40
2	ISO3		200	509.00	43.00	690	0.56	181.70
3	ISO4		200	509.00	43.00	690	0.56	181.70
4	CB2B-1	(Masmoudi, et al., 1998)	200	252.55	52.00	773	0.56	57.90
5	CB2B-2		200	252.55	52.00	773	0.56	59.80
6	CB3B-1		200	252.55	52.00	773	0.91	66.00
7	CB3B-2		200	252.55	52.00	773	0.91	64.80
8	CB4B-1		200	207.65	45.00	773	1.38	75.40
9	CB4B-2		200	207.65	45.00	773	1.38	71.70
10	CB6B-1		200	207.65	45.00	773	2.15	84.80
11	CB6B-2		200	207.65	45.00	773	2.15	85.40
12	GB1-1	(Toutanji and Saafi, 2000)	180	268.00	35.00	695	0.52	60.00
13	GB1-2		180	268.00	35.00	695	0.52	59.00
14	GB2-1		180	268.00	35.00	695	0.79	65.00
15	GB2-2		180	268.00	35.00	695	0.79	64.30
16	GB3-1		180	255.00	35.00	695	1.10	71.00
17	GB3-2		180	255.00	35.00	695	1.10	70.50
18	GB5	(Duranovic et al., 1997)	150	210.00	24.96	1000	1.31	40.31
19	GB9		150	210.00	31.84	1000	1.31	39.73
20	GB10		150	210.00	31.84	1000	1.31	39.50
21	GB13		150	210.00	34.72	1000	0.87	34.75
22	C-212-D1	(Barris, et al., 2009)	140	163.40	59.80	1000	0.99	36.90
23	C-216-D1		140	163.40	56.30	1000	1.78	44.04
24	C-316-D1		140	163.40	55.20	1000	2.67	50.16
25	C-212-D2		160	142.50	39.60	1000	0.99	26.61
26	C-216-D2		160	140.60	61.70	1000	1.78	41.31
27	C-316-D2		160	140.60	60.10	1000	2.67	45.18
28	NCF1	(Chitsazan, et al., 2010)	130	200.00	41.40	690	0.49	33.60
29	NCF2		100	170.00	41.40	690	0.75	23.99
30	NCF3		90	190.00	41.40	690	0.74	22.94
31	NCF4		80	160.00	41.40	690	0.99	17.16
32	NCF5		130	200.00	73.90	690	0.49	25.52
33	NCF6		100	170.00	73.90	690	0.75	21.67
34	NCF7		90	190.00	41.40	690	0.74	26.19
35	NCF8		80	160.00	41.40	690	0.99	18.09
36	BG1a	(Al-Sunna, 2006)	150	220.24	40.55	665	0.43	17.30
37	BG1b		150	220.24	40.55	665	0.43	17.10
38	BG2a		150	218.65	40.55	620	0.77	30.95
39	BG2b		150	218.65	40.55	620	0.77	29.84
40	BG3a		150	171.43	39.53	670	3.93	42.99
41	BG3b		150	171.43	39.53	670	3.93	45.02
42	BC1a		150	221.83	47.09	1450	0.29	28.26
43	BC1b		150	221.83	47.09	1450	0.29	29.53
44	BC2a		150	220.24	44.71	1325	0.65	40.19
45	BC2b		150	220.24	44.71	1325	0.65	39.58
46	BC3a		150	218.65	44.03	1475	1.16	47.09
47	BC3b		150	218.65	44.03	1475	1.16	47.78
48	SG1a		500	89.33	43.35	600	0.35	07.76
49	SG1b		500	89.33	43.35	600	0.35	06.83
50	SG2a		500	84.24	39.27	665	0.79	15.11
51	SG2b		500	84.24	39.27	665	0.79	16.88
52	SG3a		500	70.48	39.02	670	3.33	23.48
53	SG3b		500	70.48	39.02	670	3.33	23.78
54	SC1a		500	85.83	42.59	1450	0.28	14.25
55	SC1b		500	83.83	42.59	1450	0.28	14.06
56	SC2a		500	77.24	43.35	1325	0.63	21.11
57	SC2b		500	80.24	43.35	1325	0.63	21.26
58	SC3a		500	71.15	42.33	1475	1.14	22.99
59	SC3b		500	77.65	42.33	1475	1.14	26.70
60	G16L	(Al-Shamaa, 2010)	125	166.00	40.23	655	1.86	23.68
61	G12L		125	168.00	41.94	690	1.19	21.24
62	G10L		125	169.00	42.45	690	0.67	14.52
63	G6L		125	171.00	40.78	867	0.30	07.92
64	G10LH		125	169.00	47.56	690	0.67	15.04
65	G10LS		125	169.00	43.34	690	0.67	14.59
66	G12N		125	168.00	42.73	690	1.19	22.96
67	G10N		125	169.00	44.78	690	0.67	15.24
68	G6N		125	171.00	42.73	867	0.30	08.48
69	B10L		125	169.00	40.23	1127	0.74	15.28
70	B6L		125	171.00	39.56	1029	0.27	09.40
71	B10LH		125	169.00	46.75	1127	0.74	16.16
72	B10LS		125	169.00	41.92	1127	0.74	17.31
73	B10N		125	169.00	43.56	1127	0.74	17.88
74	B6N		125	171.00	40.59	1029	0.27	09.72
75	B1	(Taha, 2013)	100	126.50	62.77	2300	0.15	05.43
76	B2		100	126.50	62.77	2300	0.30	10.96
77	B3		100	126.50	62.77	2300	0.45	14.49
78	B4		100	126.50	84.55	2300	0.15	05.60
79	B5		100	126.50	84.55	2300	0.30	11.80
80	B6		100	126.50	84.55	2300	0.45	17.40
81	B7		100	126.50	97.96	2300	0.30	11.52
82	B8		100	126.50	97.96	2300	0.45	18.41
83	B9		100	116.50	97.96	2300	0.65	19.46
84	B10		100	126.50	63.78	2300	0.15	05.57

85	B11	100	126.50	63.78	2300	0.30	11.90
86	B12	100	126.50	63.78	2300	0.45	13.72
87	B13	100	126.50	86.22	2300	0.15	05.57
88	B14	100	126.50	86.22	2300	0.30	12.29
89	B15	100	126.50	86.22	2300	0.45	18.80
90	B16	100	126.50	100.55	2300	0.30	12.92
91	B17	100	126.50	100.55	2300	0.45	18.24
92	B18	100	116.50	100.55	2300	0.65	19.25
93	B19	100	126.50	64.09	2300	0.15	06.27
94	B20	100	126.50	64.09	2300	0.30	09.21
95	B21	100	126.50	64.09	2300	0.45	10.68
96	B22	100	126.50	86.70	2300	0.15	05.71
97	B23	100	126.50	86.70	2300	0.30	11.80
98	B24	100	126.50	86.70	2300	0.45	14.04
99	B25	100	126.50	100.82	2300	0.30	12.57
100	B26	100	126.50	100.82	2300	0.45	18.48
101	B27	100	116.50	100.82	2300	0.65	19.60

REFERENCES

Al-Shamaa, M.F.K., 2010. *Behaviour of Lightweight Concrete Beams Reinforced with Fibre Reinforced Polymer Bars*, PhD. University of Technology Baghdad, Iraq.

Al-Sunna, R.A.S., 2006. *Deflection Behaviour of FRP Reinforced Concrete Flexural Members*, PhD. University of Sheffield.

Barris, C. et al., 2009. An experimental study of the flexural behaviour of GFRP RC beams and comparison with prediction models. *Composite Structures*, 91, pp.286-95.

Benmoktane, B., Chaallalt, O. and Masmoudi, R., 1995. Flexure Response of Concrete Beams Reinforced with FRP Reinforcing Bars. *ACI Structural Journal*, 9(2), pp.46-55.

Chitsazan, I., Kobraei, M., Jumaat, M.Z. and Shafig, P., 2010. An experimental study on the flexural behavior of FRP RC beams and a comparison of the ultimate moment capacity with ACI. *Civil Engineering and Construction Technology*, 1(2), pp.27-42.

Duranovic, N., Pilakoutas, K. and Waldron, P., 1997. Tests on Concrete Beams Reinforced with Glass Fiber Reinforced Plastic Bars. In *Third International Symposium on Non-metallic (FRP) Reinforcement for Concrete Structures*. Sapporo, Japan, 1997. Japan Concrete Institute.

Hall, M. et al., 2009. The WEKA Data Mining Software: An Update. *SIGKDD Explorations*, 11(1), pp.10-18. Available at: http://www.cs.waikato.ac.nz/~ml/weka/index.html .

Lee, S. and Lee, C., 2014. Prediction of shear strength of FRP-reinforced concrete flexural members without stirrups using artificial neural networks. *Engineering Structures*, 61, pp.99-112.

Leung, C.K.Y., Ng, M.Y.M. and Luk, H.C.Y., 2006. Empirical Approach for Determining Ultimate FRP Strain in FRP-Strengthened Concrete Beams. *Journal of Composites for Construction*, 10(2), pp.125-38.

Mashrei, M.A., Seracino, R. and Rahman, M.S., 2013. Application of artificial neural networks to predict the bond strength of FRP-to-concrete joints. *Journal of Construction and Building Materials*, 40, pp.812-21.

Masmoudi, R., Theriault, M. and Benmokrane, B., 1998. Flexural Behavior of Concrete Beams Reinforced with Deformed Fiber Reinforced Plastic Reinforcing Rods. *ACI Structural Journal*, 96(6), pp.665-76.

Metwally, I.M., 2013. Prediction of Punching Shear Capacities of Two-way Concrete Slabs Reinforced with FRP Bars. *HBRC Journal*, 9, pp.125-33.

Muhammad Ali, P.J., 2014. Predicting the Gender of the Kurdish Writers in Facebook. *Sulaimani Journal for Engineering Sciences*, 1(1), pp.18-28.

Muhammad Ali, P.J., Surameery, N.M.S., Yunis, A.M. and Abulrahman, L.S., 2013. Gender Prediction of Journalists from Writing Style Style. *Aro, the Scientefic Journal of Koya University*, 1(1), pp.22-28. Retrieved from http://dx.doi.org/10.14500/aro.10031.

Perera, R., Tarazona, D., Ruiz, A. and Martín, A., 2014. Application of artificial intelligence techniques to predict the performance of RC beams shear strengthened with NSM FRP rods. Formulation of design equations. *Journal of Composites: Part B*, 66, pp.162-73.

Taha, B.O., 2013. *Flexural Response of High Strength Concrete Beams Reinforced with CFRP Rebars*, PhD. University of Salahadeen, Erbil, Iraq.

Toutanji, H.A. and Saafi, M., 2000. Flexural Behavior of Concrete Beams Reinforced with Glass Fiber-Reinforced Polymer (GFRP) Bars. *ACI Structural Journal*, 97(5), pp.712-19.

Yousif, S.T. and Al-Jurmaa, M.A., 2010. Modeling of ultimate load for R.C. beams strengthened with Carbon FRP using artificial neural networks. *Al-Rafidain Engineering Journal*, 18(6), pp.28-41.

Comparative Study of Terrazzo Tiles Produced in Koya and Erbil, and its Suitability for Construction Purposes

Sarmad F. Abdullah, Sarkawt A. Saeed and Shler S. Qadir

Department of Civil Engineering, Koya University
Danielle Mitterrand Boulevard, Koya KOY45, Kurdistan Region of F.R. Iraq

***Abstract*—Tiles are durable and have a long lifespan. They may be used as a floor finish for both interior and exterior applications. Experimental and field studies were conducted to investigate the parameters and properties of terrazzo tiles from different regions, namely Erbil and Koya being represented by factories (A) and (B) respectively. These parameters and properties are dimensions, water absorption, modulus of rupture and impact resistance. Test results indicate that the dimensions and modulus of rupture for the tiles from both factories (A) and (B) are conformable with Iraqi specifications, but water absorption of terrazzo tiles from factory (B) does not conform with the Iraqi specification and having surface and total absorption values which are 55.1% and 23.8% higher than that for factory (A) tiles, respectively. The results show that terrazzo tiles of factory (A) have an impact resistance value which is 50% higher than that of tiles from factory (B). The field study which includes questionnaire procedure indicates that 63% of the residents agreed that the terrazzo tiles are beautiful as a floor finishing material and at the same time 94% agreed that this material is expensive. This study shows also that only 20% of Koya residents are satisfied with the quality of the production of factory (B), whereas, 90% of Erbil residents are satisfied with the production of factory (A).**

***Index Terms*—Impact resistance, modulus of rupture, terrazzo tiles, water absorption.**

I. Introduction

There are many different types of flooring which make it difficult to know just what type we can select for floor finishing and how to maintain and care for each type of floor. Tiles provide one of the most cost-effective and environmentally friendly flooring choices. Its manufacturing does not necessitate the use of heavy chemicals or other harmful substances used to make other flooring types in forms of ceramic, porcelain, quarry, agglomerate and terrazzo tiles. They are durable and have a long lifespan, may be used as a wall or floor finish for both interior and exterior applications (National Terrazzo and Mosaic Association, 1994).

Tile is rated and placed in one of five grades or groups based on its relative hardness, ability to stand up to wear and percentage of water it will absorb. Group I is for area of light traffic such as a residential bathroom floor. Group II is for most areas inside the home except the kitchen and entry ways. Group III is for anywhere within a home. Group IV is for homes and light to medium commercial areas. Group V is for extra heavy traffic areas and can be used anywhere.

Terrazzo tiles get their name from the Italian word for "terraces" and were created several hundred years ago in Europe when Venetian workers discovered a new use for discarded marble remnants (National Terrazzo and Mosaic Association, 2014). Since that time it has become a logical, practical solution for contemporary design and construction. The beauty and versatility of terrazzo offers today's architects and designers a contemporary flooring and wall material for interior and exterior design use. Fifteenth century Venetian marble workers began to use odd-size marble pieces, remaining from the custom made marble slabs, to surface the terraces around their living quarters. The uneven, rough surfaces created when the spells were set in clay to anchor them, convinced the workers that flattening the surface would produce a smoother surface which is more comfortable for walking. And so they began to rub the surfaces with hand stones achieving a smoother, flat surface (National Terrazzo and Mosaic Association, 2014). The workers soon advanced their technique for rubbing the surfaces by designing a long handle with a weighted end to which they could fasten their rubbing stones. Now they were able to rub the terraces in a more comfortable stand-up position, using their body weight to provide the pressure to abrade the surface faster. With this crude equipment and back-breaking labor they achieved a smoother, flat surface but still lacking the true marble color that only resulted when the surface was wet. Ceramic Institute

ARO, The Scientific Journal of Koya University
Volume III, No 2(2015), Article ID: ARO.10053, 07 pages
DOI: 10.14500/aro.10053
Received 16 September 2014; Accepted 22 April 2015
Regular research paper: Published 03 September 2015
Corresponding author's e-mail: sarkawt.saeed@koyauniversity.org

 http://dx.doi.org/10.14500/aro.10053

of America mentioned that the first president, George Washington, selected terrazzo floors for many of his important rooms. Soon American terrazzo was created from the wealth of marble in the United States, and American ingenuity advanced installation techniques. This made terrazzo materials available for all concepts of construction. Terrazzo has proven itself throughout history as the sensible choice for floor surfaces that require resistance to heavy abuse, while still retaining beauty and low maintenance costs. (Karam and Tabbara, 2009) specify that the material is a composite of natural marble chippings set in a matrix of cement with a color pigment added to it. The range of aggregates in size and color is vast and they can be set into practically any color cement to create an endless number of finishes. Once laid, the terrazzo is ground down and polished to expose the aggregate. A minor disadvantage of using terrazzo tiles is that after the initial heavy polishing at the time the tiles are laid it is essential to polish the tiles from time to time. This is necessary to maintain the shine and appearance of the floors.

II. Experimental Program

Experimental studies and field works are made to study the method of manufacturing and properties of terrazzo tiles from different regions "Erbil (factory A) and Koya (factory B)". The properties and parameters of the tiles were measured and recorded for each factory according to Iraqi specification (No.1042, 1984) including dimensions, surface water absorption, total water absorption and rupture strength. In addition to these properties the impact property for tiles was studied. The field work including questionnaire procedure for 50 houses in both regions made to study the usage of terrazzo tiles as finishing materials for floors, this study contains different opinions about the terrazzo tiles including peeling off, erosion, beauty, cost and others.

A. Manufacturing and Curing of Terrazzo Tiles

Square terrazzo tiles, of sizes 400×400×30 mm^3 and 300×300×30 mm^3 (length × width × thickness), where manufactured at local factories (A) in Erbil and (B) in Koya. The manufacturing process in factory (A) was accomplished with a good quality control according to the general of Iraqi Specification (No.1042,1984) casted in tempered steel moulds consisting of two layers: a 15 mm thick white hydraulic cement layer enclosing marble chips which were brought from Permam and Sulaimani then vibration was applied to the extent that it allows the trapped air to get out from the surface then a 15 mm thick regular gray hydraulic Portland cement mortar backing then maintaining a standard pressure of 150 bar to get sufficient merging of the two layers as shown in Fig. 1. Grain size distribution of the marble chips, marble powder filler, and aggregates for the mortar backing were all selected according to Iraqi specification recommendations. Finally a careful polishing process eliminates a 3 mm upper layer and reveals the beauty of the marble chips mixed in colored cement. On the other hand, the manufacturing process at factory (B) was accomplished without any quality control casted in steel moulds consisting of two layers: a 15 mm thick white hydraulic cement layer enclosing marble chips brought from Gorashin then vibration was applied to allow the trapped air to get out from the surface then a 15 mm thick regular gray hydraulic Portland cement mortar backing followed by maintaining a standard pressure of 100-200 bar to get sufficient merging of the two layers as shown in Fig. 2. Finally a careful polishing process eliminates a 3 mm upper layer and reveals the beauty of the marble chips mixed in colored cement.

B. Curing

Factory (A) followed two methods for curing of terrazzo tiles:

1) Putting the tiles in a vapor room for six hours then taking them out into sunlight for 2 hours.
2) Putting the tiles in clean water for 1-2 weeks (which is close to the method recommended by Iraqi specifications).

But tiles in factory (B) were cured by putting them in water containing impurities for 4-days only.

C. Test Technique

Dimensions and Shape

The dimension and shape were determined according to Iraqi specification (No.1042, 1984) using 400×400×30 mm terrazzo tiles at the age of 28 days. The dimensions determined by using simple measuring devices like steel ruler, angles and T-square in order to check the sides, edges of the tile and the accuracy of the angles in addition to the thickness of surface layer and thickness of terrazzo tile. The average values of three samples were recorded.

Fig. 1. Manufacturing machine for terrazzo tile in factory (A).

Fig. 2. Manufacturing machine for terrazzo tiles in factory (B).

Water Absorption

Water absorption includes:

1) Face Absorption

The face absorption test was determined according to Iraqi specification (No.1042, 1984) using 300×300×30 mm terrazzo tiles at the age of 28-days. In this test the samples were dried for 8 hours by placing them in oven at temperature of (100±5)°C then cooled for 24 hours at laboratory temperature then recording the weight which will be the dry weight. After that, tile is immersed on its face in water for 24 hours with attention that the height of water is 5 mm from the thickness of the sample and the tile should not be totally immersed in water. Then the sample is taken out from water and the surface is dried with a dry cloth and the weight is recorded which will be the wet weight. The face absorption is calculated by:

$$Face\ \ Absorption = \frac{B - A}{Surface\ \ area} \quad (1)$$

Where:-

A = Dry weight of the sample (gm).

B = Wet weight of the sample (gm).

2) Total Absorption

The total absorption was determined according to Iraqi specification (No.1042, 1984) using (300×300×30) mm terrazzo tiles at the age of 28-days. In this test the samples were dried for 8 hours by placing them in oven at a temperature of (100±5)°C then cooled for 24 hours at laboratory temperature after which the weight is recorded which will be the dry weight (A). After immersing the tile in water for 24 hours with attention that the tile should be totally immersed in water, the sample was taken out from water and dried with a dry cloth, then the weight was recorded which will be the wet weight (B). The total absorption is calculated, by:

$$Total\ \ Absorption = \frac{B - A}{A} \times 100 \quad (2)$$

Modulus of Rupture (M.O.R)

Modulus of rupture value was determined according to Iraqi specification (No.1042, 1984) and carried out using (300×300×30) mm terrazzo tiles simply supported with clear span of 200 mm at the age of 28 days. This test was carried out by placing the tile on the two supports of testing apparatus in symmetrical way, applying a continuous load until a homogeneous fracture happened, then recording the load that causes total failure of the tile. The Modulus of Rupture is calculated by:

$$M.O.R = \frac{3PL}{2bd^2} \quad (3)$$

Where;

$M.O.R$ = Modulus of rupture (MPa).

P = Load at failure (N).

L = Clear loaded span (mm).

b = Width of the tile (mm).

d = Thickness of the tile (mm).

Impact Resistance Test

The impact resistance value can be measured by a test method that is simple and easy to carry out and has been developed by ACI committee 54, (1986) which recommends the use of repeated impact drop weight test to estimate this important property since there is no recognized standard test to assess the impact resistance of tiles. In this research a simple repeated drop-weight of 1.25 Kg used to fall down from 1 meter height on (400×400×30) mm terrazzo tiles through a tube of circular section with diameter of 3 inches which acts as a drop weight guide and held vertically above the center of the tile as shown in Fig. 3.

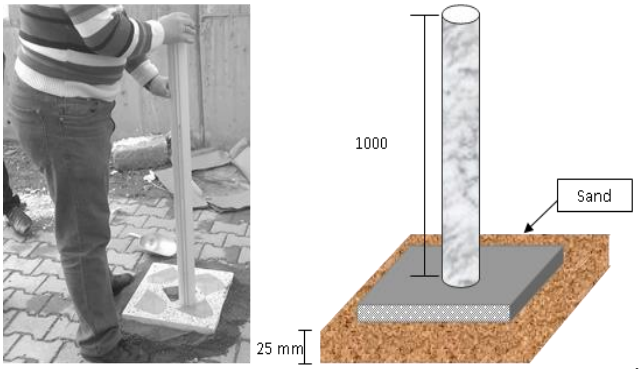

Fig. 3. The impact resistance test.

Questionnaires Procedure

Questionnaire procedure is another field study which was made for different 50 houses in both regions to study the usage of terrazzo tiles as finishing materials for floors. This study contains different opinions about the terrazzo tiles which were derived from the residents occupying these houses, including peeling off, erosion of face layer, beauty, cost and others.

III. Results and Discussion

A. Manufacturing and Curing of Terrazzo tile

From the field vision in both factories the following results can be obtained:-

1) Marble chips used to make a terrazzo tiles in factory (A) were washed and stored into four silos classified according to the size as shown in Fig. 4-a, while the chips used to make the tiles in factory (B) were stored in an open area and used without washing or cleaning as shown in Fig. 4-b.
2) Mix proportion of base layer in both factories was 1:4 (cement: sand) which is not adequate to the standard Iraqi specification (No.1042, 1984) which recommended that the mix proportion should be 1:3 or 1:3.5.
3) Pressing pressure in factory (B) was estimated by workers between (100-200) bars while in factory (A) it was

http://dx.doi.org/10.14500/aro.10053

controlled at 150 bars.

4) Terrazzo tiles in factory (A) were made by automatically operating machine with a good quality control and they used binders for surface (face) layer while that for factory (B) the mixture was made on the floor then poured into the mould manually by hand, as shown in Fig. 2, without binders used in face layer.
5) Production of factory (A) is (3000) tiles/day which is 233.33% higher than that of factory (B) (900) tiles/day due to using of multi moulds machine for making tiles as shown in Fig. 1.
6) Curing tiles in factory (B) is not confirmable with the Iraqi specification (No. 1042, 1984) which recommended curing the tiles in a humid condition for 9 days; 2 days in clean water then sprinkling the tiles with water for 7 days.

(a) (b)

Fig. 4. Marble chips storing; (a) In factory (A) and (b) In factory (B).

B. *Dimensions and Shape*

The average dimensions of six terrazzo tiles from factories (A) and (B) are shown in the Table I. These dimensions confirm to the Iraqi specification article (No.6, 1984) which allow tolerance (± 1mm) in length and (±3mm) in thickness after polishing and grounding. The tiles from factory (A) were polished and grounded better than tiles from factory (B) with surface clean from cracks and flaws and homogeneity distribution of marble chips, both group of tiles (factories A and B) are square in shape with vertical edges these properties confirming with the Iraqi specification article (No.7 , 1984).

TABLE I
DIMENSIONS OF THE TERRAZZO TILES

Source of Terrazzo tiles	Erbil (Factory A)			Koya (factory B)		
Dimensions (mm)	*l*	*w*	*t*	*l*	*w*	*t*
	399	399	29.1	399	399	29.8
Iraqi specification (400×400×300 mm^3)	±1	±1	±3	±1	±1	±3
	Conformable			Conformable		

l is the length, w *is the width and t is the thickness*

C. *Water absorption*

Surface Absorption

The surface absorption results of six samples which were taken from factory (A) and other six samples from factory (B) are presented in Table II and Fig. 5. From these results, it is indicated that the surface absorption of factory (B) terrazzo tiles is 55.1% higher than surface absorption of factory (A) terrazzo tiles: This can be attributed to high absorption of the marble chips used in face layer of terrazzo tiles and insufficient compaction of the face layer. It is noticed that the surface absorption of factory (B) terrazzo tiles is not conformable with the Iraqi specification (No.1042 article No.9-1-1, 1984) which recommends that the surface absorption should not exceed 0.4 gm/cm^2.

TABLE II
SURFACE ABSORPTION OF THE TERRAZZO TILES

Source of Terrazzo tiles	Erbil (Factory A)	Koya (Factory B)
Surface Absorption (gm/cm^2)	0.22	0.49
Iraqi specification (Not exceed 0.4 gm/cm^2)	Conformable	Not Conformable

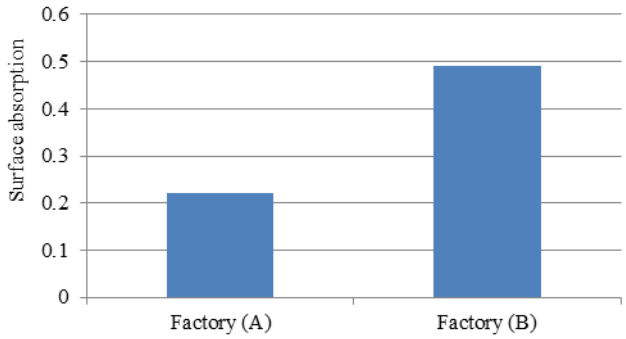

Fig. 5. Surface absorption (gm/cm^2) of the terrazzo tiles in factories (A) and (B).

Total Absorption

The total absorption values of six samples which were taken from factory (A) and another six samples from factory (B) are presented in Table III and Fig. 6. These values indicate that total absorption of factory (B) terrazzo tiles is 23.8% higher than total absorption of factory (A) terrazzo tiles; this is due to high voids content in the mixture as a result of insufficient vibration applied during the production. It is noticed that the total absorption of factory (B) terrazzo tiles is not conformable with the Iraqi specification (No.1042 article No.9-1-2, 1984), which recommends that the total absorption should not exceed 8%.

TABLE III
TOTAL ABSORPTION OF THE TERRAZZO TILES

Source of Terrazzo tiles	Erbil (Factory A)	Koya (factory B)
Total Absorption%	8	10.5
Iraqi specification (Not exceed 8%)	Conformable	Not CONFORMABLE

D. *Modulus of Rupture (M.O.R.)*

The modulus of rupture results of six samples which were taken from factory (A) and other six samples from factory (B)

are presented in Table IV and Fig. 7. From these results, it is indicated that the modulus of rupture for both factories (A) and (B) terrazzo tiles are conformable with the Iraqi specification (No.1042 article No.9-2, 1984) which recommends that the modulus of rupture of terrazzo tiles should not be less than 3 N/mm^2. It also indicates that the modulus of rupture for factory (A) tiles is 1.72% higher than that for factory (B). This is due to controlled pressing pressure applied during manufacture.

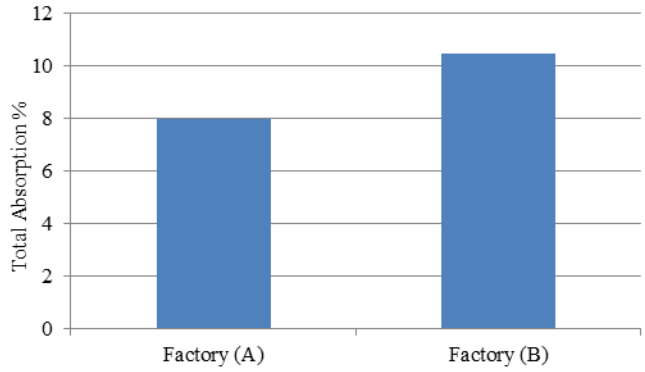

Fig. 6. Total absorption of the terrazzo tiles.

TABLE IV
MODULUS OF RUPTURE OF THE TERRAZZO TILES

Source of Terrazzo tiles	Erbil (Factory A)	Koya (factory B)
Modulus of rupture (N/mm^2)	5.23	5.14
Iraqi specification (Not less than 3 N/mm^2)	Conformable	Conformable

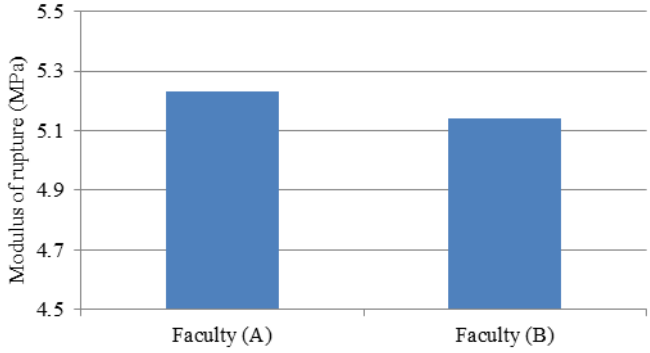

Fig. 7. Modulus of rupture of the terrazzo tiles.

E. Impact resistance

The impact resistance results of six samples which were taken from factory (A) and other six samples from factory (B) are presented in Table V and plotted in Fig. 8. From these results, it can be recognized that the impact resistance for factory (A) tiles is twice higher than that for factory (B) terrazzo tiles. This can be attributed to sufficient pressing pressure being applied during manufacturing. The important visual observation which can be drawn from Figs. 9 and 10 is the symmetrical failure of factory (A) tiles compared with a non-uniform failure of factory (B) tiles and the marble chips of the face layer in factory (B) tiles split from the surface at the line of failure compared with factory (A) tiles. This can be attributed to the bad bond between the materials (cement and marbles) due to insufficient pressing used in the manufacturing which was selected by workers.

TABLE V
IMPACT RESISTANCE OF THE TERRAZZO TILES

Source of Terrazzo tiles	Erbil (Factory A)	Koya (factory B)
Impact resistance (No. of blows)	6	3

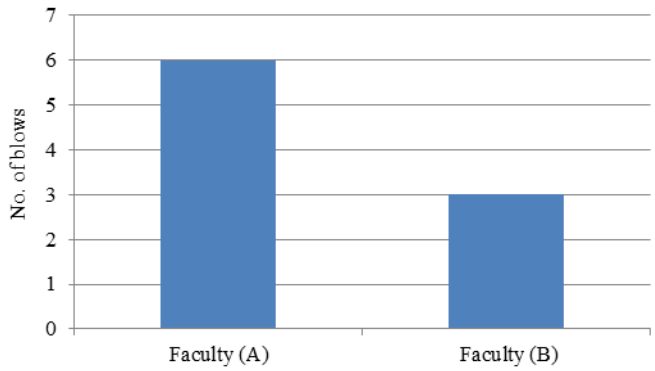

Fig. 8. Impact resistance (No. of blows) of the terrazzo tiles.

Fig. 9. Splitting failure of terrazzo tiles of factory (A).

Fig. 10. Splitting failure of terrazzo tiles of factory (B).

F. Questionnaire Procedure

The questionnaire procedure is another field study which was made for different 50 houses in both regions to study the usage of terrazzo tiles as finishing materials for floors. This

http://dx.doi.org/10.14500/aro.10053

study includes different opinions about the types of flooring (ceramic, granite, porcelain and terrazzo tiles), and which one the residents preferred. The reasons behind using of terrazzo tiles in flooring were also discussed in this study which was derived from the opinion of the residents occupying these houses, including beauty, peeling off, erosion, cost and others.

Table VI and Fig. 11 show that the terrazzo tiles have a high usage percentage as a flooring finish material compared with other types. 63% of the participants in both regions, Erbil and Koya agreed that the terrazzo tiles are beautiful and 94% have agreed that this type of flooring is expensive, as shown in Table VII and Fig. 12.

TABLE VI
PERCENTAGE OF USAGE FOR THE DIFFERENT TYPES OF FLOORING

Flooring types	Granite	Ceramic	Porcelain	Terrazzo Tiles
(%) preferring to use this type in both Erbil and Koya	4.66	27.48	6.66	61.2

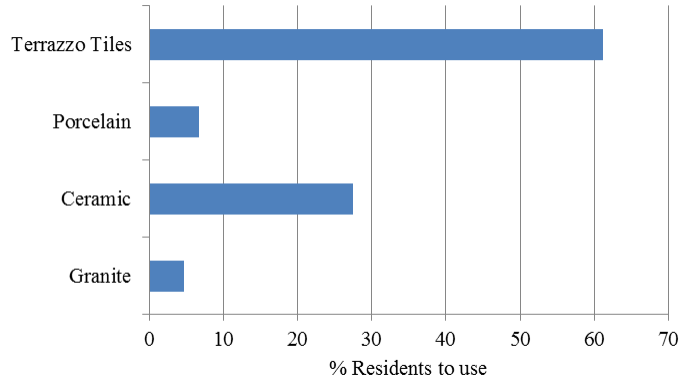

Fig. 11. Percentage of usage for the different types of flooring.

TABLE VII
PERCENTAGE OF RESIDENT'S OPINIONS ABOUT PROPERTIES OF THE TERRAZZO TILES

Property	Beauty	Peeling off	Erosion	Cost
Residents' opinion (%) (Erbil & Koya)	63	52	50	94 (expensive)

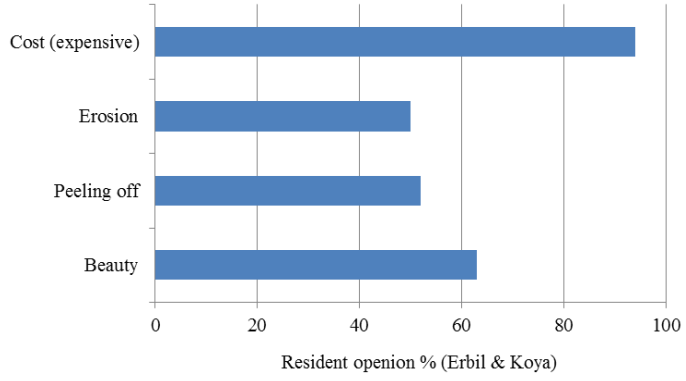

Fig. 12. Percentage of residents' opinion about the properties of the terrazzo tiles.

Table VIII and Fig. 13 show that 20% of the participants in Koya are satisfied with the type of terrazzo tiles used, while about 90% of those from Erbil show satisfaction with the same floor finishing material. This can be attributed to the manufacturing and properties of factory (B) terrazzo tiles.

TABLE VIII
PERCENTAGE OF RESIDENTS' SATISFACTION WITH THE TERRAZZO TILES

Property	Erbil	Koya
Satisfaction (%)	89.33	20

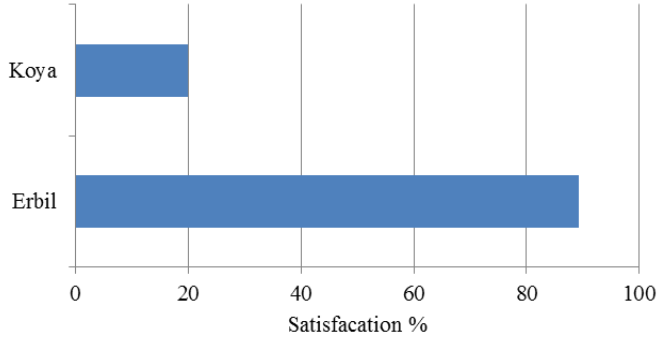

Fig. 13. Percentage of residents' satisfaction with the terrazzo tiles.

IV. CONCLUSION

The following conclusions can be drawn from this study:-

1) Factory A produced tiles according to Iraqi specification requirements and has better production than factory B.
2) Both factories did not achieve the Iraqi specification (No. 1042, 1984) related to the base layer.
3) Surface absorption of factory (B) terrazzo tiles is 55% higher than factory (A) terrazzo tiles and did not conform with the Iraqi specifications (No. 1042, 1984).
4) Total absorption of factory (B) tiles is 23.8% higher than factory (A) terrazzo tiles and did not conform with the Iraqi specifications.
5) Modulus of rupture of terrazzo tiles from both regions (Erbil and Koya) are confirm with Iraqi specifications (No. 1042, 1984).
6) Impact resistance of factory (A) terrazzo tiles is twice higher than factory (B) tiles with a symmetrical failure.
7) Terrazzo tiles have a higher percentage (61.2%) for being used as a floor finishing material compared with granite, ceramic and porcelain, based on questionnaire results in Koya and Erbil.
8) The residents' questionnaire procedure has indicated that only 20% of the participants in Koya show their satisfaction with the type of terrazzo tiles they used while about 90% of those from Erbil show satisfaction with the same floor finishing type.

V. Recommendations

According to the experimental work in this investigation, the following is recommended:

1) Marble chips used for making the face layer of terrazzo tiles should be tested for water absorption and washed by clean water before using them in the manufacturing of terrazzo tiles.
2) The manufacturing components of terrazzo tiles should be automatically mixed and poured with sufficient vibration for both surface and base layers.
3) Pressing pressure should be sufficient to obtain tiles with good properties and without splitting of marble chips from the face layer.
4) Erosion percentage and mechanical properties of the tiles should be tested.

References

ACI Committee 54, 1986. State-of-the art report on fiber reinforced concrete. Report No.544.IR-82.

Ceramic Institute of America, 1996. *Tile types uses & standards*. CTIOA report 83-1-1.

Karam, G., Tabbara, M., 2009. Properties of pre-cast terrazzo tiles and recommended specifications. *Cerâmica Journal*, 55(333), pp.84-87.

Iraqi specification, 1984. *Standard test methods for terrazzo tiles. No.1042:1984.*

Terrazzo Ideas and Design Guide. 1994. *National Terrazzo and Mosaic Association*. [online] Available at: <http://www.ntma.com > [Accessed 9 May 2014].

A brief history of terrazzo, 2014. *National Terrazzo and Mosaic Association*. [online] Available at: <http://www.ntma.com> [Accessed 12 April 2014].

Discover Different Flooring Options for Your Home, 2015. *Ultimate Flooring Company*. [online] Available at: <http://www.ultimateflooringco.com/types-of-flooring.php > [Accessed 10 April 2014].

 http://dx.doi.org/10.14500/aro.10068

The Suitability of Limestone from Pilaspi Formation (Middle-Late Eocene) for Building Stone in Koya Area, NE Iraq

Hemn M. Omar and Nawzat R. Ismail

Department of Geotechnical Engineering, Faculty of Engineering, Koya University
Daniel Mitterrand Boulevard, Koya KOY45, Kurdistan Region of F.R. Iraq

***Abstract*—Suitability of limestone rocks has a crucial importance when stones are used for constructing modern structure. The purpose of this study is to clarify the links between physical, mechanical properties of limestone rocks, also their quality to use as building materials. A total of six limestone rock samples were collected from three different outcrops locations within Pilaspi Formation in Koya area. Engineering geological and geotechnical properties of the limestone rocks in the study area were determined based on the field studies and laboratory tests. The field studies included observations/ measurements of rock mass characteristics such as color, grain size, orientation, bedding thickness and weathering state of the rock materials also spacing, persistence, roughness and infilling material of the discontinuities. Laboratory tests were carried out for determining water content, water absorption, density, uniaxial compressive strength, slake durability and porosity of the rock materials. The study results go well with the national and international standards (Iraqi Standards, 1989; American Society for Testing and Materials, 2004; International Society for Rock Mechanics, 1981) and have shown that the limestone rocks are acceptable for building stone.**

***Index Terms*—Building materials, limestone, physical properties, Pilaspi formation, slake durability.**

I. Introduction

Limestone is one of the most common rock types in the world and is widely exploited for use in construction materials and other engineering works. Because of its range of properties and a good quality, it is easily adapted to use in a variety of structural and architectural application. There are other reasons to choose an advocate of these rocks for study, according to, first, the high prevalence and thickness of these rocks in large areas of Iraq particularity in the Kurdistan region, whether that is as the outcrops or subsurface rocks, second, the rocks of limestone of significant economic importance in engineering industries in terms of quality and quantity values, third, the result of this study becomes of importance not only to the study site, but vast areas of Kurdistan province. These have been done to prepare a study on the physical and mechanical properties of these rocks. Some studies were carried out on the same purpose, (Dhaher, 2009) examined the physical and geochemical properties of some rock units of Pilaspi Formation in Shaqlawa area, and he concluded that the rocks are durable and strong enough to be used as engineering purposes. Saleh (2012) used several samples were taken from different limestone quarries located in Nineveh governorate (NW Iraq), the results have led to widely used in decoration, covering of the outer walls as well as concrete aggregate. The results confirm the suitability of some limestone samples for using as a building stone. This research programmed concerned with the selection of three different outcrops location of limestone within Pilaspi Formation in Koya area in order to point out the different parameters which are links with field studies and laboratory tests to evaluate the suitability of limestone for construction purposes. The locations of studied samples are bounded by UTM grid 3994000 and 3997000 North, (38) 464000 and (38) 469000 East, as shown in (Fig. 1 and Table I).

TABLE I
LOCATIONS OF THE STUDIED LIMESTONE SAMPLES

Location No.	Formation	Coordinates (North and East lines)
1	Pilaspi	3996333 N and (38) 498267 E
2	Pilaspi	3994233 N and (38) 470067 E
3	Pilaspi	3995333 N and (38) 464466 E

ARO, The Scientific Journal of Koya University
Volume III, No 2(2015), Article ID: ARO.10068, 06 pages
DOI: 10.14500/aro.10068
Received 08 January 2015; Accepted 10 August 2015
Regular research paper: Published 11 September 2015
Corresponding author's e-mail: hemn.omar@koyauniversity.org

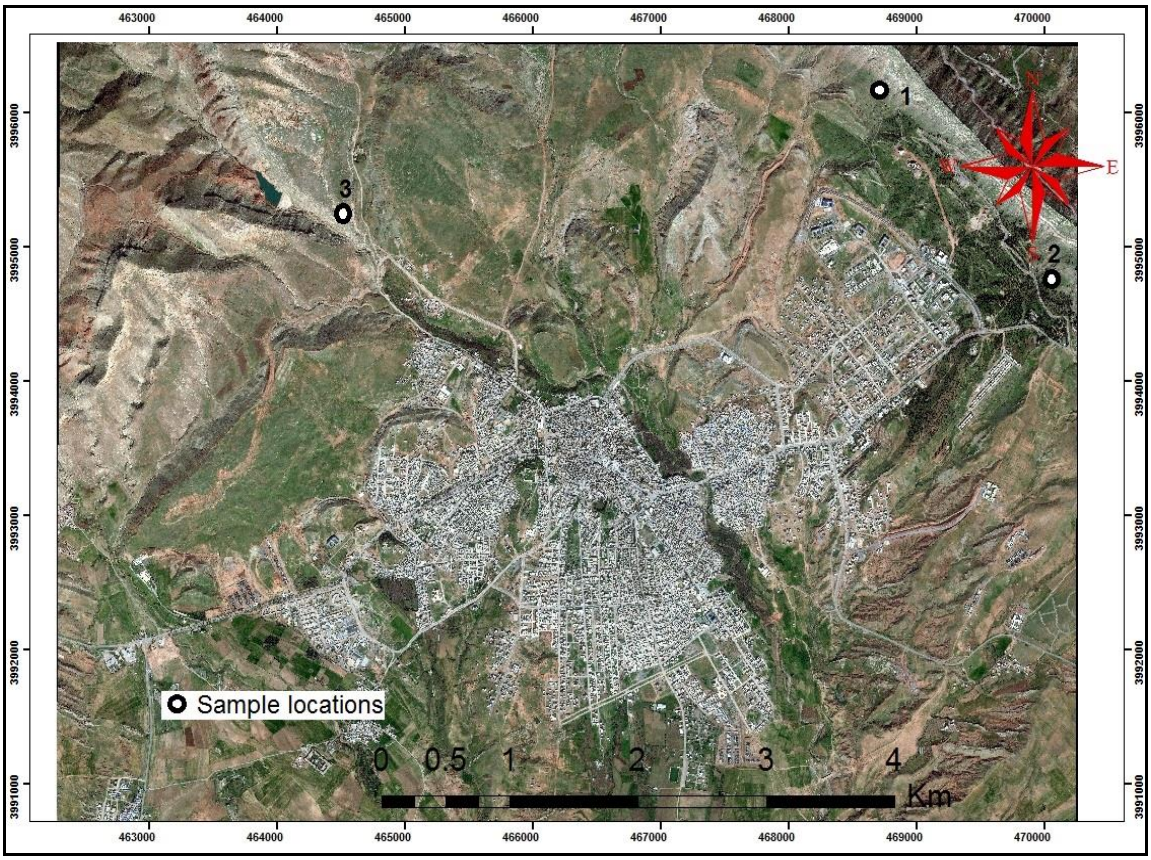

Fig. 1. Satellite image of Koya city which indicates the sample locations.

II. Geological Setting

Tectonically the studied area is located in the High Folded Zone of the Unstable Shelf area and according to geography it is located of NE Iraq, Haibat-Sultan homocline structure is considered part of the southwest limb of Haibat-Sultan anticline which is asymmetrical anticline extending in the (NW-SE) trend, that is parallel to the Zagros fault thrust zone (Buday, 1980; Buday and Jassim, 1987; Jassim and Goff, 2006). The studied samples were collected from three different outcrops locations in Koya area are belonging to Pilaspi Formation (Middle-Late Eocene). The Pilaspi Formation is exposed in the entire studied region; it is seen as continuous high ridges surrounding the anticlinal structures with very common flat iron morphology, while in the other places it forms the carapace of main body of the Haibat-Sultan homocline structure. According to (Bellen, et al., 1959) the Pilaspi Formation was first described by Lees in 1930 from the Pilaspi area of High Folded Zone also they added that the original type section was submerged under the reservoir of the Darbanikhan dam during the sixtieth of the last century. The resistant Pilaspi Formation forms a conspicuous ridge between the less resistive Gercus and Fatha Formations throughout the high folded zone. It is about (100 – 200 m) thick, variation in thickness such as in the Pirmam area (120 m), Koysanjaq (56 m), Shaqlawa (70 m), and in Hareer (52 m) due to different in the weathering processes action and rapidly subsidence of the sedimentary basin from one region to another (Bellen et al. 1959; Buday, 1980; Youkhana and Sissakian, 1986; Jassim and Goff, 2006). In the studied area the Pilaspi Formation forms continuous steep ridges of Hogback type at the crest of Haibat-Sultan homocline structure it consists mainly of grey, light grey, yellowish white color well bedded limestone, and sometime crystalline to dolomitic limestone.

III. Methodology

Engineering geological and geotechnical properties of the limestone rocks in the study area were determined based on the field studies and laboratory tests. The description of rock material and the main discontinuities were based on the suggested methods by (Anon, 1972; New Zealand Geotechnical Society, 2005). The field studies included observations/ measurements of the rock mass characteristics such as color, grain size, orientation, bedding thickness and

 http://dx.doi.org/10.14500/aro.10068

weathering state of the rock materials, also spacing, persistence, roughness and infilling material of the discontinuities (except the bedding plane, the rock mass are intersecting by two set of joints), as shown in Tables II and Table III.

TABLE II
ROCK MATERIAL PROPERTIES OF THE STUDY AREA

Location No.	Lithology	Color	Grain size	Weathering state
1	Limestone	Yellowish gray to Light gray	Fine	Fresh to slightly weathered
2	Limestone	Yellowish gray	Fine	Fresh to slightly weathered
3	Limestone	Light gray	Fine	Fresh to slightly weathered

Six limestone rock samples were collected from three different outcrop locations at the field for laboratory testing. Some physical and mechanical tests have been done on the limestone samples according to the requirements of the national and international standards (Iraqi Standards, 1989; American Society for Testing and Materials, 2004 and International Society for Rock Mechanics, 1981), Tables IV and V. Laboratory tests are included water content (w%), density & water absorption, uniaxial compressive strength by using point load test, slake durability & porosity, as shown in Tables VI, VII, VIII and IX, respectively.

TABLE III
MAIN DISCONTINUITY (BEDDING PLANE AND JOINTS) PROPERTIES OF THE STUDY AREA

Location No.	Orientation (dip dir./ amount)	Thickness of layers (m)	Spacing (m)	Persistence	Roughness	Infilling materials
1	230/ 42°	0.18 – 0.9	0.2 – 0.5	0.7 m to < 7 m	Smooth- rough	Thin layers of clay (0.3 cm)
2	228/ 48°	0.4 – 1.0	0.3 – 0.6	0.7 m to < 7 m	Smooth- rough	Thin layers of clay (0.2 cm)
3	220/ 45°	0.3 – 0.6	0.15 – 0.5	0.3 m to < 6 m	Smooth- rough	Thin layers of clay (0.5 cm)

TABLE IV
STANDARD SPECIFICATION OF PHYSICAL AND MECHANICAL PROPERTIES OF LIMESTONE FOR CONSTRUCTION MATERIALS (IRAQI STANDARDS, 1989 AND AMERICAN SOCIETY FOR TESTING AND MATERIALS, 2004)

Type	Class	Density (gm/ cm^3)	Absorption %	Compressive strength (MPa)	Grade
I	A	1.76 – 2.16	12	12	Low
II	B	2.16 – 2.56	7.5	28	Moderate
III	C	≥ 2.564	3	55	High

TABLE V
STANDARD SPECIFICATION OF SLAKE DURABILITY INDEX (Id_1)% ACCORDING TO (INTERNATIONAL SOCIETY FOR ROCK MECHANICS, 1981)

(Id_1) %	Grade	Class
< 60	Very low	A
60 – 85	Low	B
85 – 95	Medium	C
95 – 98	Medium to high	D
98 – 99	High	E
> 99	Very high	F

TABLE VI
RESULTS OF WATER CONTENT (W%)

Location No.	Sample No.	Wet weight (gm)	Dry weight (gm)	Natural water content (w %)
1	S1	221.58	220.7	0.3987
	S2	193.4	192.9	0.2592
2	S3	242.7	242	0.2892
	S4	176.7	176.2	0.2837
3	S5	607.9	607.4	0.08231
	S6	352.4	352.2	0.05678

TABLE VII
RESULTS OF DENSITY AND WATER ABSORPTION

Location No.	Sample No.	Weight in air (g)	Weight of stone after (24 hrs) been in water (g)	Pore water weight (when the rock sample is fully saturated)	Weight in water (g)	Weight of total displaced water (W_B)	Weight of displaced water by solid (W_S)	Water content in saturated state (m %)	Dry density (g/cm^3)
1	S1	220.7	225.8	5.1	135.6	90.2	85.1	2.31	2.45
	S2	192.9	197.1	4.2	116.5	80.6	76.4	2.18	2.39
	Average							2.2	2.42
2	S3	242.9	248.1	5.2	177.2	70.9	65.7	2.31	2.0
	S4	176.2	180.6	4.4	107.3	73.3	68.9	2.5	2.4
	Average							2.4	2.2
3	S5	607.4	620.7	13.3	384.3	236.4	223.1	2.19	2.57
	S6	352.2	355.6	3.4	220.1	135.5	132.1	1.0	2.59
	Average							1.6	2.58

TABLE VIII
RESULTS OF THE POINT LOAD TESTS AND RELATED UNIAXIAL COMPRESSIVE STRENGTH OF THE COLLECTED ROCK SAMPLES FROM THE STUDY AREA

Location No.	Test No.	Diameter (mm)	Load P (MN)	Is = P/ D^2 (MPa)	$Is_{(50)}$ (MPa)	Uniaxial Compressive Strength (UCS) = 22.5 × $Is_{(50)}$ (MPa)	Average UCS and description
1	1	46	0.009	4.5	4.275	96.18	(81) Strong
	2	52	0.006	3.0	3.03	68.18	
	3	43	0.0011	6.11	5.71	128.47	
	4	55	0.0081	2.667	2.79	62.82	
	5	63	0.0079	1.994	2.211	49.75	
2	1	60	0.012	3.338	3.62	81.52	(84) Strong
	2	60	0.0045	1.25	1.35	30.52	
	3	52	0.0012	4.655	4.73	106.52	
	4	57	0.0013	4.052	4.29	96.7	
	5	45	0.0099	4.89	4.67	105.1	
3	1	42	0.012	7.05	6.486	145.93	(182) Very strong
	2	48	0.01	10	10	225	
	3	50	0.025	10.08	8.35	188.04	
	4	56	0.02	6.451	6.77	152.32	
	5	44	0.18	9.47	8.94	201	

TABLE IX
RESULTS OF SLAKE DURABILITY AND POROSITY OF LIMESTONE SAMPLES

Location No.	Sample No.	Slake durability (Id_1)	Porosity (n%)
1	S1	99.3	5.65
	S2	99.1	5.21
	Average	99.2	5.43
2	S3	99.0	7.33
	S4	99.0	6.00
	Average	99.0	6.66
3	S5	99.55	5.62
	S6	99.75	2.50
	Average	99.65	4.06

IV. RESULTS AND DISCUSSION

The results obtained from the field studies led to that the limestone rocks have fine grain size, fresh to slightly weathered, moderately to thickly bedded. The discontinuities are moderately spaced, smoothly rough with thin layers of clay materials and their persistence ranges from 0.3 m to < 7 m. The physical and mechanical properties were investigated according to the national and international standard specification. To obtain the best representative value for rock property, six samples within three different outcrop locations in Koya area were collected, tests for each sample were done and so the results of these tests were discussed herein, in order to evaluate the quality of studied limestone rocks as construction and building materials. Tables VI and VII give the result of some physical properties such as natural water

content ranges from 0.05% to 0.39% with an average value of 0.22%, water content in saturated state with an average ranges from 2.2% to 2.58%, dry density with an average value ranges from 1.6 to 2.4 g/cm^3. This shows that samples have low effective porosity (Khanal and Tamrakar, 2009). Building stones that exhibit low water absorption or low porosity values are generally found to be relatively more durable. Water will be disable to penetrate non-pores stone types, therefore disable to promote damage in construction model structure (Miglio and Willmott, 2010), also (Jacobsen and Aarseth, 1999) proved that the building material′s surface with low degree of water absorption and porosity will be little or no effect by weathering agents such as wind or rainfall.

Table VIII shows the results of mechanical property such as compressive strength of limestone ranges from 81 to 182 MPa pointed out that this range have strong to very strong and inversely proportional with the lower water absorption (Naghoj, et al., 2010). As a result all these physical and mechanical properties pointed out that the studied limestone samples are belonging to Class C and Type III (high density), Table IV, according to (Iraqi Standards, 1989; American Society for Testing and Materials, 2004) respectively. Table IX gives the results of the slake durability tests with average value range from 99% to 99.65%, and porosity from 2.5% to 7.33%. These physical properties were carried out to examine by (International Society for Rock Mechanics, 1981) and indicated that the studied limestone samples are belong to Class F (very high) slake durability with lower porosity, Table V.

According to the obtained results, the investigated limestone rocks are acceptable, compact, strong to very strong enough and have very high slake durability. They show fresh-slightly weathering processes without micro cracks or fractures. As a result of the study, it is concluded that the studied limestone in Koya area within Pilaspi Formation could be used as construction material in accordance with national and international standard specification. A durable building stone is one which resists the weathering elements in the atmosphere, stone durability is closely related to both pore structure and strength, building material must be resist to physical and chemical weathering processes which are considered the main causes of building stone decay, therefore durability test method must be used to assess and select the stone which is most suitable for building materials (Ross, et al., 1990; Benavente, et al., 2004).

V. Conclusion

Based on the results of this study the following conclusions have been reached out:

- The distinct rock have been recognized as limestone shows fine grained size, fresh-slightly weathering, high durable, strong-very strong and free from visible defect which affect on the appearance or strength.
- The thickness of rock mass layers are moderately to thickly bedded and the discontinuity spacing are closely to moderately spaced give an indication of the large size of blocks that are suitable for using as dimension stone.
- Based on national and international standards specification for using of limestone in construction materials. The limestone rocks in the study area proved that they are belonging to Class C, Type III (high density), Class F (very high slake durability with low porosity) according to Iraqi Standards (1989), American Society for Testing and Materials (2004) and International Society for Rock Mechanics (1981), respectively, to be used as construction and building materials such as walls, foundations and covering building for beautiful appearance, etc.

References

American Society for Testing and Materials, 2004. C568: 2004 *Standard specification for limestone dimension stone.* America: ASTM.

Anon, 1972. The preparation of maps and plans in term of engineering geology, *Quarterly Journal of Engineering Geology*, 5(4), pp.293-383.

Bellen, R, Dunnigton, H, Wetzel, R & Morton, D 1959, *Lexique stratigraphique international Intern Geol. Conger. Comm.*, 3, 10 Asie, Iraq, 333pp.

Benavente, D., Garcia del Cura, M, A., Fort, R. and Ordonez, S., 2004. Durability estimation of porous building stone from pore structure and strength. *Journal of the Engineering Geological*, 74(1-2), pp.113-127.

Buday, T., 1980. *The Regional geology of Iraq, vol. 1: stratigraphy and paleontology*. Baghdad: Publication of GEOSURV.

Buday, T. and Jassim, S., 1987. *The Regional geology of Iraq, vol. 2: Tectonism, Magmatism and Metamorphism.* Baghdad: Publication of GEOSURV.

Dhaher, K.A., 2009. *Study of physical and geotechnical properties of some rock units of Pilaspi, Fatha and Injana Formations in Shaqlawa area, northern Iraq*, M. Sc., University of Baghdad.

International Society for Rock Mechanics, 1981. *Suggested methods for determining swelling and slake durability index properties. ISRM Suggested Method: Rock characterization testing and monitoring*. Oxford: ISRM.

Iraqi Standards, 1989. IS No. 1387: 1989 *Natural building stone*. Baghdad, IS.

Jacobsen, S. and Aarseth, LI., 1999. Effect on wind on drying fram wet porous building material surfaces- A simple model in steady state. *Journal of Material and Structure*, 32, pp.38-44.

Jassim, S.Z. and Goff.J. C., 2006. *Geology of Iraq*. Prague: Dolin.

Khanal, S. and Tamrakar, N. K., 2009. Evaluation of quality of crushed limestone and-siltstone for road aggregates. *Bulletin of Department of Geology*, 12, pp.20-42.

Miglio, B. and Willmott, T., 2010. Durability of stone for construction. *Journal of ASTM International Selected Technical Papers STP 1514; durability of Building and construction, Sealants and Adhesives*, 3, pp.241-246.

Naghoj, N.M., Yuossef, N. A. R. and Maaitah, O. N., 2010. Mechanical properties of natural building stone: Jordanian building limestones as an example, *Jordan Journal of Earth and Environmental Sciences*, 3(1), pp.37-48.

New Zealand Geotechnical Society, 2005. *Field description of soil and rock*, New Zealand: Publication of NZ Geotechnical Society.

Ross, K.D., Hart, D. and Butlin, R. N., 1990. Durability tests for natural building stone. *Proceedings of the Fifth International Conference on Durability of Building Materials and Components*. Brighton, pp.97-111.

Saleh, D.G., 2012. The suitability of limestone of Fatha Formation for building and road aggregates in Nineveh governorate/ North Iraq, *Journal of University of Anbar for Pure Science*, 6(2), pp.1-13.

Youkhana, R. and Sissakian,V., 1986. Stratigraphy of Shaqlawa-Koisanjaq area. *Journal of the Geological Society of Iraq*, 19(3), pp.137-154.

 http://dx.doi.org/10.14500/aro.10072

Objective Gender and Age Recognition from Speech Sentences

Fatima K. Faek

Electrical Department, Engineering College, Salahaddin University
Zanko Street, Kirkuk road, Erbil, Kurdistan Region of F.R. Iraq

***Abstract*—In this work, an automatic gender and age recognizer from speech is investigated. The relevant features to gender recognition are selected from the first four formant frequencies and twelve MFCCs and feed the SVM classifier. While the relevant features to age has been used with k-NN classifier for the age recognizer model, using MATLAB as a simulation tool. A special selection of robust features is used in this work to improve the results of the gender and age classifiers based on the frequency range that the feature represents. The gender and age classification algorithms are evaluated using 114 (clean and noisy) speech samples uttered in Kurdish language. The model of two classes (adult males and adult females) gender recognition, reached 96% recognition accuracy. While for three categories classification (adult males, adult females, and children), the model achieved 94% recognition accuracy. For the age recognition model, seven groups according to their ages are categorized. The model performance after selecting the relevant features to age achieved 75.3%. For further improvement a de-noising technique is used with the noisy speech signals, followed by selecting the proper features that are affected by the de-noising process and result in 81.44% recognition accuracy.**

***Index Terms*—Age classification from speech, gender classification from speech, MFCC based gender and age recognition, SVM classifier.**

I. INTRODUCTION

The problems to be faced in the process of automatic speech-based age estimation are: Firstly, a large balanced database for different speaker age ranges is needed. Secondly, speech contains other speaker characteristics, including the speaker's weight, height and emotional condition, these characteristics may interact with age. (Bahari and Van hamme, 2011; Dobry et al. 2011; Florian, et al., 2007).

ARO, The Scientific Journal of Koya University
Volume III, No 2(2015), Article ID: ARO.10072, 06 pages
DOI: 10.14500/aro.10072
Received 11 February 2015; Accepted 03 July 2015
Regular research paper: Published 06 October 2015
Corresponding author's e-mail: fatima.faek@su.edu.krd

Automatic gender and age classification from speech can be performed using different approaches. For instance cepstral features, like Mel frequency cepstral coefficients (MFCC), are used by Florian, et al. for age recognition (Florian, et al., 2007). MFCC is reported to produce poor results for gender and age classification with recorded signals, either by using different microphones or in different places (noisy, and non-noisy) (Tiwari, et al., 2011). To avoid this problem, Sas, et al enhanced the MFCC features by analyzing the parameters that affect the process of extracting the features. Additionally the impact of these parameters on the gender recognition accuracy is studied (Sas, et al., 2013). Other researchers have used pitch or prosodic features with MFCC together; this improves the results of the gender and age recognizer (Harnsberger, et al., 2008).

While (Golfer and Mikes, 2005) studied the automatic gender classification from the speech signals of adult speakers using features related to the fundamental frequency (F0) and the first four formant frequencies**.** This approach is very active for gender classification of three classes, adult males, adult females, and children without gender discrimination, since the F0 and the formant frequencies, (especially the second and third formants), of children are higher than that of adults, i.e. the range of formant decreases with age (Potamianos and Narayanan, 2003). Female range changes are more gradual than male and the main differences become more significant after age twelve (Potamianos and Narayanan, 2003).

Different classifiers can be used for gender and age classification; Gaussian mixture models (GMM), hidden Markov models (HMM), support vector regression (SVR), and multilayer perceptrons (MLP) are proposed and tested by Hugo, et al., for gender classification, where the result was 95%. This result is for male/female classification and does not concern children (Hugo and Isabel, 2011). Sedaaghi used different classifiers for age estimation, like support vector machine (SVM), k-nearest neighbor (k-NN), probabilistic neural network (PNN), and GMM, when a result of 88% was obtained (Sedaaghi, 2009). Mirhassani, et al., used single layer feed forward neural network to estimate the age of children, and they used fuzzy data fusion to make the overall decision (Mirhassani, et al., 2014). Thomas et al combines three MLP outputs trained with Perceptual Linear Prediction (PLP)

features (Thomas, et al., 2014).

As any pattern recognition task the model performance depends on the robustness of the features and the classifier.
Many features are suggested by previous studies. However, this work focuses on the use of MFCC and formant frequencies. The work investigates the contribution of different MFCC and formant frequencies in age and gender recognition, especially in terms of the contribution of different frequency bands represented in their relative formants and MFCCs. The goal of this work is to use a few number of MFCC and formant frequency features, which are relevant features for gender and age classification.

In this work, the support vector machine and the k-NN are used as classifiers. SVM is one of the popular on-the-shelf classification method for its ability to separate the classes by an optimized hyper plain since it maximize the margin distance from the separator hyper plain to the support vector.

The data used in this work is a mix of noisy and clean speech signals, therefore this work follows a pre-processing (de-noising) technique and feature selection among the 12 MFCC, that are affected by the de-noising process for further improving the result of the age classifier (Faek and Al-Talabani, 2013).

II. The Database

The database consists of recorded speech sentences uttered by 114 Kurdish speakers (males and females), their ages lying between five and sixty-five years. This data has been recorded and collected by the author. The age recognizing algorithm is evaluated using the 114 speech samples after distributing the database in the following manner:

a) Children: less than 13 years (32 speakers).
b) Young: 14-19 years, (15 male speakers), and (15 female speakers).
c) Adults: 20-55 years, (17 male speakers), and (19 female speakers).
d) Seniors: up to 56 years, (9 male speakers), and (7 female speakers).

The two classes gender recognizer is evaluated using 82 adult males (40 speakers), and females (42 speakers), whereas, the 114 speech samples are used for the evaluation of the three classes gender recognizer, adult males (40 speakers), adult females (42 speakers), and children (32 speakers).

III. The Gender Classifier

In this work, the robust features among the first four formant frequencies are used as features for gender classification. Formants are the peaks of the speech signal spectrum. Formant frequencies are an acoustic resonance of the human vocal tract which is measured as an amplitude peak in the frequency spectrum of the sound. Extraction of Formant frequencies is achieved using linear prediction coefficients (LPC) based formants estimation technique as shown in Fig. 1 (Golfer and Mikes, 2005).

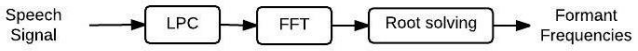

Fig. 1. Block diagram of extracting the formant frequency features.

The robust MFCC features are combined with the aforementioned features, since the MFCCs are the standard features in speech processing. They present the energy distribution of the speech signal in the frequency domain. This method is based on the Mel frequency scale and is related to human hearing. The technique of extracting MFCC features can be described by the block diagram shown in Fig. 2.

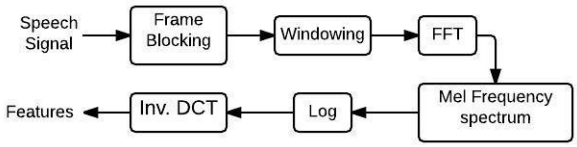

Fig. 2. Block diagram of extracting the MFCC features.

In the frame blocking section, the speech signal is divided into frames. Windowing minimizes the discontinuities present in the signal. The FFT is used for conversion of each frame from the time domain to the frequency domain which gives information about the energy rate at each frequency band. The Mel frequency spectrum is obtained by arranging the spectrum according to human hearing. Human hearing does not follow the linear scale but the Mel-spectrum scale which is a linear spacing below 1000 Hz and logarithmic scaling above 1000 Hz. Finally, the Mel-spectrum is converted back to the time domain by using the inverse DCT (Tiwari, et al., 2011).
Cepstral features are calculated from the log filter bank amplitudes (mj), as shown in Fig. 3. These features are calculated using the discrete cosine transformation as expressed below:

$$ci = \sqrt{\frac{2}{N}} \sum_{j=1}^{N} mj \cos\left(\frac{\pi j}{N}(j - 0.5)\right) \quad (1)$$

N is the number of filter bank channels which is set to 24. The SVM, with linear and non-linear separation function (LSF and NLSF) is tested as a classifier for two classes (adult males and females) gender recognition. SVM is a classifier that constructs an N-dimensional hyper-plane that separates the data optimally into two classes. With the SVM, the weights of the network are found by solving a quadratic programming problem; the separation function between classes in SVM may be linear, or non-linear. (Bocklet, et al., 2008; Santosh, et al., 2012).

http://dx.doi.org/10.14500/aro.10072

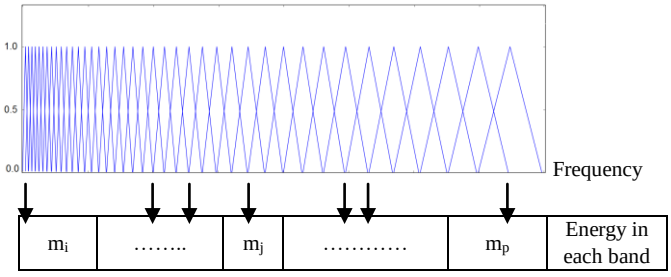

Fig. 3. Frequency response of a typical Mel-scaled triangular filter bank.

The goal of SVM modelling is to find the optimal hyper-plane that separates clusters of vector, (a set of features that describes one class), in such a way that the features that belong to the first class will be on one side of the plane and the features of the other class will be on the other side of the plane. The data close to the hyper-plane are the support vectors (Bocklet, et al., 2008; Santosh, et al., 2012).

IV. The Age Classifier

The robust formant frequencies in addition to the robust MFCCs to age classification are used as features. MFCCs are the best performing features for age recognition, but the drawback of these features is that they are not suitable for analyzing noisy signals (Tiwari, et al., 2011). So, for a further improvement of the age recognizer, a wavelet based, de-noising algorithm is followed to clean up the noisy speech signals as a pre-processing method (Faek and Al-Talabani, 2013), selecting robust features after the de-noising process is also of prime importance, to obtain the best results.

The k-Nearest-Neighbors (k-NN) is used as classifier, since it is a simple arbitrary classifier. This classifier is highly applicable in many cases. Simply this classifier classifies each set of the data in sample into one of the groups in training (Faek and Al-Talabani, 2013).

V. Feature Selection

In this work, the different features are analyzed, and the robust features are selected based on the frequency range that the feature represents. This process leads to obtain a good classification results with a few number of features. According to previous researchers, formants 2 and 3 differ from children to adults and from adult males to adult females (Potamianos and Narayanan, 2003), so these two formant features hold gender information and can be selected for better results, and the mid-frequency MFCC features are selected in this work for the same reason.

On the other hand, unlike the mid-frequency band; low and high frequency bands of a speech signal hold age information, especially the high frequency components of human voice, for they decrease with age. So based on this knowledge the low and high MFCCs are selected in this work, in addition to formants 1 and 4 for better age recognition results.

VI. Results and Discussion

A. Gender Classification Results

The results of the gender recognition of two classes(adult males and females), are shown in Table I, and Figs. 4, 5, 6, 7, 8 and 9, using different formant frequencies (F1, F2, F3 and F4) as features and SVM with linear separation function as a classifier. This algorithm is applied on a data consisting of 82 speakers (adult males and females).

TABLE I
Gender Recognizer Results of Tow Classes Using Different Formant Frequencies as Features, and SVM with Linear Suppuration Function as a Classifier

Feature	Recognition rate %
F2 and F4	85%
F3	89%
F2 and F3	90%
F3 and F4	89%
F1, F2 and F3	90%
F2, F3 and F4	89%
F1 and F3	90%
F1 and F4	81%
F1 and F2	83%
F1, F2, F3 and F4	88%

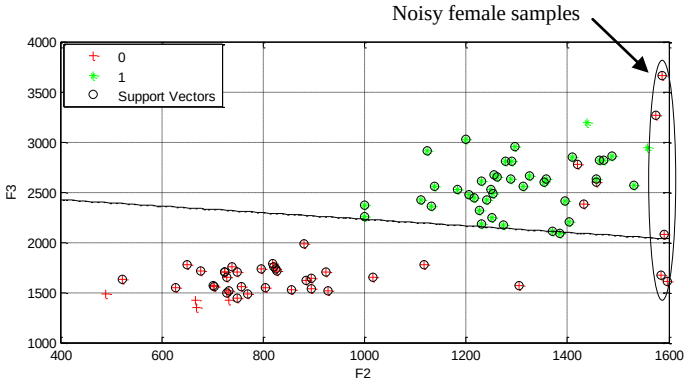

Fig. 4. Gender classification result using F2, F3 and SVM with LSF.

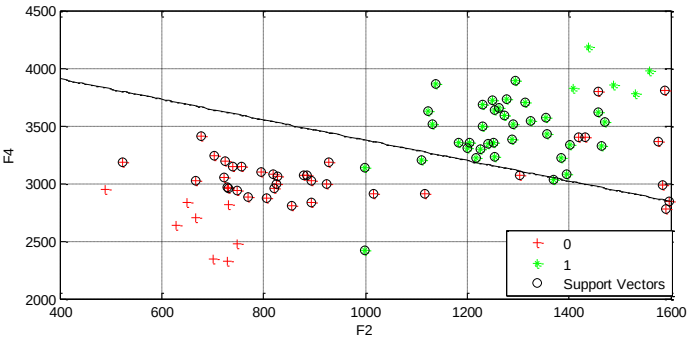

Fig. 5. Gender classification result using F2, F4 and SVM with LSF.

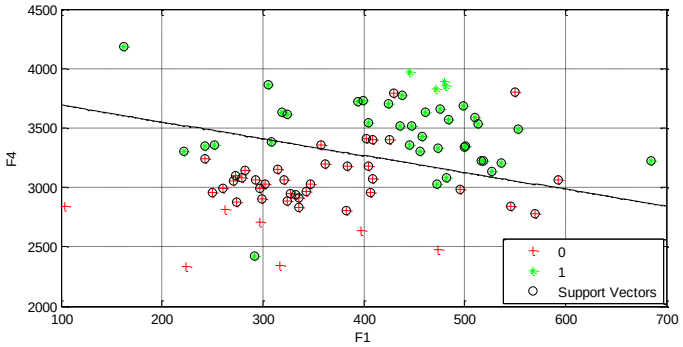

Fig. 6. Gender classification result using F1, F4 and SVM with LSF.

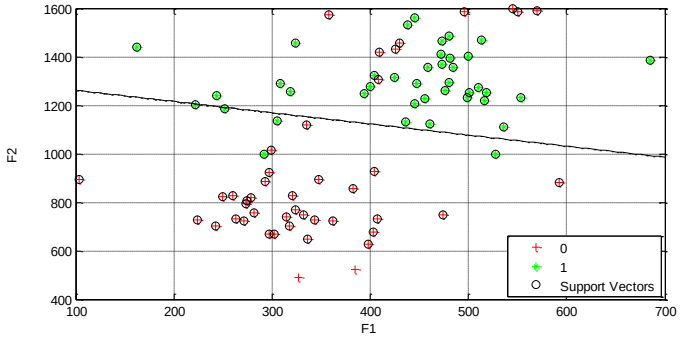

Fig. 7. Gender classification result using F1, F2 and SVM with LSF.

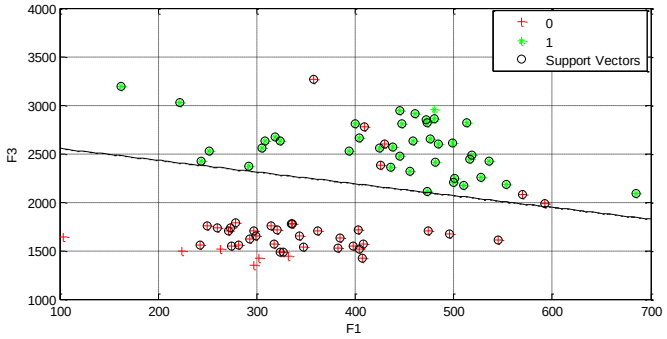

Fig. 8. Gender classification result using F1, F3 and SVM with LSF.

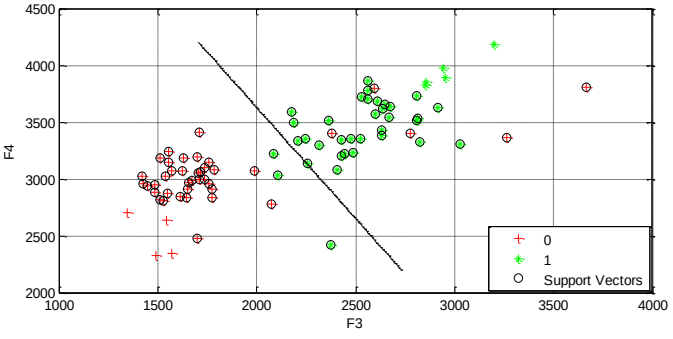

Fig. 9. Gender classification result using F3, F4 and SVM with LSF.

When using the SVM with non-linear separation function, the results of the gender recognition of two classes are as shown in Table II and Figs. 10, 11, 12, 13, 14, and 15.

TABLE II
GENDER RECOGNIZER RESULTS OF TOW CLASSES USING DIFFERENT FORMANT FREQUENCIES AS FEATURES, AND SVM WITH NON- LINEAR SUPPURATION FUNCTION AS A CLASSIFIER

Feature	Recognition rate %
F2 and F4	90%
F3	94%
F2 and F3	96%
F3 and F4	92%
F1, F2 and F3	91%
F2, F3 and F4	94%
F1 and F3	87 %
F1 and F4	83 %
F1 and F2	85 %
F1, F2, F3 and F4	90%

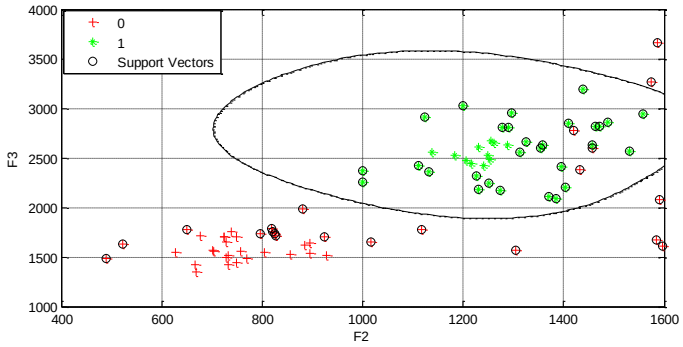

Fig. 10. Gender classification result using F2, F3 and SVM with NLSF.

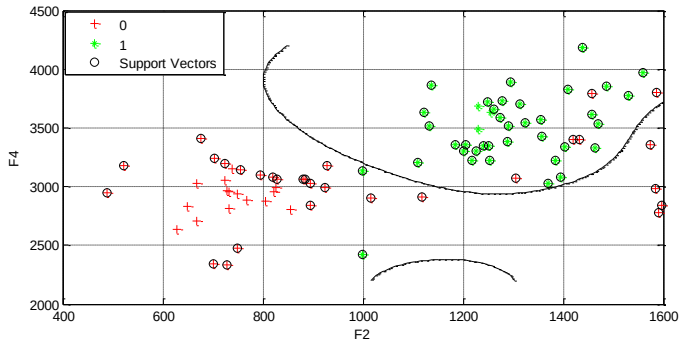

Fig. 11. Gender classification result using F2, F4 and SVM with NLSF

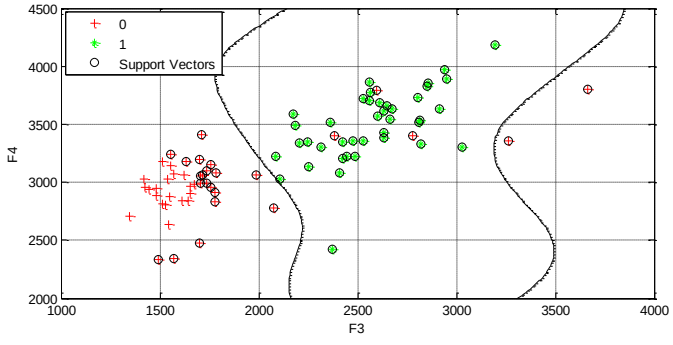

Fig. 12. Gender classification result using F3, F4 and SVM with NLSF.

The noise affects the formants of both genders but the formants of females change (increase) more than that of males. This problem appeared when using SVM with linear separated

http://dx.doi.org/10.14500/aro.10072

function; Non-linear separated function is more active with noisy signals, especially when using F2 and F3 as shown in Fig. 10.

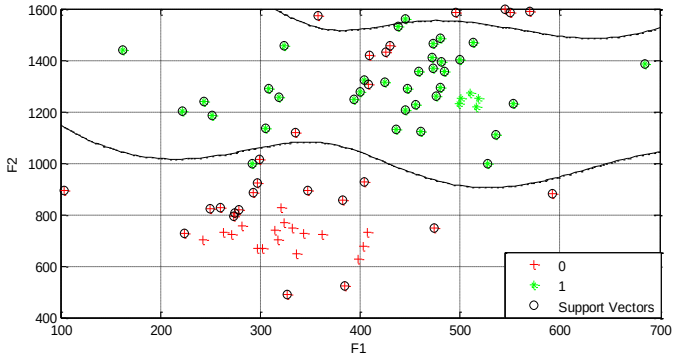

Fig. 13. Gender classification result using F1, F2 and SVM with non-linear separation function.

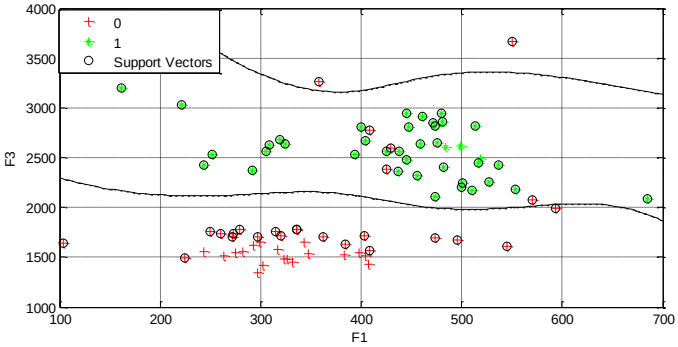

Fig. 14. Gender classification result using F1, F3 and SVM with NLSF.

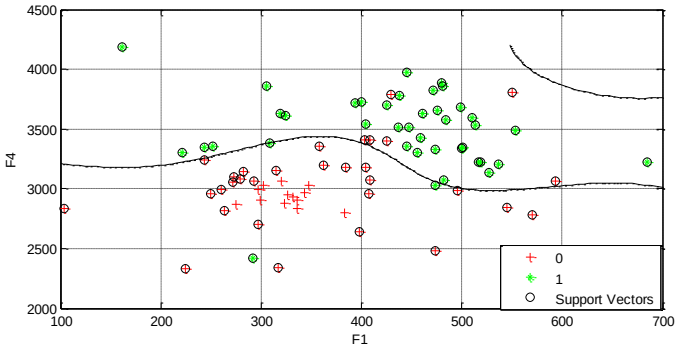

Fig. 15. Gender classification result using F1, F4 and SVM with NLSF.

It is clear that the best result is obtained using the second and third formants as feature.

Combining the MFCC with the formant frequencies as features, the results shown in Table III are achieved. The SVM with non- linear separation function is used as a classifier.

MFCCs (4-10) represent the mid frequency MFCC features. So it can be expected that these features in addition to formant 2 and 3 hold gender information, since they give the best results.

The results of the three classes' gender recognition are shown in Table IV, using different formant frequencies and different MFCC features, as well as the k-NN classifier. This algorithm is applied to (114) speakers (children without gender discrimination, adult males, and females).

Again the best result is obtained using F2, F3 and the mid MFCC features.

TABLE III
GENDER RECOGNIZER RESULTS OF TOW CLASSES USING MFCC AND FORMANT FREQUENCY AS FEATURES, AND SVM WITH NON- LINEAR SUPPURATION FUNCTION AS A CLASSIFIER

Feature	Recognition rate %
12 MFCC + F1, F2, F3 and F4	88%
4-9 MFCC + F1, F2, F3 and F4	92%
4-9 MFCC	96%
4-10 MFCC	93%
3-9 MFCC	92%
12 MFCC + F2 and F3	88%
4-9 MFCC + F2 and F3	96%

TABLE IV
GENDER RECOGNIZER RESULTS OF THREE CLASSES USING MFCC AND FORMANT FREQUENCY AS FEATURES, AND K-NN AS A CLASSIFIER

Feature	Recognition rate %
12 MFCC + F1, F2, F3 and F4	85%
F2 and F3	94%
12 MFCC + F2 and F3	85%
F1, F2 and F3	93%
F1 and F4	79%
4-9 MFCC + F2 and F3	94%
4-9 MFCC	94%
F1, F2, F3 and F4	92%

B. Age Classification Results

The results of the age classifier, using the first formant frequencies, and the 12 MFCC as features, and k-NN as a classifier, are shown in Table V. This algorithm is applied on a database of 114 speakers of different ages; five to sixty-five years. It is clear from the results of this part that F1 and F4 are important features for age classification, especially when combing them with the low and high frequency MFCC features. As a result, it can be expected that the low and high frequency features, (formants and MFCC), carry age information other than mid-frequency features.

TABLE V
AGE RECOGNIZER RESULTS USING MFCC AND FORMANT FREQUENCY AS FEATURES, AND K-NN AS A CLASSIFIER

Feature	Recognition rate %
F1and F4	66%
F2 and F3	52%
F2, F3 and F4	52%
F3 and F4	59%
F1, F2 and F3	54%
F1, F3 and F4	68%
F1, F2, F3, F4 and12 MFCC	69%
F1, F4 and 12 MFCC	57%
F1, F4 and MFCC 1, 2, 3, 4, 8, 9, 10, 11 and 12	75.3%

It can be observed from the results of gender recognition shown in Tables III, and the above results that MFCC's 4, 8 and 9 are useful for both gender and age classification.

The results of the age classifier, after de-noising the noisy speech signals, and using the aforementioned features and classifier are shown in Table VI. In this case, F1 and F4 are also of prime importance and the high frequency MFCC features have a great effect on the results, since they are affected by the de-noising technique used in this part.

The time cost for the all experiments done in this paper using SVM, is not exceeding 7 seconds. While in the case of k-NN the time cost is not more than 1.5 second. In both cases the complexity is not assigned as a serious drawback.

TABLE VI
AGE RECOGNIZER RESULTS AFTER THE DE-NOISING PROCESS USING MFCC AND FORMANT FREQUENCY AS FEATURES, AND K-NN AS A CLASSIFIER

Feature	Recognition rate %
F1 and F4	67%
F2 and F3	56%
F2, F3 and F4	56%
F3 and F4	59%
F1, F2 and F3	62%
F1, F3 and F4	69%
F1, F2, F3, F4 and12 MFCC	76%
F1, F4 and 12 MFCC	78%
F1, F4 and MFCC 7, 8, 9, 10, 11 and 12	81.44%

VII. CONCLUSION

The best gender classification results are obtained in the case of two classes and three classes with the second and third formant frequencies as features, since these formants differ from children to adults and from adult females to males. The mid-frequency MFCC features also hold gender information, so these MFCC features can be selected for better gender classification results.

Since the database is a mix of clean and noisy recorded speech sentences, SVM with a non-linear separated function is more active with the noisy speech signals than the linear separated function.

The experiments done in this work show that F1 and F4 are more relevant to human age recognition than F2 and F3, consequently they were selected for the age recognition model.

The 12 MFCC are also important features for age recognition, especially the low and high MFCCs, as they hold age information. However, the drawback of these features is that they are affected by noise. De-noising criteria as a pre-processing method leads to better results especially after selecting the robust features that are affected by the de-noising process among the twelve MFCCs, which are the high frequency features, in addition to the F1 and F4 features.

The selected features in this work are picked according to a pre-knowledge scheme, and not selected automatically. Consequently the obtained results need to be generalized to other datasets.

REFERENCES

Bahari, M.H. and Van hamme, H., 2011. Speaker age estimation and gender detection based on supervised non-negative matrix factorization, In: IEEE, *IEEE Workshop on Biometric Measurements and Systems for Security and Medical Applications*, Italy, 28 September 2011. USA.

Bocklet, T., Maier, A. and North, E., 2008. Age Detection of Children in Preschool and primary School Age with GMM-Based Super vector and Support Vector Machines/regression. In: *11th International Conference, TSD 2008*, Bron, Czech Republic, 8-12 September 2008.

Dobry, G., Hetch, M., Avegal, M., and Zigel, Y., 2011. Super vector Dimension Reduction for Efficient Speaker Age Estimation Based on the Acoustic Speech Signal, *IEEE Trans. Audio, Speech and Language Processing*, 19(7), pp.1975–1985.

Faek, F.K., Al-Talabani, A.K., 2013. Speaker recognition from noisy spoken sentences, *International Journal of Computer Applications*. 70(20), pp.11-14.

Metze, F., Ajmera, J., Englert, R., Bub, U., Burkhardt, F., Stegmann, J., Muller, C., Huber, R., Andrassy, B., Bauer, J.G., Littel, B., 2007. Comparison of four approaches to age and gender recognition for telephone applications, In: IEEE, *IEEE international conference on Acoustics, Speech and Signal Processing (ICASSP)*, Honolulu, 15-20 April 2007. USA.

Golfer, M. and Mikes, V. 2005. The relative contributions of speaking fundamental frequency and formant frequencies to gender identification based on isolated vowels, *Journal of Voice*, 19 (4), pp.544-554.

Harnsberger, J.D., Shrivastav, R., Brown, W.S., Rothman, H. and Hollien, H., 2008. Speaking rate and fundamental frequency as speech cues to perceived age, *Journal of Voice*, 22(1), pp.58-69.

Hugo, M. and Isabel, T., 2011. Age and gender detection in the I-DASH project ACM, *Transactions on Speech and Language Processing*, 7(4), 16 pages. DOI 10.1145/1998384.1998387.

Li, M., Han, K.J. and Narayanan, S., 2012. Automatic speaker age and gender recognition using acoustic and prosodic level information fusion. *Computer Speech and Language*, 27, pp.151-167.

Mirhassani, S.M., Zourmand, A. and Ting, H.N., 2014. Age Estimation Based on Children's Voice: A Fuzzy-Based Decision Fusion Strategy. *Scientific World Journal*, [online] Available at: < http://www.ncbi.nlm.nih.gov/pmc/articles/PMC4070543/> [Accessed 22 November 2014].

Potamianos, A. and Narayanan, S., 2003. Robust recognition of children's speech. *IEEE Trans. Speech Audio Processing*, 11(6), pp.603–616.

Santosh, G., Bharti, G. and Mehrotra, S.C., 2012. Gender identification using SVM with Combination of MFCC, *Advances in Computational Research*, 4(1), pp.69-73.

SAS. J. and SAS., A., 2013. Gender recognition using neural network and ASR techniques, *Journal of medical information and technologies*, 22, pp.179-187.

Sedaaghi, M.H., 2009. A comparative study of gender and age classification in speech signals, *Iranian Journal of Electrical & Electronic Engineering*, 5(1), pp.1-12.

Thomas, P., Vahid, H., Isabel, T., Annika, H., Miguel, S., 2014, Speaker age estimation for elderly speech recognition in European Portuguese. In: *The 15th Annual Conference of the International Speech Communication Association - INTERSPEECH 2014*, Singapore, 14-18 September 2014.

Tiwari, V., Ganga, G., Singhai, J. and Azad, M., 2011. Wavelet based noise robust features for speaker recognition, *Signal Processing: An International Journal (SPIJ)*, 5(2), pp.52-64.

 http://dx.doi.org/10.14500/aro.10080

Comparative Study of Different Methods to Determine the Role of Reactive Oxygen Species Induced by Zinc Oxide Nanoparticles

Nigar A. Najim[1, 2]

[1]Department of Pharmacognosy and Pharmaceutical Chemistry, School of Pharmacy, Faculty of Medical Sciences, University of Sulaimani, Sulaimani, Kurdistan Region - F.R. Iraq

[2]Centre of Synthesis and Chemical Biology, Institute of Science, University Technology MARA, 40450 Shah Alam, Malaysia

***Abstract*—Accumulation of reactive oxygen species (ROS) followed by an increase in oxidative stress is associated with cellular responses to nanoparticle induced cell damages. Finding the best method for assessing intracellular ROS production is the key step in the detection of oxidative stress induced injury. This study evaluates and compares four different methods for the measurement of intracellular ROS generation using fluorogenic probe, 2′,7′-dichlorofluorescein diacetate (DCFH-DA). Hydrogen peroxide (H_2O_2) was utilised as a positive control to assess the reactivity of the probe. Spherically shaped zinc oxide (ZnO) nanoparticles with an average particle size of 85.7 nm were used to determine the diverse roles of ROS in nanotoxicity in Hs888Lu and U937 cell lines. The results showed that different methods exhibit different patterns of ROS measurement. In conclusion this study found that the time point at which the DCFH-DA is added to the reaction, the incubation time and the oxidative species that is responsible for the oxidation of DCFH, have impact on the intracellular ROS measurement.**

***Index Terms*—DCFH-DA, nanotoxicity, nanoparticle, ROS, ZnO.**

I. Introduction

Reactive oxygen species are important intermediates constantly produced *in vivo* through a variety of normal metabolic processes as well as being common intermediates generated after exposure to drugs or ionizing radiation (Curtin, et al., 2002). The nanoparticles have small size and a large surface area that can lead to the sequential oxidation-reduction reactions at nanoparticles surface to produce reactive species such as hydrogen peroxide (H_2O_2) and hydroxyl radial (Donaldson, et al., 2003; Lin, et al., 2009; Oberdorster, 2004; Xia, et al., 2008; Xia, et al., 2006).

Fluorogenic probes have been widely employed to monitor oxidative activity. Among these, 2′,7′-dichlorofluorescein diacetate (DCFH-DA) has been utilised as an assay to evaluate oxidative stress in cells (Wang and Joseph, 1999). This hydrophobic non-fluorescent molecule penetrates rapidly into the cell and is hydrolysed by intracellular esterase to give the dichlorofluorescin (DCFH), which is trapped inside the cells. In the presence of hydrogen peroxide (H_2O_2) and other ROS, DCFH molecule is oxidised to its highly fluorescent product 2′,7′-dichlorofluorescein (DCF) (Foucaud, et al., 2007; Loetchutinat, et al., 2005; Rota, et al., 1999).

The DCF fluorescence intensity can be easily measured and its fluorescence intensity is proportional to the amount of ROS. This probe has been used extensively for quantifying nanomaterial-induced ROS in a range of cell types, some examples of which include LNZ308 (glioma) cells exposed to ZnO nanoparticles (Ostrovsky, et al., 2009), ZnO induced ROS in Ana-1 (mouse macrophage) cells (Song, et al., 2010), ROS induced in A549 (human lung epithelial) cells after exposure to ZnO and silica nanoparticle (Lin, et al., 2006; Lin, 2009) and by ambient ultrafine particles, cationic polystyrene nanospheres, TiO2 and fullerol nanoparticles in RAW264.7 phagocytic cells (Xia, 2006).

In a previous study (Najim, et al., 2014) we demonstrated that the presence of zinc oxide (ZnO) nanoparticles with an average particle size of 85.7 nm induced cytotoxicity towards human histiocytic lymphoma (U937), neuron-phenotypic cells (SH-SY5Y), neuroblastoma (SH-SY5Y) and normal lung (Hs888Lu) cell lines.

Moreover, our data have also indicated that the cytotoxicity of ZnO was concentration dependent. The mechanism of nanoparticles cytotoxicity is not clear, however the generation of reactive oxygen species (ROS) was considered as one of the main causes of the nanotoxicity by the nanoparticles as shown

ARO, The Scientific Journal of Koya University
Volume III, No 2(2015), Article ID: ARO.10080, 05 pages
DOI: 10.14500/aro.10080
Received 23 April 2015; Accepted 01 September 2015
Regular research paper: Published 24 October 2015
Corresponding author's e-mail: nigar.najim@univsul.edu.iq

in previous studies (Li, et al., 2008; Oberdorster, 2004; Reeves, et al., 2008; Sharma, et al., 2009).

This study was designed to investigate the underlying mechanisms of nanoparticles induced cytotoxicity. While there is a number of different cellular injury responses to ROS generated from nanoparticles, we developed a rapid screening procedure for ZnO toxicity premised on oxidative stress injury. In this study four different methods for intracellular ROS detection were compared for their compatibility by using the same representative characterised probe, 2′,7′-dichlorofluorescein diacetate (DCFH-DA) (Grabinski, et al., 2007; Lin, 2009; Ostrovsky, 2009; Song, 2010; Wang and Joseph, 1999).

II. Materials and Methods

A. Materials

ZnO Nanoparticles

The ZnO nanoparticles were synthesised using a method detailed elsewhere (Rusdi, et al., 2011). The ZnO nanoparticles were characterized using scanning electron microscopy (SEM), X-Ray diffraction (XRD) and transmission electron microscopy (TEM) techniques (Najim, 2014; Rusdi, 2011). ZnO average particle size used in these experiments was 85.7 nm.

The 100 mM stock solution of ZnO nanoparticles was prepared in 0.01 M phosphate buffer saline (PBS, Sigma, USA) and sonicated for 30 minutes. The stock solution was stored at 4ºC until required. ZnO nanoparticles stock concentration was vigorously vortexed and then diluted with complete medium prior to each experiment, to obtain concentrations of 100, 200, 500 and 1000 µM.

Cell lines and Culture Conditions

Lymphoma U937 cell line was provided by Dr. Mohamed Saifulaman (Faculty of Applied Sciences, UiTM, Malaysia). Normal lung Hs888Lu cell line was purchased from the American Type Culture Collection (ATCC, The Global Bioresource Centre, Manassas, USA). The U937 cells were cultured in Dulbecco's Modified Eagle's Medium (DMEM, Sigma, USA) with glucose (4500 mg/L), 1% non-essential amino acids (at a strength of 100 ×) (PAA Laboratory GmbH, Austria), 1% L-Glutamine (200 mM) (Sigma, USA), 1% Gentamicin (10 mg/mL) (PAA Laboratory GmbH, Austria) and supplemented with 10% fetal bovine serum (FBS, PAA Laboratory GmbH, Austria). Hs888Lu cells were adapted to grow in DMEM with glucose (4500 mg/L), 1% non-essential amino acids, 2% L-Glutamine (200mM), 1% of Penicillin/Streptomycin (10,000 units/mL of penicillin and 10 mg/mL of streptomycin) (PAA Laboratories GmbH, Austria), 1% sodium pyruvate (1 mM) (Sigma-Aldrich, USA) and supplemented with 10% FBS. All cell lines were maintained at 37ºC in a 5% CO_2 atmosphere with 95% humidity (Incubator, Contherm Scientific Ltd, New Zealand).

Intracellular ROS Measurements

In order to establish the role of oxidative stress induced by ZnO nanoparticles, intracellular reactive oxygen species (ROS) generation was measured. In addition, 2′,7′-dichlorofluorescein diacetate (DCFH-DA, Sigma, USA) was used to detect and quantify the ROS level within the cells (Wang and Joseph, 1999). DCFH-DA stock solution (in methanol) of 10 mM was diluted in Hank's balanced salt solution (HBSS, with Ca^{2+} and Mg^{2+}, without phenol red, Gibco, USA) to yield a 20 µM working solution. Cells were plated in 96-well plate and incubated for 24 hours at 37°C before the experiment. Subsequently, various methods were applied to assess the ROS production.

Hydrogen peroxide (30% H_2O_2, Merck, Germany) was used as a positive control in these experiments to assess the reactivity of the probe (Ostrovsky, 2009; Winterbourn and Sutton, 1984) and also to validate the study. H_2O_2 final concentrations in media were 100 and 200 µM. Four different methods were used to determine their efficiency in the measurements of intracellular ROS, with variation in incubation time and termination of dye. The applied methods were a modification of that described by Wang and Joseph (1999), Grabinski (2007), Lin (2009), Song (2010), and Ostovsky (2009). Prior to each experiment for ROS measurements, cells (1×10^5 cells/mL) were seeded in 96-well plates and left to grow overnight in humidified atmosphere containing 5% CO_2 at 37 ºC incubator.

B. Methods

Method 1 (Coded as M1)

On the day of the experiments, after removing the medium, the cells were washed twice with PBS and then incubated with 50 µL/well of 20 µM of DCFH-DA (working solution) for 30 minutes in a dark environment at 37°C incubator. Immediately following incubation, DCFH-DA was removed and the cells were washed with PBS and treated with various concentrations of H_2O_2 (100 and 200 µM) or ZnO nanoparticles (ranging from 100 µM to 1 mM) for 24 hours. The fluorescence intensity from each well was measured with a 485 ± 10 nm excitation wavelength and a 520 ± 12.5 nm emission wavelength on a Glomax multi detection system (Promaga, USA). Results were representative of six independent experiments and were expressed as percentages of the value observed with control (no H_2O_2 or ZnO treatments) (Grabinski, 2007; Wang and Joseph, 1999).

Method 2 (Coded as M2)

On the day of the experiments, after removing the medium, the cells were washed twice with PBS and then incubated with 50 µL/well of 20 µM of DCFH-DA (working solution) for 30 minutes in a dark environment at 37°C incubator, followed by incubation with various concentrations of H_2O_2 or ZnO nanoparticles for 24 hours (Lin, 2009). The fluorescence intensity from each well was measured as described in the first method.

http://dx.doi.org/10.14500/aro.10080

Method 3 (Coded as M3)

For the treatments, the steps in method 2 were followed. After the treatment with H_2O_2 or ZnO nanoparticles, the cells were washed twice with PBS to eliminate DCFH-DA that did not enter the cells (Song, 2010). One hundred µL of media was added to each well and the fluorescence intensity was measured as described in method 1.

Method 4 (Coded as M4)

On the day of the experiments, after removing the medium, the cells were washed twice with PBS and then treated with various concentrations of H_2O_2 or ZnO nanoparticles. After 24 hours of exposure to ZnO nanoparticles, the cells were washed twice with PBS and then incubated with 50 µL/well of 20 µM of DCFH-DA (working solution) for 30 minutes in a dark environment at 37°C incubator. The fluorescence intensity from each well was measured as described in method 1 (Lin, 2006; Ostrovsky, 2009).

III. Statistical Analysis

GraphPad PRISM® version 5.0 program was used for statistical analysis. Means and standard deviations were determined from six independent experiments. All comparisons were made using two-tailed Student's *t*-test and when positive indicated by asterisks (*p<0.05, **p<0.01 and ***p<0.001).

IV. Results and Discussion

A. Comparison of intracellular ROS detection methods

To obtain optimal results from intracellular ROS assay, two different cell lines such as normal lung (Hs888Lu) and lymphoma (U937) were used, because the quality of DCFH-DA relies on the cell types and culture conditions. In the presence of hydrogen peroxide (H_2O_2) and other ROS as well as heme protein catalysts such as peroxidases or cytochrome *c*, DCFH is oxidized to highly fluorescent DCF in cells (Burkitt and Wardman, 2001; Ischiropoulos, et al., 1999; LeBel, et al., 1992; Ohashi, et al., 2002). Thus, H_2O_2 was used as a positive control in this study to assess the reactivity of the probe and also to validate the method.

DCF- fluorescence intensity was measured (proportional to the intracellular ROS) in Hs888Lu and U937 cells exposed to H_2O_2 or ZnO according to the methods described earlier (Fig. 1 and Fig. 2). The results showed that different methods exhibit different pattern of ROS measurement. Higher amount of intracellular ROS was detected using method 2. H_2O_2 content increased the intensity of DCF- fluorescence in a dose-dependent manner. There were significant differences between intracellular ROS production in different cell lines. Using this method the percentages of fluorescence intensity were 164% and 1011% in Hs888Lu cell lines (p<0.05) and U937 cell lines (p<0.01) respectively after exposure to 200 µM H_2O_2 (Fig. 1 and Fig. 2).

Following methods 1, 3 and 4, the results did not indicate any change in DCF- fluorescence intensity thereafter in ROS measurements in selected cell lines exposed to H_2O_2 (Fig. 1 and Fig. 2).

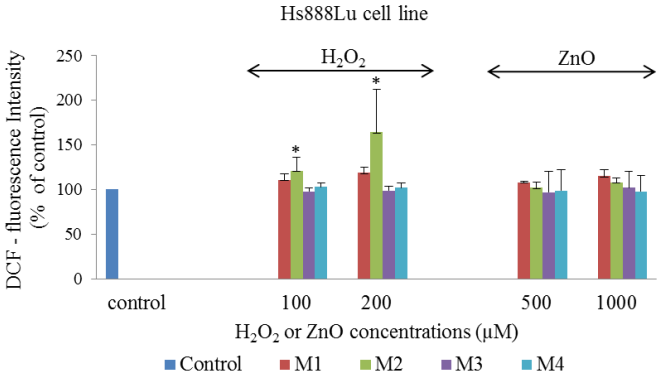

Fig. 1. Comparison of four methods (M1, M2, M3 and M4) to determine the intracellular ROS in Hs888Lu cell line. DCF-fluorescence intensities in Hs888Lu cell lines are exposed to different concentrations of H_2O_2 or ZnO. The control represents ROS measurement in non-treated cells.

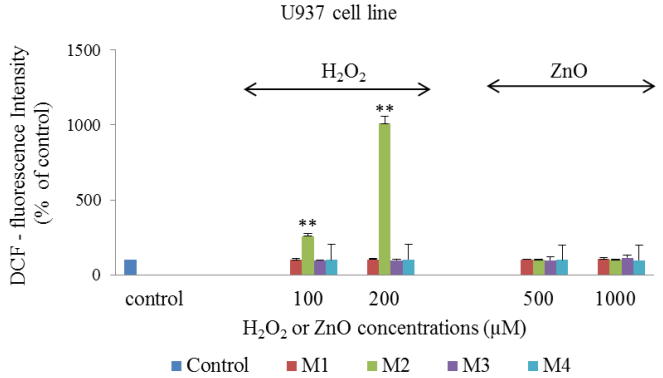

Fig. 2. Comparison of four methods (M1, M2, M3 and M4) to determine the intracellular ROS in U937 cell line. DCF-fluorescence intensities in U937 cell lines are exposed to different concentrations of H_2O_2 or ZnO. The control represents ROS measurement in non-treated cells.

After comparison of ROS-induction by H_2O_2 using the selected methods as a representative analysis of optimization experiments, ZnO nanoparticles – induced ROS in human cell lines was quantified according to the methods described earlier.

Following all methods 1, 2, 3 and 4, results did not show increase in DCF-fluorescence intensity in all cell lines compared to the control after exposure to 100 and 200µM ZnO nanoparticles (data not shown), but results showed 10% increase in DCF-fluorescence intensity in all cell lines compared to the control after exposure to ZnO nanoparticles (500 and 1000µM). Therefore, the results did not indicate significant changes in fluorescence intensity thereafter in ROS

measurements in a nanoparticle dose-dependent study (Fig. 1 and Fig. 2). In addition, hydrogen peroxide produced significant increase in DCF- fluorescence compared to ZnO nanoparticles under the experimental conditions of method 2.

Following methods 1, 3 and 4 results indicated that the H_2O_2 and ZnO were weak inducer of DCF-fluorescence in both cell lines (Fig. 1 and Fig. 2). In contrast, previous studies (Grabinski, 2007; Ostrovsky, 2009; Song, 2010) were demonstrated different pattern of the ROS measurement with the selected methods. In previous studies, mouse keratinocyte (HEL-30) cells exposed to H_2O_2 in a dose-dependent manner showed an increase in the ROS production according to the method 1 by Grabinski (2007). According to method 3, Song and co-workers (2010) have illustrated an increase in intracellular levels of ROS after exposure to all particle size of ZnO nanoparticles (30 nm, 100 nm) in mouse macrophage (Ana-1) cell line. Ostrovesky and co-workers (2009) have reported an increase in the fluorescence intensity of DCF in the normal human astrocyte and human glioma (U87) cell lines exposed to H_2O_2 according to method 4. In addition, they found an increase in the fluorescence intensity of DCF after 24 hours exposure to 10 mM ZnO nanoparticles in the human glioma (U87) cells. The ZnO nanoparticles induced a smaller increase in the fluorescence intensity of DCF in the normal astrocytes cells as a compared to H_2O_2 (positive control) (Ostrovsky, 2009).

Researchers in previous works used dilution of DCFH-DA in HBSS free of Ca^{2+} and Mg^{2+} (Li, et al., 2002; Reinisch, et al., 2000). Thus, the above methods (M1, M2, M3 and M4) were repeated using HBSS without Ca^{2+} and Mg^{2+}. The results (Data not shown) were very similar to the results shown in Fig. 1 and Fig. 2. This may imply that Ca^{2+} and Mg^{2+} in the medium of reaction were not contributing to the formation of DCF and thereafter to the intracellular ROS measurement.

It must be pointed out that the importance of the mechanisms and the possibilities that lead to the formation of highly fluorescent DCF must be carefully understood. Previous research works focused on the effects of endogenous and exogenous ROS in a variety of cell types, using 2′,7′-dichlorofluorescein diacetate (DCFH-DA) (Grabinski, 2007; Lin, 2009; Loetchutinat, 2005; Ohashi, 2002; Ostrovsky, 2009; Song, 2010; Xia, 2008; Xia, 2006).

Although there is clear evidence that DCFH-DA is de-acetylated to form DCFH by cellular esterase which is then oxidised to DCF by oxidising species in most cell lines. Some limitations of utilising this probe exist. Not all cell types possess sufficient esterase activity to produce the DCFH needed for accurate measurements of ROS. This may limit the availability of DCFH and result in an underestimation of intracellular ROS levels (Brubacher and Bols, 2001). In addition, DCF, oxidised fluorescent product of DCFH, is membrane permeable and can leak out of cells over time (Ubezio and Civoli, 1994). Incomplete DCF trapping may complicate interpretation of the data and hinder the precise evaluation of intracellular oxidation.

It remains unclear which reactive oxygen species are responsible for the oxidation of DCFH in cells, even though it is often assumed to be H_2O_2 (in the presence of cellular peroxidases and similar catalysts). It was reported that other biologically relevant ROS, including peroxynitrite and hydroxyl radicals (˙OH), can oxidize DCFH (Kooy, et al., 1997; Myhre, et al., 2003; Possel, et al., 1997). Others have found that DCFH showed rather low sensitivity towards oxidation by NO, $O_2^{\cdot -}$ (Myhre, 2003; Rota, 1999). Rota and co-workers (1999) implied that DCFH cannot be used to measure superoxide free radical formation in cells because the oxidation of this compound leads to the formation of superoxide. Moreover, some oxidants require small quantities which rapidly increase DCF formation, whereas other oxidants may need higher concentrations and more time (Myhre, 2003). In addition, H_2O_2 cannot oxidise DCFH directly. The oxidation occurs as a result of the reaction of H_2O_2 with cellular peroxidase, cytochrom *c*, or Fe^{2+} (LeBel, 1992; Rota, 1999; Royall and Ischiropoulos, 1993).

An important question is which reactive oxygen species induced from ZnO nanoparticles responsible for the oxidation of DCFH in biological systems? One of the possible mechanisms of free radical induction by ZnO nanoparticles was proposed by Ai and co-workers (2003) which is that sequential oxidation-reduction reaction may occur at ZnO particle surface to produce reactive species such as H_2O_2 and hydroxyl radical (Ai, 2003). Some limitations of utilising this probe exist, even though it is often assumed that H_2O_2 (in presence of cellular peroxidases and similar catalysts) and hydroxyl radicals (˙OH) can oxidise DCFH (Ai, 2003).

V. Conclusion

This comparative analysis found different results for the measurements of ROS depending on which method was used, although same concentrations of H_2O_2 and DCFH-DA, same cells lines and cell culture conditions were used. The methods are varying in the step sequence of exposure to DCFH-DA and H_2O_2 or ZnO, elimination of DFH-DA and termination of DCF. There are several significant factors affecting the measurements such as the timing of loading DCFH-DA to the reaction, duration of DCFH-DA incubation and the oxidative species responsible for the oxidation of DCFH. All these will have an impact on the formation of DCF and thereafter on the intracellular ROS measurement. Our data show that the higher amounts of intracellular ROS were detected after exposure to H_2O_2 using method 2. In addition, there is no evidence of ROS production due to ZnO nanoparticle toxicity in lymphoma and normal lung cell lines.

Acknowledgment

This study is supported by Institute of Science (IOS) research grant, Universiti Teknologi MARA/ Malaysia.

REFERENCE

Ai, H., Bu, Y., and Han, K., 2003. Glycine-Zn+/Zn2+ and their hydrates: On the number of water molecules necessary to stabilize the switterionic glycine-Zn+/Zn2+ over the nonzwitterionic ones. *Journal of Chemical Physics*, 118 (24), pp.10973-10985 .

Brubacher, J.L., and Bols, N.C., 2001. Chemically de-acetylated 2',7'-dichlorodihydrofluorescein diacetate as a probe of respiratory burst activity in mononuclear phagocytes. *Journal of Immunological Methods*, 251(1-2), pp.81-91.

Burkitt, M.J., and Wardman, P., 2001. Cytochrome c is a potent catalyst of dichlorofluorescin oxidation: Implications for the role of reactive oxygen species in apoptosis. *Biochemical and Biophysical Research*, 282(1), pp.329-333.

Curtin, J.F., Donovan, M., and Cotter, T.G., 2002. Regulation and measurement of oxidative stress in apoptosis. *Journal of Immunological Methods*, 265(1-2), pp.49-72.

Donaldson, K., Stone, V., Borm, P.J., Jimenez, L.A., Gilmour, P.S., Schins, R.P., Knaapen, A.M., Rahman, I., Faux, S.P., Brown, D.M., and MacNee, W., 2003. Oxidative stress and calcium signaling in the adverse effects of environmental particles (PM10). *Free Radical Biology and Medicine*, 34 (11), pp.1369-1382.

Foucaud, L., Wilson, M.R., Brown, D.M., and Stone, V., 2007. Measurement of reactive species production by nanoparticles prepared in biologically relevant media. *Toxicology Letters*, 174(1-3), pp.1-9.

Grabinski, C., Hussain, S., Lafdi, K., Braydich-Stolle, L., and Schlager, J., 2007. Effect of particle dimension on biocompatibility of carbon nanomaterials. *Carbon*, 45(14), pp.2828-2835.

Ischiropoulos, H., Gow, A., Thom, S.R., Kooy, N.W., Royall, J.A., and Crow, J.P., 1999. Detection of reactive nitrogen species using 2,7-dichlorodihydrofluorescein and dihydrorhodamine 123. *Methods in Enzymology*, 301, pp.367-373.

Kooy, N., Royall, J., and Ischiropoulos, H., 1997. Oxidation of 2',7'-dichlorofluorescein by peroxynitrite. *Free Radical Research*, 27(3), pp.245-254.

LeBel, C.P., Ischiropoulos, H., and Bondy, S.C., 1992. Evaluation of the probe 2‘,7‘-dichiorofluorescin as an indicator of reactive oxygen species formation and oxidative stress. *Chemical Research in Toxicology*, 5(2), pp.227-231.

Li, N., Xia, T., and Nel, A.E., 2008. The role of oxidative stress in ambient particulate matter-induced lung diseases and its implications in the toxicity of engineered nanoparticles. *Free Radical Biology and Medicine*, 44(9), pp.1689-1699.

Li, Y., Nishimura, T., Teruya, K., Maki, T., Komatsu, T., Hamasaki, T., Kashiwagi, T., Kabayama, S., Shim, S.Y., Katakura, Y., Osada, K., Kawahara, T., Otsubo, K., Morisawa, S., Ishii, Y., Gadek, Z., and Shirahata, S., 2002. Protective mechanism of reduced water against alloxan-induced pancreatic β-cell damage: Scavenging effect against reactive oxygen species. *Cytotechnology*, 40(1-3), pp.139-149.

Lin, W., Huang, Y., Zhou, X.D., and Ma, Y., 2006. In vitro toxicity of silica nanoparticles in human lung cancer cells. *Toxicology and Applied Pharmacology*, 217(3), pp.252-259.

Lin, W., Xu, Y., Huang, C.C., Ma, Y., Shannon, K.B., Chen, D.-R., and Huang, Y.-W., 2009. Toxicity of nano- and micro-sized ZnO particles in human lung epithelial cells. *Journal of Nanoparticle Research*, 11(1), pp.25-39.

Loetchutinat, C., Kothan, S., Dechsup, S., Meesungnoen, J., Jay-Gerin, J.-P., and Mankhetkorn, S., 2005. Spectrofluorometric determination of intracellular levels of reactive oxygen species in drug-sensitive and drug-resistant cancer cells using the 2',7'-dichlorofluorescein diacetate assay. *Radiation Physics and Chemistry*, 72(2-3), pp.323-331.

Myhre, O., Andersen, J.M., Aarnes, H., and Fonnum, F., 2003. Evaluation of the probes 2',7'-dichlorofluorescin diacetate, luminol, and lucigenin as indicators of reactive species formation. *Biochemical Pharmacology*, 65(10), pp.1575-1582.

Najim, N., Rusdi, R., Zain, M.M., Hamzah, A.S., Shaameri, Z., and Kamarulzaman, N., 2014. Effects of the absorption behaviour of ZnO nanoparticles on the optical measurements of cytotoxicity studies: In normal and cancer cell lines. *Journal of Nanomaterials*, 2014, pp.1-8.

Oberdorster, E., 2004. Manufactured nanomaterials (fullerenes, C60) induce oxidative stress in the brain of juvenile largemouth bass. *Environmental Health Perspectives*, 112(10), pp.1058-1062.

Ohashi, T., Mizutani, A., Murakami, A., Kojo, S., Ishii, T., and Taketani, S., 2002. Rapid oxidation of dichlorodihydrofluorescin with heme and hemoproteins: formation of the fluorescein is independent of the generation of reactive oxygen species. *FEBS Letters*, 511(1-3), pp.21-27.

Ostrovsky, S., Kazimirsky, G., Gedanken, A., and Brodie, C., 2009. Selective cytotoxic effect of ZnO nanoparticles on glioma cells. *Nano Research*, 2(11), pp.882-890.

Possel, H., Noack, H., Augustin, W., Keilhoff, G., and Wolf, G., 1997. 2',7'-Dihydrodichlorofluorescein diacetate as a fluorescent marker for peroxynitrite formation. *FEBS Letters*, 416(2), pp.175-178.

Reeves, J.F., Davies, S.J., Dodd, N.J.F., and Jha, A.J., 2008. Hydroxyl radicals (•OH) are associated with titanium dioxide (TiO2) nanoparticle induced cytotoxicity and oxidative DNA damage in fish cells. *Mutation Research*, 640(1-2), pp.113-122.

Reinisch, N., Wiedermann, C.J., and Ricevuti, G., 2000. Inhibition of human peripheral blood neutrophil respiratory burst by alcohol-based venipuncture site disinfection. *Clinical and Diagnostic Laboratory Immunology*, 7(6), pp.980-982.

Rota, C., Chignell, C.F., and Mason, R.P., 1999. Evidence for free Radical Formation during the oxidation of 2'-7'-dichlorofluorescin to the fluorescent dye 2'-7'-dichlorofluorescein by horseradish peroxidase: possible implications for oxidative stress measurements. *Free Radical Biology and Medicine*, 27(7), pp.873-881.

Royall, J., and Ischiropoulos, H., 1993. Evaluation of 2',7'-dichlorofluorescein and dihydrorhodamine 123 as fluorescent probes for intracellular H2O2 in cultured endothelial cells *Archives of Biochemistry and Biophysics*, 302(2), pp.348-355.

Rusdi, R., Rahman, A., Mohamed, N., Kamarudin, N., and Kamarulzaman, N., 2011. Preparation and band gap energies of ZnO nanotubes, nanorods and spherical nanostructures. *Powder Technology*, 210(1), pp.18-22.

Sharma, V., Shukla, R.K., Saxena, N., Parmar, D., Das, M., and Dhawan, A., 2009. DNA damaging potential of zinc oxide nanoparticles in human epidermal cells. *Toxicology Letters*, 185(3), pp.211-218.

Song, W., Zhang, J., Guo, J., Zhang, J., Ding, F., Li, L., and Sun, Z., 2010. Role of the dissolved zinc ion and reactive oxygen species in cytotoxicity of ZnO nanoparticles. *Toxicology Letters*, 199(3), pp.389-397.

Ubezio, P., and Civoli, F., 1994. Flow cytometric detection of hydrogen peroxide production induced by doxorubicin in cancer cells. *Free Radical Biology and Medicine*, 16(4), pp.509-516.

Wang, H., and Joseph, J.A., 1999. Quantifying cellular oxidative stress by dichlorofluorescein assay using microplate reader. *Free Radical Biology and Medicine*, 27(5-6), pp.612-616.

Winterbourn, C.C., and Sutton, H.C., 1984. Hydroxyl radical production from hydrogen peroxide and enzymatically generated paraquat radicals: Catalytic requirements and oxygen dependence. *Archives of Biochemistry and Biophysics*, 235(1), pp.116-126.

Xia, T., Kovochich, M., Liong, M., Madler, L., Gilbert, B., Shi, H., Yeh, J.I., Zink, J.I., and Nel, A.E., 2008. Comparison of the mechanism of toxicity of zinc oxide and cerium oxide nanoparticles based on dissolution and oxidative stress properties. *ACS nano*, 2(10), pp.2121-2134.

Xia, T., Kovochich, M., and Nel, A., 2006. The role of reactive oxygen species and oxidative stress in mediating particulate matter injury. *Occupational and Environmental Medicine*, 5(4), pp.817-836.

In Vitro Screening of Antibacterial Properties of *Rhus coriaria* and *Origanum vulgare* Against Some Pathogenic Bacteria

Hêro F.S. Akrayi, Rebwar M.H. Salih and Pishtiwan A. Hamad

Department of Biology, College of Education, Salahaddin University–Erbil, Kurdistan Region of F.R. Iraq

***Abstract*—This study investigates the antibacterial property of *Rhus coriaria* (Sumac) and *Origanum vulgare* (Jatra) aqueous extracts against *Escherichia coli* ATCC 25922, *Klebsiella pneumoniae*, *Proteus mirabilis* and *Pseudomonas aeruginosa* ATCC 27835. Results confirm the resistance of the bacterial isolates against more than three antibiotics. The aqueous extract of *R. coriaria* showed the highest activity as an inhibitor against tested bacteria, while the aqueous extract of *O. vulgare* shows low effect against the above mentioned bacteria. MIC for *R. coriaria* and *O. vulgare* aqueous extracts were determined for four bacterial isolates. The MIC of *O. vulgare* against tested bacteria was >12%, while the MIC of *R. coriaria* was 4% for *E. coli*, <0.025% for both *K. pneumoniae* and *P. mirabilis* and 2% for *P. aeruginosa*. The phytochemical groups of both plants extract were analyzed; the results indicated both plants contain tannins, phenols and saponins, flavonoid, alkaloid, and phlobatanin. The antimitotic effect of both plants extracts were investigated on *Allium cepa*, and the extracts showed inhibitory role in the root growth in contrast to the control when grown in the tap water for 5 days. In addition, the 24 hours treatment of grown roots in tap water with both extracts resulted in significant decrease in mitotic index.**

***Index Terms*—Antibacterial agents, antimitotic index, *E. coli*, *K. pneumoniae*, plant extracts, *P. aeruginosa*, *P. mirabilis*.**

I. Introduction

Due to the rapid increase in the rate of infections, antibiotic resistance in microorganism increase, in addition to the side effects that are caused by synthetic antibiotics (Levy and Marshall, 2004), medicinal plants are gaining popularity over these drugs. The use of plants in medicine goes far back as thousands of years and continues today. Plants integrate incorporate substances that have potential therapeutic values for the cure of disease. These natural products from plants including saponin, alkaloids, tannins, cardiac glycosides and anthraquinones, are synthesized for defense purposes (Adebisi and Ojokoh, 2011). Medicinal plants have been found useful in the cure of a number of diseases including bacterial diseases, because they are a rich source of antimicrobial agents. Although medicinal plants lead to slow recovery, the therapeutic use of medicinal plant is becoming popular because of their lesser side effects and low resistance in microorganisms (Solanki, 2010). Antibiotic resistant bacteria may keep people sick longer, and sometimes people are unable to recover at all. Because of the concerns about the side effects of conventional medicine, the use of natural products as an alternate to conventional treatment in healing and treatment of various diseases has been on the rise in the last few decades (Frieden, 2013). The exchanging of genetic material between microorganisms through transformation, conjugation or transduction processes or may by mobile genes (transposons) have been proposed as a major contribution in the rapid evolution of microorganisms resistance to antibiotics. On the other hand using inaccurate concentrations of antibiotics or drugs or unnecessary of medicine appointment (medical checkups) lead to the resistance to multiresistance, in addition to weakening the immune system in some human due to poor nutrition or hereditary factors make bacteria to be more resistant (Salah, 2007; Levy and Marshall, 2004). Increasing of infections based on antibiotic resistant microorganisms call for new strategies and use of natural antimicrobials (Keskin and Toroglu, 2011).

People need to be documented and investigated for modern therapeutics. Due to lack of modern medical facilities, expensive drugs and poor transportation, patients of these localities normally suffer for a long. In these unfavorable situations, traditional herbal therapeutics of these remote locations plays a vital role to provide them with alternative sources of therapeutic facilities for their primary healthcare. Subsequently, with the advanced in the techniques of phytochemistry and pharmacology, a number of active ingredients of medicinal plants were isolated and introduce as valuable drugs in medicine (Kumari, *et al.*, 2011).

ARO, The Scientific Journal of Koya University
Volume III, No 2(2015), Article ID: ARO.10085, 07 pages
DOI: 10.14500/aro.10085
Received 27 April 2015; Accepted 20 September 2015
Regular research paper: Published 2 December 2015
Corresponding author's e-mail: hero.salah@su.edu.krd

R. coriaria (Anacardiaceae) is a notoriously used in the Mediterranean region and Middle East as a spice, sauce and drink. The fruits have been reported to possess antimicrobial and antioxidant properties (Kossah, *et al.*, 2009). *O. vulgare* L. is a perennial, aromatic, hairy herb; belonging to Lamiaceae family. It is one of the most popular herbs that have widely been used in Mediterranean cooking. It is traded both as 'whole' dried leaves and in ground form. The leaves and dried herb of Oregano as well as its essential oil are used medicinally. The volatile oil of Oregano has been used traditionally for respiratory disorders, indigestion, dental caries, rheumatoid arthritis and urinary tract illnesses (Shivali and Kamboj, 2009; AL–Neemy and AL–Jebury, 2006). Mitosis is a process of cell division, it occurs in the somatic cells, and it is meant for the multiplication of cell number during embryogenesis and blastogenesis of plant and animals. An agent that prevents or disrupts mitosis is called as antimitotic agent, so that beneficial in life threatening diseases like cancer. Anti-mitotic constituents can stop the mitosis anywhere in the cell cycle (Gaikwad, *et al.*, 2011).

This study was conducted to investigate the possible antibacterial at different concentrations and antimitotic activity of the Sumac and Oregano extracts against four isolates of pathogenic bacteria.

II. Materials and Methods

A. Bacterial Strains

The bacterial strains used in this study were *E. coli* ATCC 25922, *P. aeruginosa* ATCC 27835, *K. pneumoniae* (was obtained from Lab of Bacteriology, Erbil Teaching Hospital) and *P. mirabilis* was obtained from Microbiology Lab, Department of Biology, College of Education.

B. Phytochemical Screening of Extract

The methods described by (Odebiyi and Sofowora, 1978; Salna, *et al.*, 2011) are used to test for the presence of saponins, tannins, alkaloids, flavonoids and in the test samples.

Saponins

Each of the plant extracts (0.5 g) was separately stirred in a test tube, foaming which persisted on warming was taken as an evidence for the presence of saponins (Odebiyi and Sofowora, 1978).

Tannins

Extract of each sample (0.5 g) was separately stirred with 10ml of distilled water and then filtered. To the filtrate two drops of 5% Iron (III) Chloride ($FeCl_3$) reagent was added. Blue–black or blue–green coloration or precipitate was taken as an indication of the presence of tannins (Odebiyi and Sofowora, 1978).

Alkaloids

Extract of each plant sample (0.5 g) was separately stirred with 1% hydrochloric acid (HCl) on a steam bath. The solution obtained was filtered and 1ml of the filtrate was treated with two drops of Mayer's reagent. The two solutions were mixed and made up to 100 ml with distilled water. Turbidity of the extract filtrate on addition of Mayer's reagent was regarded as evidence for the presence of alkaloids in the extracts (Odebiyi and Sofowora, 1978).

Phenols

Two ml of test solution, added alcohol and then few drops of neutral ferric chloride solution were added. The test result was observed (Odebiyi and Sofowora, 1978).

Quinones

To the test substance, sodium hydroxide was added. Blue green or red color indicates the presence of Quinone (Odebiyi and Sofowora, 1978).

Flavonoids

Four ml of extract solution was treated with 1.5 ml of 50% methanol solution. The solution was warmed and metal magnesium was added. To this solution, 5–6 drops of concentrated hydrochloric acid was added and red color was observed for flavonoids and orange color for flavones (Salna, *et al.*, 2011).

Anthroquinone

About 0.5 g of the extracts was boiled with 10% HCl for few minutes in a water bath. It was filtered and allowed to cool. Equal volume of $CHCl_3$ was added to the filtrate. Few drops of 10% NH_3 were added to the mixture and heated. Formation of rose–pink color indicates the presence of anthraquinones (Salna, *et al.*, 2011).

C. Plant Extraction for Antibacterial and Antimitotic Experiments

Collection and Preparation of Plant Sample

The plants Sumac and dry Oregano were purchased from market in Erbil city, Iraq. Sumac was converted into powder by using mortar (household flourmill), then the ground (extract powder) plant was separated from its stone form (dry powder), while dry Oregano was ground and both were stored in polyethylene bags in the refrigerator at 4˚C for further processing.

Extracts Preparation

Three hundred ml of sterilized distilled water was added to 30 g of ground dried plant, heated below the boiling point and stirred for 2 ½–3 hrs. The extract was filtered by muslin cloth, then by filter paper (Whatman No. 1) and then stored in the refrigerator at 5 ˚C for using (modified method of Babpour, *et al.*, 2009).

D. Sensitivity to Antimicrobial Agents

Antimicrobial susceptibility testing for isolates was done following Kirby–Bauer disk diffusion method by using fifteen different antimicrobial agents as mentioned in Table I.

E. Screening of Antibacterial Activity

The antimicrobial assay was performed using the standard procedure as described (Bauer and Kirby, 1966) with some modifications. The previously prepared inoculums were adjusted to 0.5 McFarland standards, which are equal to 1×10^8 CFU/ml and then 0.1 ml was transferred to Mueller Hinton agar (MHA) plates and spread with cotton swabs. One hundred microliters of extract were poured on wells with 8 mm diameter made by cork borer in MHA. Inoculated plates were incubated at 37 ˚C overnight. After incubation period for 24 hours, the inhibition zone diameters (mm) were measured.

F. Measurement of minimal inhibition concentration (MIC) using agar well diffusion technique

According to NCCLS agar dilution method (Alderman and Smith, 2001), the MIC of plant extracts was tested with some modifications. Briefly, a series dilution of each extract ranging from (0.025%, 0.05%, 1% (v: v) to 10% (v: v)) was prepared with Mueller Hinton agar media. Bacterial strains grown on nutrient agar at 37°C for 18 hours were suspended in a saline solution (0.85% NaCl) and adjusted to a turbidity of 0.5 McFarland standards. Briefly, 50 µl inoculum was used to inoculate 90 mm diameter petri plates containing 25 ml Mueller Hinton Agar, with a sterile nontoxic cotton swab on a wooden applicator. Wells with 6 mm diameter were punched in the agar and filled with 100 µl extract solution. Inoculated plates were incubated at 37 ˚C for 24 hrs. Minimum inhibitory concentrations (MICs) were determined as lowest concentration of extracts by measuring the inhibition zones which are produced by inoculated bacteria (Oskay *et al.*, 2009).

G. Antimitotic Activity

Local *A. cepa* test has been used for evaluating cytotoxicity of substances, small onion bulbs were cultivated on top of test tubes filled with the aqueous extracts. Tap water was used as a control. The test tubes were kept in an incubator at 24±2 ˚C and the test samples were changed daily. After 5 days the roots were counted and their lengths were measured for each onion. The above step was repeated by cultivating the onion bulbs on top of test tubes filled with tap water, when the roots were about 5 mm long the bulbs were placed on test tubes containing the extracts such that the roots were immersed in the extracts. The duration of extract treatments for each bulb was 24 hrs. Three bulbs were used for each extract at the whole duration of the treatment. The sprouted roots were also treated with distilled water (Control group). The root tips were cut and transferred for fixation. The fixative was glacial acetic acid/absolute alcohol (1/3 v/v). The root tips were kept in the aceto–alcohol solution for 24 hrs. For mitotic effect examination, slides were prepared by putting the plant root tips into a watch glass to which 9 drops of Giemsa and 1 drop of 1 M HCl were added and warmed over a flame of spirit lamp for 2–3 min. These were kept at room temperature for 15–30 min. After removing the root caps from well stained root tips, 1 mm of the mitotic zones were immersed in a drop of %45 acetic-acid on a clean slide and squashed under a cover glass. In order to spread the cells evenly on the surface of the slide, squashing was accomplished with a bouncing action by striking the cover glass with a matchstick (Ozzmen, *et al.,* 2007).

H. Statistical analysis

The data obtained from antimitotic activity of mentioned plant extracts were analyzed using one–way analysis of variance (ANOVA). The level of significance was determined in comparison with the control group. Statistical significance was accepted for $p<0.01$.

MI was expressed in terms of divided cells/ total cells. A statistical analysis was performed on the collected data. The means of the control and extracts were obtained from descriptive. Mitotic index was calculated using the following formula and all experiments were applied in triplicates:

$$Mitotic\ Index = \frac{Number\ of\ Dividing\ Cell}{Total\ Number\ of\ Cells} \times 100 \qquad (1)$$

III. Results

The results of antibiotic susceptibility in the present study, as elucidated in Table I, showed that tested bacterial isolates were resisting to most antibiotics. *E. coli* ATCC 25922 was resistant to each of AK, AMC, CTR, CE, DO, G, NIT, NV and TE, intermediate to MY and TIC and susceptible to CFM, OB, ME, and PRL. *K. pneumoniae* was resistant to AMC, DO, G, NIT, NV and TE, intermediate to CTR, MY and TIC and susceptible to AMC, CFM, CE, OB, ME, and PRL antibiotics.

TABLE I
RESISTANCE OF BACTERIA UNDER STUDY TO ANTIBIOTICS

Antibiotics µg/disc	Zone of inhibition (mm)			
	E. coli ATCC 25922	*K. pneumonia*	*P. aeruginosa* ATCC 27835	*P. mirabilis*
Amikacin (A)30	R	R	R	R
Amoxicillin- acid 30 (AMC)	R	S	R	S
Cefixime (CFM)5	S	S	S	S
Ceftriaxone (CTR)30	R	M	R	S
Cephradine (CE)30	R	S	S	S
Cloxacillin (OB)5	S	S	S	S
Doxycycline (DO)30	R	R	R	R
Gentamycin (G)10	R	R	R	R
Lincomycin (MY) 15	M	M	S	R
Methicillin (ME)10	S	S	S	S
Nitrofurantoin (NIT) 300	R	R	R	R
Novobiocin (NV)30	R	R	S	R
Pipercillin (PRL)100	S	S	S	S
Tetracycline (TE)30	R	R	R	R
Ticarcillin (TIC)75	M	M	R	S

R: Resistant, M: Intermediate or Moderate of Resistant, S: Sensitive.

 http://dx.doi.org/10.14500/aro.10085

P. aeruginosa ATCC 27835 was resistant to AK, AMC, CTR, DO, G, NIT, TE and TIC, and was susceptible to CFM, CE, OB, MY, ME, NV and PRL antibiotics. While *P. mirabilis* was resistant to AK, DO, G, MY, NIT, NV and TE and was susceptible to AMC, CFM, CTR, CE, OB, ME, PRL and TIC antibiotics.

A. Antibacterial activity of R. coriaria and O. vulgare

The antibacterial activity of aqueous extracts of *R. coriaria* and O. vulgare plants against each isolates of *E. coli* ATCC 25922, *P. aeruginosa* ATCC 27835, *K. pneumoniae* and *P. mirabilis* as clarified in Table II; the aqueous extract of *R. coriaria* demonstrates the high activity playing the role of inhibitory agent against tested bacteria, while the aqueous extract of O. vulgare show less effects against bacterial isolates, on the other hand the tested bacteria showed a variation in their susceptibility for these extracts. MIC of aqueous extract of both plants was determined for all bacteria, where the MIC of O. vulgare against all bacteria was 12%, while the MIC of *R. coriaria* was 4% for *E. coli* ATCC 25922, 2% for *P. aeruginosa* ATCC 27835 and 0.025% for both *K. pneumoniae* and *P. mirabilis*.

TABLE II
ANTIBACTERIAL ACTIVITY OF *R. CORIARIA* AND *O. VULGARE* AQUEOUS EXTRACT AGAINST TESTED BACTERIA

Scientific Name	Concentration					MIC (V:V) %
	Zone of inhibition/mm *R. coriaria*					
	100 %	75 %	50 %	25 %	12.5 %	
E. coli ATCC 25922	30	29	28	24	20	4
K. pneumoniae	30	26	20	19	17	<0.025
P. aeruginosa ATCC 27835	30	26	24	22	22	2
P. mirabilis	28	25	25	23	20	<0.025
	Zone of inhibition/mm *O. vulgare*					
E. coli ATCC 25922	18	17	15	-	-	12
K. pneumoniae	13	-	-	-	-	12
P. aeruginosa ATCC 27835	18	18	15	13	-	12
P. mirabilis	-	-	-	-	-	12

(-) : Inhibition zone not appeared.

Table III shows the phytochemical groups of both plant extracts, in which the tested plants contain tannins, phenols, saponins, flavonoid, alkaloid, while both plants do not contain anthraquinone and quinone.

TABLE III
PHYTOCHEMICAL SCREENING OF BOTH PLANT AQUEOUS EXTRACTS

Plant Extract	Tanin	Phenol	Quinone	Anthraquinone	Alkaloid	Flavonoid	Saponin
R. coriaria	+	+	-	-	+	+	+
O. vulgare	+	+	-	-	+	+	+

+: Positive (present), -: Negative (absent)

B. Antimitotic Effect of Aqueous extract of both R. coriaria and O. vulgare

Table IV illustrates the antimitotic effect of aqueous extract of both *R. coriaria* and O. vulgare on *A. cepa*, in comparison with control; the onions that treated with the extracts for 5 days did not show any growth in roots, in addition to those that treated with the mentioned extracts for 24 hours showed a significant decreasing in mitotic index.

TABLE IV
THE AVERAGE OF ROOT LENGTHS AND NUMBERS IN CONTROL AND IN EXTRACTS AFTER 5 DAYS AND MITOTIC INDEX AFTER 1 DAY

Extract	Average of Roots Number (±SD)	Average of Roots Length/ cm (±SD)	MI% (±SD)
Control	16±1	7± 2.64	70 ± 6.55
R. coriaria	-	-	29.19 ±1.84
O. vulgare	-	-	15 ± 2.63

IV. DISCUSSION

To help characterizing the evolution of drug resistance in tested bacteria since antimicrobial drugs were first widely used, we tested existing strain collections of *E. coli*, *K. pneumoniae*, *P. aeruginosa* and *P. mirabilis* for their susceptibility to a common panel of 15 antibiotic agents, and for treatment of bacterial infections, antibiotics are widely used and this has led to the emergence and spread of resistant bacterial strains. The appearance of multiple drug resistant bacteria has become a major cause of failure of the treatment of infectious disease (Ibrahim, *et al.*, 2011). The resistance of bacteria may return to overuse, abuse, and misuse of antibiotics and also bacteria different mechanisms as efflux pump to protect it selves (Coyle, 2005; Lewis *et al.*, 2002). Resistant bacteria might have antibiotic resistance genes carried on either their DNA chromosome or on plasmids. It is well known that plasmids are major vectors for the dissemination of both antibiotic resistance and virulence determinants among bacterial populations (Hamada, *et al.*, 2008). The other major factor in the growth of antibiotic resistance is spread of the resistant strains of bacteria from person to person, or from the non-human sources in the environment, including food (Frieden, 2013).

The rapid spread of bacteria expressing multidrug resistance (MDR) has necessitated the discovery of new antibacterial and resistance modifying agents (Tariro and Stanley, 2011). Since the initial discovery of bacterial efflux pumps in the 1980s, many have been characterized in community and hospital acquired pathogens, (Stavri, *et al.*, 2007). Efflux pumps are able to extrude structurally diverse compounds, including antibiotics used in a clinical setting, rendering the drugs therapeutically ineffective (Amusan, *et al.*, 2007). Antibiotic resistance can develop rapidly through changes in the expression of efflux pumps. It is, therefore, imperative that new antibiotics, resistance-modifying agents and, more specifically, efflux pump inhibitors (EPIs) are characterized (Stermitz, *et al.*, 2000). The use of bacterial resistance modifiers such as EPIs could facilitate the re-introduction of

therapeutically ineffective antibiotics back into clinical use and might even suppress the emergence of MDR strains (Stavri, *et al*., 2007).

In the present study, *E. coli* was resist to Amikacin, Amoxiclave, Ceftriaxone, Cephradine, Doxycycline, Gentamycin, Nitrofurantoin, Novobiocin and Tetracycline. Daniel *et al.* (2012) demonstrated that the isolates of *E. coli* show the different percentage of resistance against Sulfonamide, Tetracycline, Chloramphenicol, Gentamycin, extended spectrum cephalosporins (Ceftiofur and Ceftriaxone) and they clarified the resistant genes are commonly associated with mobile genetic elements, and these elements play a major role in dissemination of multiple antimicrobial drug resistance genes in *E. coli* isolates. Schito, *et al*, (2009) testified in their research that among 2315 isolates of *E. coli*, 48.3% show resistance to Amoxiclave, 3.8% to Ampicillin, 2.4% to Cefotaxime, 8.6% to Nalidixic acid, 8.1% to Ciprofloxacin, 29.4% to Sulphamethaxazole–Trimethoprim and 1.6% to Nitrofurantoin. *In vitro* data showed a wide range of resistant of *K. pneumoniae* toward beta lactams, aminoglycosides, quinolones and other antibiotics, which we found that *K. pneumoniae* resist to Amoxiclave, Doxycycline, Gentamycin, Nitrofurantoin, Novobiocin and Tetracycline antibiotics. Toroglu and Keskin (2011) demonstrate that resistance rate of twenty two isolates of *K. pneumoniae* which collected from urine, vaginal fluid, wound, cerebrospinal fluid and blood against eleven antibiotics were 95% to Penicillin G, 82% to Amoxiclave, 77% to Ceftazidime, 59% to Ceftriaxone and Tetracycline, 46% to Gentamycin, 332% to Nitrofurantoin, 27% to Cefoxitin and Ofloxacin, 23% to Sulphamethaxazole–Trimethoprim and 19% to Chloramphenicol. Plasmid encoded resistance to broad spectrum cephalosporins is becoming a widespread phenomenon in clinical medicine. These antibiotics are inactivated by an array of different extended spectrum beta lactamases (ESBLs) which have evolved by stepwise mutation of TEM/SHV type beta lactamases. Plasmid encoding these enzymes has been encountered in several members of the family Enterobacteriaceae, but are, for unknown reasons, most often harbored by *K. pneumoniae* (Sikarwar and Batra, 2011). In concordance to these results, Egbebia and Famurewa (2011) study on 970 samples which collected from urine, high vaginal swab, blood, ear, sputum, pus, cerebrospinal fluid, semen, stool and nasal fluids. Among of all samples they detected 544 isolates of *K. pneumoniae* (56.1%), when 120 isolates (96%) resist to Cefixime, 117 (93.6%) to Amoxiclave, 109 (87.2%) to Cefotaxime, and 106 (84.4%) to Cefadroxil. In the other hand, Ghafourian *et al.*, (2011) isolated and identified 113 isolates of *K. pneumoniae* which taken from respiratory tract infections (RTIs). They found that 19 isolates (28.3%) resist to Amikacin, 67 (100%) to Amoxiclave, 62 (92.5%) to Cefixime, 46 (68.6%) to Cefotaxime, 11 (16.4%) to Ciprofloxacin, 62 (92.5%) to Cefoperazone and 0.00% to Imipenem.

Increasing resistance to different anti–pseudomonal drugs particularly among hospital strains has been reported world–wide and this is a serious therapeutic problem in the management of diseases due to these organisms. The resistance profiles of *P. aeruginosa* to the fifteen antimicrobial agents tested varied among the isolates investigated. One striking feature in this study was that all the *P. aeruginosa* isolates were found to resist Amikacin, Amoxiclave, Ceftriaxone, Doxycycline, Gentamycin, Nitrofurantoin, Tetracycline and Ticarcillin antibiotics. Younis (2011) reported that 397 samples (13.8%) are positive growths of bacterial genera among 2872 patients were admitted with clinical diagnosis of neonatal sepsis. *P. aeruginosa* comprise with 14 (3.5%). He reported that the resistance percent to Amoxiclave was 86%, Gentamycin 71%, Amikacin 29%, Cefoperazone 43%, Cefixime 86%, Cefotaxime 43%, Imipenem 28.5% and the rates of resistances of Ciprofloxacin was 36%. The cause of the multi–drug resistant among *P. aeruginosa* strains due to: First, including the community acquired isolates of *P. aeruginosa* along with hospital isolates would have provided a much better picture of resistance patterns of strains in this geographical area. Second, molecular typing and plasmid profile of the *P. aeruginosa* isolates would provide the much needed details about the strains and lastly extended spectrum beta lactam (ESBL) producing *P. aeruginosa* which have become a major cause of nosocomial infections with MDR strains should be analyze (Anil and Shahid, 2013). While *P. mirabilis* was resistant to Amikacin, Doxycycline, Gentamycin, Lincomycin, Nitrofurantoin, Novobiocin and Tetracycline antibiotics. The main problem associated with infections caused by biofilm forming bacteria is the low sensitivity of the *P. mirabilis* to the antimicrobials used and there exists a possible level of correlation between the ability of the *P. mirabilis* to form biofilm and the isolation site of the strain (Wasfi, *et al.*, 2012).

The antibacterial activity of aqueous extract of *R. coriaria* was the most effective against bacteria and this could be linked to the chemical constitutes of the plant including the phytochemical groups and the rate of these substances in screened extracts, where most of these groups have the antibacterial properties (Cowan, 1999). Plants have formed the basis of classy traditional medicine system and natural products make excellent lead for new drug development. The World Health Organization (WHO) is encouraging, promoting and facilitating the effective use of herbal medicine in developing countries for health programs (Ibrahim, *et al.*, 2011). *R. coriaria* contains phenols, tannins, and as in many research explained the action of hydrophobic property of phenolic compounds in impairing the cellular function and membrane integrity as mentioned in (Seyyednejad, *et al.*, 2008) and also interpreted that the aqueous extracts of *R. coriaria* and *O. vulgare* have contain phenols, tannins and others integrates and these may have influence on enzymatic system of bacteria especially those that prevent the plasmid replication or may affected on cell membrane specially on mesosome which is considered as the attachment point for plasmids. The effect of tannins may be related to their ability to inactivate microbial adhesions, enzymes, and cell envelope transport proteins, etc. they also complex with polysaccharide (Ya *et al.*, 1989). Sumac is rich in water soluble tannins, and the antimicrobial activity of tannins is well documented

(Salna, *et al.*, 2011). Roopashree *et al.*, (2008) have demonstrated that not only the organic acids but also the other substances in water extracted sumac were found to be effective antimicrobial agents. It is generally believed that the fully protonated species of organic acids can diffuse into the bacterial cells, and cause cell death, and also the activity of phenols and glycosides of *R. coriaria* belonging to rich in anthocyanin and hydrolysable tannins, gallic acid (the main phenolic acid in *R. coriaria*), anthocyanin fraction contained cyanidin, peonidin, pelargonidin, petunidin, and dolphinidin glucosides and coumarates (AL–Jubory, *et al.*, 2010; Chaudhry, *et al.*, 2007). The most important components of Oregano are the limonene, gamma cariofilene, rho-cymenene, canfor, linalol. Alpha pinene, carvacol and thymol. Among them thymol and carvacrol are the main components of the essential oil of Oregano, which are responsible for its antioxidative, antimicrobial and antifungal effects (Kırmusaoğlu, *et al.*, 2007).

In the present study, both aqueous extracts show significant effect as antimitotic in comparison with the control (Distilled water). The mechanism of inhibiting mitosis growth that the extract may bind with the cell proteins responsible for cell division (Vidyalakshmi, *et al.*, 2007); and this action may be return to the presence of glycoside especially anthraquinone glycosides, and phenolic compounds responsible for antimitotic activity (Gaikwad, *et al.*, 2011). They exhibit cytotoxic effect by interfering with cell cycle kinetics. However most of the cytotoxic drugs exhibit side effects, and hence, there is a need for drugs that are efficient and have less side effects as plant extracts (Bhujbal, *et al.*, 2011).

V. Conclusion

It is concluded that aqueous extract of *R. coriaria* and *O. vulgare* have the antibacterial potency, and they were vary in their effect against four isolates of bacteria. The aqueous extract of *R. coriaria* was the strongest extract as bacterial inhibitory agent when compared to *O.* vulgare. On the other side, the aqueous extract of each plant showed antimitotic activity. We recommend using both plants as antitumor agents after separate all components and performance each of them separately.

References

Adebisi, O. and Ojokoh, A.O., 2011. Antimicrobial activities of green and red calyx extracts of *Hibiscus sabdariffa* on some microorganisms. *Journal of Agriculture and Biological Sciences*, 2(2), pp.038–042.

Alderman, D.J. and Smith, P., 2001. Development of Draft Protocols of Standard Reference Methods for Antimicrobial Agent Susceptibility Testing of Bacteria Associated with Fish Diseases. *Aquaculture*, 196(3–4), pp.211–243.

AL-Jubory, S.Y.O., Salah, S.S. and AL-Saltany, A.A.M., 2010. Antimicrobial study of active constituents of *Rhus coriaria. Kufa Journal for Veterinary Medical Sciences*, 2(1), pp.91.

AL-Neemy, U.M. and AL-Jebury, S.H., 2006. The Inhibitory Effect of Some Medicinal Plant Extracts to *Streptococcus pyogenes*. *Duhok Zanko Journal*, 11(1), pp.45–51. Proceedings of 1st Kurdistan Conference on Biological Science, Duhok.

Amusan, O.O.G., Sukati, N.A., Dlamini, P.S., and Sibandze, F.G., 2007. Some Swazi phytomedicines and their constituents. *African Journal of Biotechnology*, 6, pp.267–272.

Anil, C., and Shahid, R.M., 2013. Antimicrobial Susceptibility Patterns of *Pseudomonas aeruginosa* Clinical isolates at a Tertiary Care Hospital in Kathmandu, Nepal. *Asian Journal of Pharmaceutical and Clinical Research*, 6(3), pp.235–238.

Babpour, E.S. Angaji, A. Angaji, S.M., 2009. Antimicrobial effects of four medicinal plants on dental plaque. *Journal of Medicinal Plants and Researches*, 3(3), pp.132–137.

Bauer, A.W., Kirby, W.M., Sherris, J.C., and Turck, M., 1966. Antibiotic susceptibility testing by standardized single disc diffusion method. *American Journal of Clinical Pathology*, 45: pp.493 – 496.

Bhujbal, S.S. Deshmukh, R.P. Bidkar, J.S. Thatte, V.A. Awasare, S.S. and Garg, P.P., 2011. Evaluation of cytotoxic activity of barks of *Mimusops elengi*. *European and Asian Journal of Bioscience*, 5, pp.73–79.

Chaudhry, N.M.A., Saeed, S. and Tariq, P., 2007. Antibacterial effects of Oregano (*Origanum vulgare*) against gram negative bacilli. *Pakistan Journal of Botany*, 39(2), pp.609–613.

Coyle, M.B., 2005. Manual of Antimicrobial Susceptibility Testing. *American Society for Microbiology*.

Daniel, A.T., Shaohua, Z., Emily, T., Sherry, A., Aparna, S., Mary, J.B., and Patrick, F.M., 2012. Antimicrobial Drug Resistance in Escherichia coli from Humans and Food Animals, United States, 1950–2002. *Emerging Infectious Diseases*, 18 (5), pp.741–749.

Egbebia, O. and Famurewa, O., 2011. Antibiotic Resistance of *Klebsiella* Isolated from Some Hospitals in South West, Nigeria to Third Generation Cephalosporin's. *Advance Tropical Medicine and Public Health International*, 1(3), pp.95–100.

Frieden, T., 2013. Antibiotic Resistance Threats in the United States. *Centers for Disease Control and Prevention* (CDC), pp.1–114.

Gaikwad, S.B. Krishna, M.G. and Anerthe, S.J., 2011. Antimitotic activity and brine shrimp lethality test of *Tectona grandis* Linn. Bark. *Research Journal of Pharmaceutical, Biological and Chemical Science*, 2(4), pp.1014–1022.

Ghafourian, S., Bin-Shekawi, Z., Sadeghifard, N., Mohebi, R., Neela, V.K., Maleki, A., Hematian, A., Rahbar, M., Raftari, M. and Ranjbar, R., 2011. The Prevalence of ESBLs Producing *Klebsiella pneumoniae* Isolates in Some Major Hospitals, Iran. *The Open Microbiology Journal*, 5, pp.91–95.

Hamada, T.A., Mahmood, A.R. and Ahmed, I.B., 2008. Antibiotic resistance in pathogenic bacteria isolated from utis in Tikrit province. *Tikrit Medical Journal*, 14(1): pp.203–210.

Ibrahim, T.A. Opawale, B.O. and Oyinloye, J.M.A., 2011. Antibacterial activity of herbal extracts against multi drug resistant strains of bacteria from clinical origin. *Life Science and Leaflets*, 15, pp.490–498.

Keskin, D. and Toroglu, S., 2011. Studies on antimicrobial activities of solvent extracts of different spices. *Journal of Environment and Biology*, 32, pp.251–256.

Kırmusaoğlu, S., Yurdugul, S. and Kocoğlu, E., 2007. Effects of Fermented Sumac on the Formation of Slime Layer of *Staphylococcus aureus. Balkan Medical Journal*, 29, pp.84–87.

Kossah, R. Nsabimana, C. Zhao, J. Chen, H. Tian, F. Zhang, H. and Chen, W., 2009. Comparative Study on the Chemical Composition of Syrian Sumac (*Rhus coriaria* L.) and Chinese Sumac (*Rhus typhina* L.) Fruits. *Pakistan Journal of Nutrition*, 8(10), pp.1570–1574.

Kumari, P., Joshi, G.C., Tewari, L.M. and Singh, B.K., 2011. Quantitative assessment and antibacterial activity of Origanum vulgare L. *Journal of Phytology*, 3(12), pp.15–21.

Levy, S.B. and Marshall, B., 2004. Antibacterial resistance worldwide: causes, challenges and responses. *Nature Medicine Supplement*, 10(12), pp.122–129.

Lewis, K., Salyers, A.A., Taber, H.W., Wax, R.G., 2002. Bacterial Resistance to Antimicrobials. Marcel Dekker, Inc. New York. USA.

Odebiyi, O.O. and Sofowora, E.A., 1978. Phytochemical screening of Nigerian medical plants II. *Lloydia*,. 41, pp.2234–2246.

Oskay, M., Oskay, D. and Kalyoncu, F., 2009. Activity of Some Plant Extracts against Multi-Drug Resistant Human Pathogens. *Iranian Journal of Pharmaceutical Research*, 8(4), pp.293–300.

Ozzmen, A. Gamze, B. and Tugba, A., 2007. Antimitotic and antibacterial effects of the *Nigella sativa* L. seed. *Caryologia*, 60: pp.270–272.

Roopashree, T.S. Raman, D. Shobha, R.R.H. and Narendra, C., 2008. Antibacterial activity of antipsoriatic herbs: *Cassia tora*, *Momordica charantia* and *Calendula officinalis*. *International Journal of Applied Researches and Natural Products*, 1(3), pp.20–28.

Salah, H.F., 2007. Effect of some medicinal plant extract on antibiotic resistance by plasmids of *Escherichia coli* isolated from different sources. M.Sc. thesis submitted to College scientific education, University of Salahaddin – Erbil, Iraq.

Salna, K.P. Sreejith, K. Uthiralingam, M. Mithu, A.P. John, M.M. and Albin, T.F.A., 2011. Comparative study of phytochemicals investigation of *Andrographis paniculata* and *Murraya koenigii*. *International Journal of Pharmacy and Pharmaceutical Science*, 3(3), pp.291–292.

Schito, G.C. Naber, K.G. Botto, H. Polou, J. Mazzei, T. Guallo, L. and Marchese, A., 2009. The ARESC (Antimicrobial Resistance Epidemiological Survey on Cystitis) Study: An International Survey on the Antimicrobial Resistance of Pathogens involved in Uncomplicated Urinary Tract Infections. *International Journal of Antimicrobial Agents*, 34(5), pp.4–12.

Seyyednejad, S.M. Maleki, S. Mirzaei, D.N. and Motamedi, H., 2008. Antibacterial activity of *Prunus mahaleb* and parsley (*Petroselinum crispum*) against some pathogen. *Asian Journal of Biological Science*, 1, pp.51–55.

Shivali, N.M., and Kamboj, P., 2009. *Hibiscus sabdariffa* Linn. An overview. *Natural Product Radiance*, 8(1), pp.77–83.

Sikarwar, A.S., and Batra, H.V., 2011. Prevalence of Antimicrobial Drug Resistance of *Klebsiella pneumoniae* in India. *International Journal of Bioscience, Biochemistry and Bioinformatics*, 1(3), pp.211–215.

Solanki, R., 2010. Some Medical Plants with Antibacterial Activity. *Pharmacie Globale* (IJCP), 4(10), pp.1–4.

Stavri, M., Piddock, L.V.J., and Gibbons, S., 2007. Bacterial efflux pumps inhibitors from natural sources. *Journal of Antimicrobial Chemotherapy*, 59, pp.1247–1260.

Stermitz, F.R., Lorenz, P., and Tawara, J.N., 2000. Synergy in a medicinal plant: antimicrobial action of berberine potentiated by 5'-methoxyhydnocarpin, a multidrug pump inhibitor. *Proceedings of the National Academy of Sciences USA*, 97: pp.1433–1437.

Tariro, A.C., and Stanley, M., 2011. *In Vitro* Antibacterial Activity of Selected Medicinal Plants from Zimbabwe. *The African Journal of Plant Science and Biotechnology*, 5 (1), pp.1–7.

Toroglu, S. and Keskin, D., 2011. Antimicrobial Resistance and Sensitivity among Isolates of *Klebsiella pneumoniae* from Hospital Patients in Turkey. *International Journal of Agriculture and Biology*, 13(6), pp.941–946.

Vidyalakshmi, K.S. Chales, D.A. and Vasanthi, H.R., 2007. Anti – Mitotic and cytotoxic effect of *Mussaenda queensirkit*. *Journal of Pharmacology and Toxicology*, 2(7), pp.660–665.

Wasfi, R., Abd El-Rahman, O.A., Mansour, L.E., Hanora, A.S., Hashem, A.M., and Ashour, M.S., 2012. Antimicrobial activities against biofilm formed by *Proteus mirabilis* isolates from wound and urinary tract infections. *Indian Journal of Medical Microbiology*, 30(1), pp.76–80.

Ya, C. Gaffney, S.H. Lilley, T.H. and Haslam. E., 1989. Carbohydrate polyphenol complication in chemistry and significance of condensed tannins. Plenum Press, New York.

Younis, N.S., 2011. Neonatal Sepsis in Jordan: Bacterial Isolates and Antibiotic SusceptibilityPatterns. *Rawal Medicine Journal*, 36(3), pp.1–16.

General Information

Aro's Mission: Aro seeks to publish those papers that are most influential in their fields or across fields and that will significantly advance scientific understanding. Selected papers should present novel and broadly important data, syntheses, or concepts. They should merit the recognition by the scientific community and general public provided by publication in Aro, beyond that provided by specialty journals.

We welcome submissions from all fields of natural science and technology, and from any source. We are committed to the prompt evaluation and publication of submitted papers. Aro is published biannually; selected papers are published online ahead of print.

Submission

Manuscripts should be submitted by the correspondent authors of the manuscript via the on-line submission page (http://aro.koyauniversity.org./authors/submit-online). Regardless of the source of the word-processing tool, only electronic Word (.doc, .docx, .rtf) files can be submitted on-line. There is no page limit. Only online submissions are accepted to facilitate rapid publication and minimize administrative costs. Submissions by any other one but the authors will not be accepted. The submitting author takes responsibility for the paper during submission and peer review. If for some technical reason submission through the email is not possible, the author can contact aro.journal@koyauniversity.org for support. Before submitting please check Aro's guide to authors thoroughly to avoid any delay in the review and publication process.

Authors are explicitly responsible for the language of their texts. Paper should be submitted in a well written in understandable English. Authors should not expect the editor or editorial board to rewrite their paper. Prior to submission, authors should have their paper proofread by a possible academic native speaker of English.

- Submit the Article with contact Information
- File name should be your article tittle
- Don't submit your article in multiple journal, we are taking only minimum time for review process. please don't waste our time
- Once the paper is accepted, it can't be withdrawn
- Please follow publication ethics and regulation
- Avoid plagiarism and copied material
- Strictly Follow Aro's Template

Terms of Submission

Papers must be submitted on the understanding that they have not been published elsewhere and are not currently under consideration by another journal or any other publisher. Aro accepts original articles with novel impacts only. Post conference papers are not accepted "as is", however, regular papers on the same topic but with a different title can be submitted. The new paper should contain significant improvements in terms of extended content, analysis, comparisons with popular methods, results, figures, comments, etc. Please do not forget that the publication of the same or similar material in Aro constitutes the grounds for filing of an (auto) plagiarism case.

The submitting author is responsible for ensuring that the article’s publication has been approved by all the other co-authors. It is also the authors’ responsibility to ensure that the articles emanating from a particular institution are submitted with the approval of the necessary institution. Only an acknowledgement from the editorial office officially establishes the date of receipt. Further correspondence and proofs will be sent to the author(s) before publication unless otherwise indicated. It is a condition of submission of a paper that the authors permit editing of the

paper for readability. All enquiries concerning the publication of accepted papers should be addressed to aro.journal@koyauniversity.org.

Peer Review

All manuscripts are subject to peer review and are expected to meet standards of academic excellence. Submissions will be considered by an editor and "if not rejected right away" by peer-reviewers, whose identities will remain anonymous to the authors.

Guide to Author

We welcome submissions from all fields of science and from any source. We are committed to the prompt evaluation and publication of submitted papers. Selected papers are published online ahead of print. Authors are encouraged to read the instructions below before submitting their manuscripts. This section arranged into an overview speedy guidelines below and more detailed at the bottom section of this page

Manuscript Preparation

Submitting your manuscript will be in two stages namely before final acceptance and after.

Stage one:

At the first stage manuscript needs to be prepared electronically and submitted online via the online submission page in a Word (.doc, .docx, .rtf) format of one column double-spaced page, Times New Roman font type, and 12 p font size. A pdf version of the submitted manuscript should be submitted too. All authors' names, affiliations, e-mail addresses, and mobile phone numbers should be typed on a cover page, indicating the correspondent author.

Stage two:

- File type: MS-Word version 2003 or later.
- Format: The preferred format of the manuscript two-column template with figures and captions included in the text. This template can be downloaded via the following link. Please follow instructions given in the template; http://aro.koyauniversity.org/authors/guide-for-author
- Text: All text is in Times New Roman font. The main text is 10-point, abstract is 9-point font and tables, references and captions are 8-point font.
- Figures: Figures should be easily viewed on a computer screen.

Units of Measurement

Units of measurement should be presented simply and concisely using System International (SI) units.

Title and Authorship Information

The following information should be included;

- Paper title.
- Full author names.
- Affiliation.
- Email addresses.

Abstract

The manuscript should contain an abstract. The abstract should be self-contained and citation-free and should not exceed 200 words.

Introduction

This section should be succinct, with no subheadings.

Materials and Methods

This part should contain sufficient detail so that all procedures can be repeated. It can be divided into subsections if several methods are described.

Results and Discussion

This section may each be divided by subheadings or may be combined.

Conclusions

This should clearly explain the main conclusions of the work highlighting its importance and relevance.

Acknowledgements

All acknowledgements (if any) should be included at the very end of the paper before the references and may include supporting grants, presentations, and so forth.

References

References must be included in the manuscript and authors are responsible for the accuracy of references. Manuscripts without them will be returned. Aro is following Harvard System of Referencing. (Learn how to import and use Harvard Styling in your Microsoft Office by following this link: http://bibword.codeplex.com/releases/view/15852)

Preparation of Figures

Upon submission of an article, authors are supposed to include all figures and tables in the PDF file of the manuscript. Figures and tables should embedded in the manuscript. Figures should be supplied in either vector art formats (Illustrator, EPS, WMF, FreeHand, CorelDraw, PowerPoint, Excel, etc.) or bitmap formats (Photoshop, TIFF, GIF, JPEG, etc.). Bitmap images should be of 300 dpi resolution at least unless the resolution is intentionally set to a lower level for scientific reasons. If a bitmap image has labels, the image and labels should be embedded in separate layers.

Preparation of Tables

Tables should be cited consecutively in the text. Every table must have a descriptive title and if numerical measurements are given, the units should be included in the column heading. Vertical rules should not be used.

Copyright

ARO Reviewer/Associate Editor Application Form

Aro is a scientific journal of Koya University (p-ISSN: 2410-9355, e-ISSN: 2307-549X) which aims to offer a novel contribution to the study of Science. The purpose of Aro is twofold: first, it will aim to become an ongoing forum for debate and discussion across the sciences and Engineering. We hope to advance our problem solving capacity and deepen our knowledge regarding a comprehensive range of collective actions. Second, Aro accepts the challenges brought about by multidisciplinary scientific areas and aspires to expand the community of academics who are able to learn from and help to produce advances in a variety of different disciplines.

The Journal is seeking reviewers who can provide constructive analysis of papers thus enhancing overall reputation of the Journal. If any expert is interested in participating of the review process, we highly encourage you to sign up as a reviewer for our Journal and help us improve our presence in domain of your expertise. Appropriate selection of reviewers who have expertise and interest in the domain relevant to each manuscript are essential elements that ensure a timely, productive peer review process. We require proficiency in English.

How to apply

To apply for becoming a reviewer or a member of the Editorial Board of Aro, please submit the application form by following the link:
http://aro.koyauniversity.org/about/application-form.

Both Associate Editor and Reviewers should specify their areas of research and expertise. Applicants must have a doctorate (or an equivalent degree), and if Master degree they need to have significant publishing experience. Please note that;

- You will need to write your full official name.
- Please provide an email which reflects your official name, such as nameOne.NameTwo@... , or your institute's official email.
- All data need to be written in English.

Note: For more information, kindly visit the following websites:

1. Aro.koyauniversity.org.
2. http://libweb.anglia.ac.uk/referencing/harvard.htm.
3. http://bibword.codeplex.com/releases/view/15852.

Koya University is located in the city of Koya (Koysinjaq), which is one hour drive to the East of the Kurdistan Region capital Erbil (Erbil, Hewlér) in North Iraq. It is on the foothills of beautiful high mountain. Its campus has been carefully laid out to embrace the beautiful mountainous nature. The Koya University was established in 2003 and has developed noticeably. In 2010, Koya University was restructured from colleges to faculty systems to enhance the interactions between similar academic fields. Today the University has 4 faculties - Engineering, Science and Health, Humanities and Social Sciences and Education, and a school of Medicine - which together compound 25 departments in different fields, such as Petroleum Engineering, Geotechnical Engineering, Clinical Psychology, Social Science and Medical Microbiology, as well as Sport Education.

Aro is a scientific journal published by the Koya University. Aro is a journal of original scientific research, global news, and commentary. The Aro Scientific Journal is a peer-reviewed, open access journal that publishes original research articles as well as review articles in all areas of Natural Science and Technology.

KOYA UNIVERSITY

ARO
The Scientific Journal of Koya University

ARO the Scientific Journal Office
Koya University Park
Danielle Mitterrand Boulevard
Koya KOY45
Kurdistan Region - F.R. Iraq

ISSN: 2410-9355 (print version),
ISSN: 2307-549X (electronic version), DOI: 10.14500/2307-549X